PRIRODOSLOVNO-MATEMATIČKI FAKULTET

Doktorski studij Biofizika

Doktorski rad

Učinak korištenja vlažnih lipidnih filmova, dobivenih fuzijom vezikula, na elektroformaciju divovskih unilamelarnih vezikula s obzirom na različite lipidne sastave i naboj, koncentraciju kolesterola i ionsku snagu otopine

Ivan Mardešić

Split, veljača 2025

FACULTY OF SCIENCE

Doctoral Study of Biophysics

Doctoral thesis

The effect of using wet lipid films, obtained by vesicle fusion, on electroformation of giant unilamellar vesicles with respect to different lipid compositions and charge, cholesterol concentration, and solution ionic strength

Ivan Mardešić

Split, 2025 February

University of Split, Faculty of Science

Department of Physics, Doctoral Study of Biophysics

The effect of using wet lipid films, obtained by vesicle fusion, on electroformation of giant unilamellar vesicles with respect to different lipid compositions and charge, cholesterol concentration, and solution ionic strength

The PhD thesis authored by Ivan Mardešić was conducted under the supervision of prof. dr.sc. Marija Raguž,

This research was undertaken as a necessary requirement to obtain the PhD title.

Achieved academic title: PhD in Natural Sciences.

Members of the Expert Board for Assessment and Defending of Doctoral Thesis:

1. Assist. Prof. Lucija Krce, Ph.D. _____
2. Assoc. Prof. Željka Sanader Maršić, Ph.D. _____
3. Assist. Prof. Martina Perić Bakulić, Ph.D. _____
4. Full Prof. Ante Bilušić, Ph.D (substitute member) _____

Hereby confirm that the PhD thesis has been defended on the date: _____

Doctoral Study Head:

Associate Professor Damir Kovačić, PhD

_____

D E A N:

Professor Mile Dželalija, PhD

_____

BASIC DOCUMENTATION CARD

University of Split   PhD. thesis
Faculty of Science

The effect of using wet lipid films, obtained by vesicle fusion, on electroformation of giant unilamellar vesicles with respect to different lipid compositions and charge, cholesterol concentration, and solution ionic strength

Ivan Mardešić
Thesis performed at University of Split School of Medicine

Abstract
The long-term aim of this research is to investigate the properties of cholesterol bilayer domains (CBDs). Before starting experimental work, we conducted a detailed literature search and wrote a review article about all membrane models and experimental methods suitable for studying properties of CBD domains. We also described in details their known properties and functions in biological membranes. Our motivation stemmed from the beneficial role of CBDs in protecting the eye lens from cataract development and maintaining its homeostasis. Based on this knowledge we chosen giant unilamellar vesicles (GUVs) as an appropriate model for studying lipid portion of the fiber cell plasma membranes of the eye lens. GUVs are widely used as membrane models in studies of membrane properties, with the electroformation method being the most common approach for their production. However, several factors can affect the success of GUV electroformation. Common challenges include high cholesterol (Chol) concentrations, the use of lipid mixtures containing charged lipids, and solutions with elevated ionic strength. High Chol concentrations pose a particular problem for the traditional electroformation protocol, which involves drying the lipid film by fully evaporating the organic solvent. During this process, anhydrous Chol crystals can form, which do not integrate into the lipid bilayer, resulting in a lower Chol concentration in the vesicle bilayer compared to the original lipid mixture. To address the issue of artifactual Chol demixing, we have modified the electroformation protocol by introducing rapid solvent exchange, ultrasonication, plasma cleaning, and spin-coating techniques for the reproducible production of GUVs from damp lipid films. A high yield of GUVs was achieved for Chol/1-palmitoyl-2-oleoyl-sn-glycero-3-phosphocholine (POPC) samples with mixing ratios ranging from 0 to 2.5. At Chol/POPC mixing ratios greater than 1,5, where the GUVs may contain Chol bilayer domains (CBDs), a significant decrease in the average GUV diameter is measured. It is about 40% lower compared to that of the pure POPC bilayer. This modified approach not only minimizes Chol demixing but also successfully produces GUVs from lipid mixtures containing charged lipids and ionic solutions as the internal medium. We prepared GUVs from mixtures with up to 60 mol% of the charged lipid 1-palmitoyl-2-oleoyl-sn-glycero-3-phospho-L-serine (POPS) and formed GUVs in low-concentration NaCl solutions.

Učinak korištenja vlažnih lipidnih filmova, dobivenih fuzijom vezikula, na elektroformaciju divovskih unilamelarnih vezikula s obzirom na različite lipidne sastave i naboj, koncentraciju kolesterola i ionsku snagu otopine

Ivan Mardešić
Rad je izrađen na Medicinskom fakultetu u Splitu

Sažetak

Dugoročni cilj ovog rada je istraživanje svojstava čiste kolesterolove domene. Prije početka eksperimentalnog rada, istražili smo literaturu te napisali detaljni pregledni članak o različitim membranskim modelima i eksperimentalnim tehnikama prikladnim za istraživanje tih domena. Sva poznata svojstva i funkcije čiste kolesterolove domene su opisane. Glavna motivacija za istraživanje su istraživanje funkcija domene u leći oka, gdje ta domena omogućuje homeostazu stanice i ima zaštitnu funkciju tijekom razvoja katarakte. Odlučili smo koristiti divovske unilamelarne vezikule (DUV) kao prikladan model za stanične membrane vlaknastih stanica leće oka. DUV-ovi se koriste kao membranski modeli za istraživanje osobina bioloških membrana, pri čemu je elektroformacija najčešće primjenjivana metoda za njihovo formiranje. Međutim, mnogo čimbenika može utjecati na uspjeh elektroformacije DUV-ova. Neki od izazova uključuju upotrebu visoke koncentracije kolesterola, nabijenih lipida i korištenje otopine s ionskom snagom. Visoke koncentracije kolesterola predstavljaju poseban problem za tradicionalni protokol, koji uključuje sušenje lipidnog filma. Tijekom ovog procesa mogu se formirati kolesterolovi kristali koji se ne ugrađuju u vezikulu, što rezultira nižom koncentracijom kolesterola u vezikuli nego u izvornoj smjesi lipida. Kako bismo se riješili problemom izlučivanja kolesterola, modificirali smo protokol elektroformacije korištenjem različitih metoda kao što su: brza izmjene otapala, sonikacija, čišćenje elektrode plazmom i brzo razmazivanje. Modificirani elektroformacijski protokol omogućuje reproducibilnu proizvodnju DUV-ova za različite omjere kolesterola i 1-palmitnska-2-oleoinska-sn-glicero-3-fosfokolina (POPC) od 0 do 2.5, uz minimiziranje izlučivanja kolesterola. Za omjere kolesterol/POPC veće od 1.5 izmjeren je pad drastični promjera DUV-ova. Promjer se smanjio oko 40% u usporedbi s čistom POPC membranom. Osim formiranja DUV-ova s visokom koncentracijom kolesterola, uspješno smo formirali DUV-ove koristeći nabijene lipide (1-palmitoil-2-oleoil-sn-glicero-3-fosfo-L-serin, POPS) i ionske otopine s niskom koncentracijom NaCl-a.

The following publications constitute the main part of the thesis:

1.   Mardešić, I.; Boban, Z.; Subczynski, W.K.; Raguz, M. Membrane Models and Experiments Suitable for Studies of the Cholesterol Bilayer Domains. Membranes (Basel). 2023, 13, doi:10.3390/membranes13030320.

2.   Mardešić, I.; Boban, Z.; Raguz, M. Electroformation of Giant Unilamellar Vesicles from Damp Lipid Films with a Focus on Vesicles with High Cholesterol Content. Membranes (Basel). 2024, 14, 79, doi:10.3390/membranes14040079.

3.   Mardešić, I.; Boban, Z.; Raguz, M. Electroformation of Giant Unilamellar Vesicles from Damp Films in Conditions Involving High Cholesterol Contents, Charged Lipids, and Saline Solutions. Membranes (Basel). 2024, 14, 215. https://doi.org/10.3390/membranes14100215

ABBREVIATIONS

CBD   Cholesterol bilayer domain

Chol   Cholesterol

CST   Cholesterol solubility threshold

CSAT Cholesterol saturation threshold

GUV   Giant unilamellar vesicle

ITO   Indium tin oxide

l_d Liquid-disordered domain

l_o Liquid-ordered domain

LUV   Large unilamellar vesicle

MLV   Multilamellar vesicle

OLV   Oligolamellar vesicle

POPC 1-palmitoyl-2-oleoyl-sn-glycero-3-phosphocholine

POPS 1-palmitoyl-2-oleoyl-sn-glycero-3-phospho-L-serine

RSE   Rapid solvent exchange

SALB Solvent assisted lipid bilayer

SLB   Supported lipid bilayer

SUV   Small unilamellar vesicle

CONTENTS

1 INTRODUCTION

1.1 Influence of cholesterol on the structure and properties of the plasma membrane

The plasma membrane is a complex, flexible barrier that separates the cell from its environment. It is composed of various lipids, primarily phospholipids, sphingolipids, and cholesterol (Chol), along with membrane proteins and carbohydrates [1,2]. Lipids differ in terms of headgroup structure, the length of hydrocarbon chains, and the degree of unsaturation. The physical properties of plasma membranes vary depending on the lipid composition [3]. Membrane thickness and rigidity [4,5], domain formation [4,5] and cell signalling [6] are influenced by the Chol content, which is particularly important in the membrane. Chol is an amphiphilic molecule, consisting of a nonpolar, rigid, planar fused ring structure with both a smooth and rough side (sterol), a short, flexible isooctyl tail, and a small hydrophilic hydroxyl (-OH) group [7]. In the membrane, Chol positions its headgroup next to the polar heads of surrounding lipids, with its sterol rings incorporated among the acyl chain regions of other lipids. In this orientation, Chol regulates the lateral organization of lipids and influences the membrane's physical properties at various depths.

The domains rich in Chol that have attracted researchers' attention over the last few decades are known as lipid rafts. Lipid rafts control signal transduction, protein sorting, and lipid trafficking [8–11]. Most plasma membranes contain around 30 mol% Chol with coexisting liquid-ordered (l_o) and liquid-disordered domains (l_d) (Figure 1). These membranes are the most commonly studied, but there are also plasma membranes with higher Chol content, exceeding the Chol saturation threshold (CSAT) (around 50 mol% Chol) in which Chol bilayer domains (CBDs) form [12]. These domains consist exclusively of Chol molecules in both bilayers and are stabilized by the surrounding l_o domains (domains rich in Chol). Chol concentrations exceeding the saturation threshold are less common in biological membranes and, as a result, have been less studied. High Chol content plays a crucial role in the normal functioning of the eye lens [13,14] and in the formation of Chol plaques in atherosclerosis [15]. CBDs are beneficial for the lipid portion of fiber cell plasma membranes of the eye lens, where they act as a buffering capacity, ensuring that the membrane is always saturated with Chol [14,16,17]. CBDs support normal physiological functions by helping to maintain lens transparency and prevent cataract formation. In other tissues or organs, high Chol content is considered as a sign of pathology. In fiber cell

plasma membranes of the eye lens, CBDs ensure consistent physical properties regardless of lipid composition changes (as the lipid composition of the eye lens is different in different species and changes with aging). CBDs also maximize the membrane's hydrophobic barrier. They form a barrier to oxygen permeation across the layers of fiber cells, thereby preventing oxidative stress, which helps avoid cataract development [17,18]. When Chol content exceeds the Chol solubility limit (CST), Chol crystals are formed. These crystals can trigger an inflammatory cascade, contributing to the development of atherosclerosis [19], but there is no evidence of harmful effects caused by Chol crystals in the eye lens [14,20].
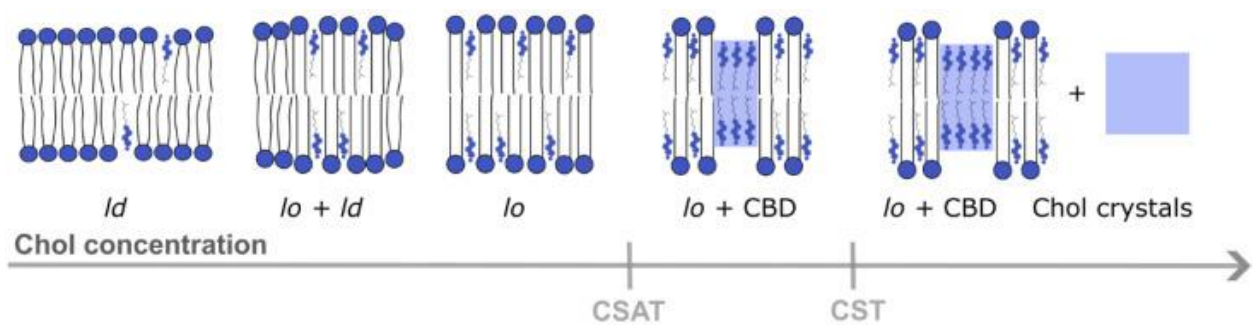
Figure 1. Different membrane domains are formed in a lipid bilayer at varying Chol concentrations. At very low Chol concentrations, the membrane contains only liquid disordered domain (l_d). Around 30 mol% Chol content, the membrane exhibits two coexisting domains: liquid ordered (l_o) and l_d. As the Chol concentration increases further, the membrane transitions entirely into the l_o domain. Cholesterol bilayr domains (CBDs) begin to form above the Chol saturation threshold (CSAT), and Chol precipitates as Chol crystals above the Chol solubility threshold (CST). Figure taken from [21].

In this work, we focused on producing artificial membrane models with high Chol content (above CSAT) as models of fiber cell plasma membranes of the eye lens. These membranes have Chol/lipid molar ratios as high as 2 in the human lens cortex and up to 4 in the lens nucleus [15,22]. They also contain significant amounts of sphingomyelin and dihydrosphingomyelin (around 66 mol% of all non-Chol lipids). These membranes also contain charged lipids (phosphatidylserine, around 8 mol%). Most of the fatty acids contained in the membranes are saturated or monounsaturated [23]. Various artificial membrane models can be used to study membrane properties, but the primary focus of this work was on developing a protocol to successfully form giant unilamellar vesicles (GUVs) that can mimic fiber cell plasma membranes of the eye lens.

2 Artificial membrane models

2.1 The vesicles

Lipid vesicles are structures consisting of at least one lipid bilayer surrounding an aqueous solution. Since they are lab-created, they can be studied under controlled conditions, making them a commonly used model for biological membranes. Vesicles are used to investigate membrane mechanical properties [24], mimic cell interaction [25,26], facilitate drug delivery [27], and study interactions with toxins [28] and nanoparticles [29]. Vesicles are generally classified based on their lamellarity: they can be unilamellar, multilamellar (MLVs), or oligolamellar (OLVs) (Figure 2). Unilamellar vesicles contain a single bilayer, MLVs have multiple concentric bilayers, and OLVs consist of bilayers enclosed within outer bilayers. Unilamellar vesicles are further categorized by size: small unilamellar vesicles (SUVs) (<100 nm), large unilamellar vesicles (LUVs) (100 nm – 1 μm), and giant unilamellar vesicles (GUVs) (>1 μm).
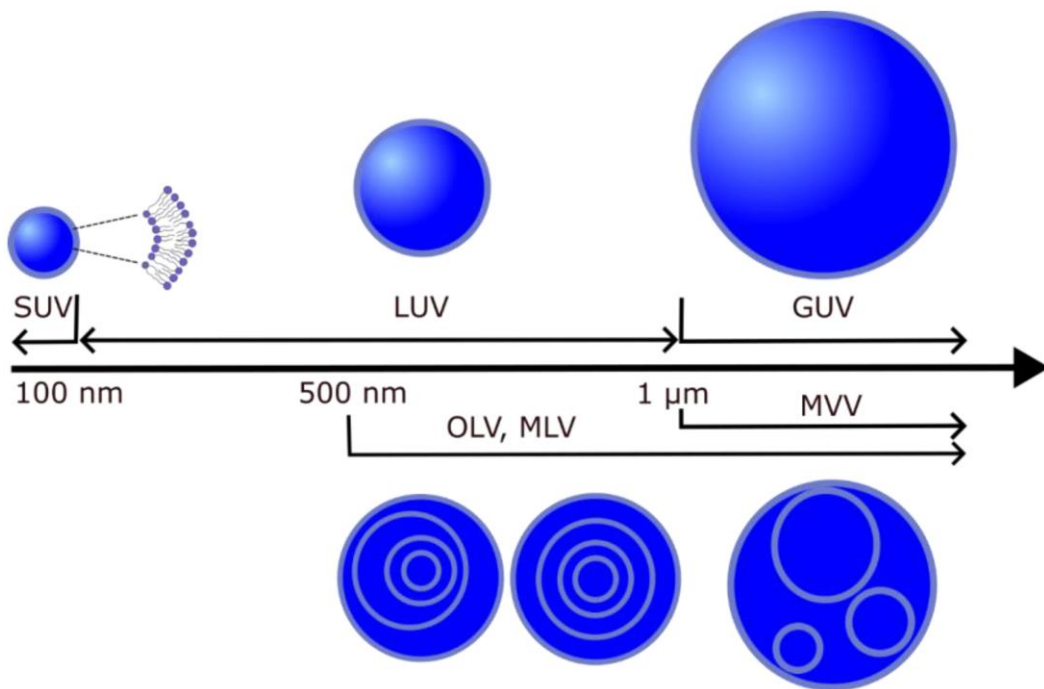
Figure 2. Different types of vesicles depending on their size and structure. Figure taken from [21].

In order to form MLVs, lipids are first dissolved in an organic solvent. They are usually deposited inside a tube or on a substrate and then dried. Vacuum drying, inert gas flow, rotary evaporation, or lyophilization can be applied to remove the organic solvent. Once a dry lipid film is formed, it is rehydrated with an aqueous solution, causing the lipids to detach and form MLVs. Shaking, vortexing, or stirring can further promote MLV formation [30]. However, a challenge

with this approach is the formation of artificial anhydrous Chol crystals during the drying process, especially when the Chol concentration is high. Upon rehydration of the lipid film, Chol molecules from anhydrous crystals do not participate in vesicle formation. As a result, the actual amount of Chol incorporated into the vesicle bilayer is lower than in the original mixture, since Chol crystals do not integrate into the vesicles.

MLVs can be used to produce SUVs or LUVs, with extrusion or sonication as the most commonly used methods. During extrusion, the MLV suspension is passed through polycarbonate filters with membranes of varying pore sizes. To achieve a uniform population of unilamellar vesicles, the MLV suspension typically needs to pass through the pores approximately 15 times. Different pore sizes allow the production of SUVs or LUVs of varying sizes. In the sonication method, applied ultrasound wave breaks up the MLVs in the sample to form smaller vesicles. The power and duration of sonication determine the final vesicle size and distribution. The advantages and disadvantages of these two methods will be discussed later in the text. SUVs and LUVs are often used as intermediate steps in protocols for GUV production [31] or in the formation of supported lipid bilayers (SLBs) [32].

2.2 The supported lipid bilayers

SLBs consist of two lipid leaflets resting on a solid support, with a 1–2 nm water layer separating the surface from the membrane [33]. Several factors influence the formation of SLBs, including the substrate, buffer, lipid composition, and concentration. Various substrates can be used, but the most commonly used ones for SLB fabrication are silica and glass [34]. One advantage of SLBs as a membrane model, compared to vesicles, is that they are better suited for 2D-sensitive experimental techniques such as atomic force microscopy [35], X-ray diffraction [36,37], fluorescence microscopy [38] and quartz crystal microbalance with dissipation monitoring [39].

Various protocols can be used to form SLBs, with vesicle fusion being the most widely used method today (Figure 3). In this method, SUVs or LUVs are deposited onto a hydrophilic surface, where they rupture and form SLBs. Although the protocol is fast and easy to use, several factors can influence SLB formation, such as vesicle size, lipid composition (including lipid charge, Chol concentration, and the degree of lipid saturation), temperature, substrate type, and ionic strength [33,40,41]. A challenge with this method is the formation of fully developed SLBs with high Chol content. Chol increases vesicle heterogeneity and rigidity, making vesicle rupture

more difficult. Another issue is that the lipid composition of the vesicles may differ from that of the resulting SLBs under these conditions [42]. Certain reagents and buffers can help mitigate these problems and promote vesicle rupture.
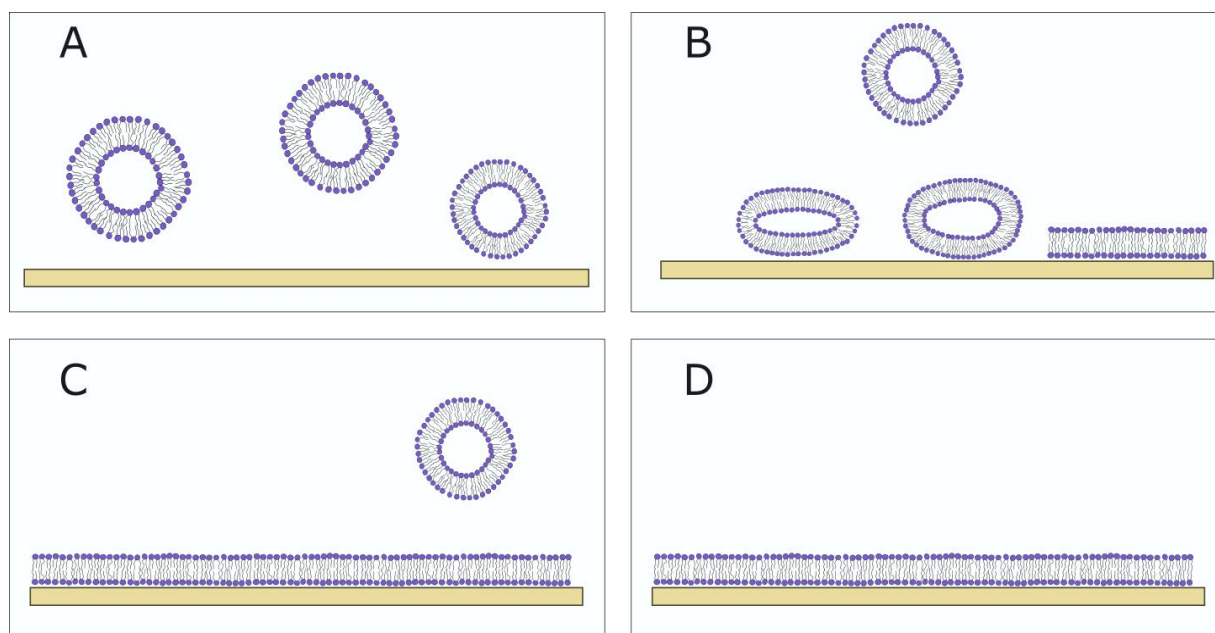
Figure 3. The supported lipid bilayer (SLB) formation using vesicle fusion method. A) Vesicles float in the bulk solution. B) If the vesicle–substrate interaction is sufficiently strong, the adsorbed vesicles rupture on the substrate. C) The SLB forms, and the unabsorbed vesicles are washed away using a buffer. D) The fully formed SLB. Figure taken from [21].

The solvent-assisted lipid bilayer (SALB) method and the bicelle-mediated method have both been shown to be suitable for forming SLBs with high Chol content (Figure 4A). The SALB method involves a gradual exchange of organic and aqueous solutions. During this process, various lipid structures are formed. First inverted micelles, then micelles and the final structure being vesicles that rupture, allowing lipids to form SLBs, similar to the vesicle fusion method. Using this approach, SLBs with high Chol content have been successfully formed [43].

The bicelle-mediated method is another protocol successfully used to create SLBs with high Chol content (Figure 4B). Bicelles are disc-shaped lipid structures composed of a combination of long-chain and short-chain lipids. When an attractive force exists between the substrate and the bicelles, the bicelles adhere to the surface and fuse together. The long-chain phospholipids stay bound to the substrate, while the short-chain phospholipids are removed as monomers with a buffer wash. The presence of short-chain phospholipids makes bicelles softer than vesicles, allowing them to rupture more easily, which is crucial for forming SLBs with high Chol content.
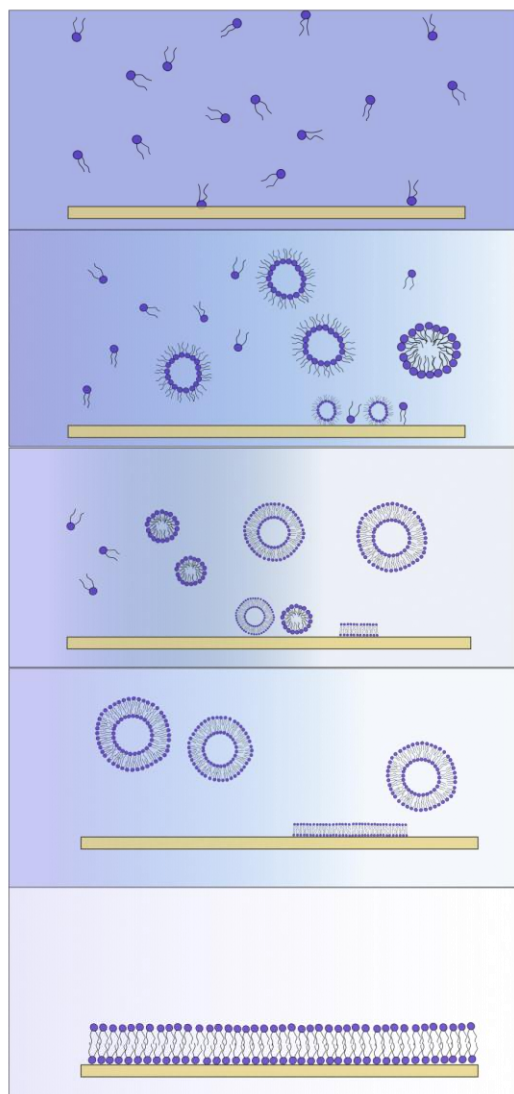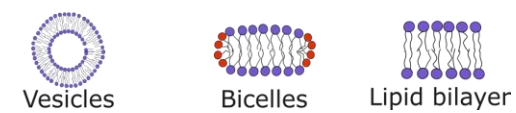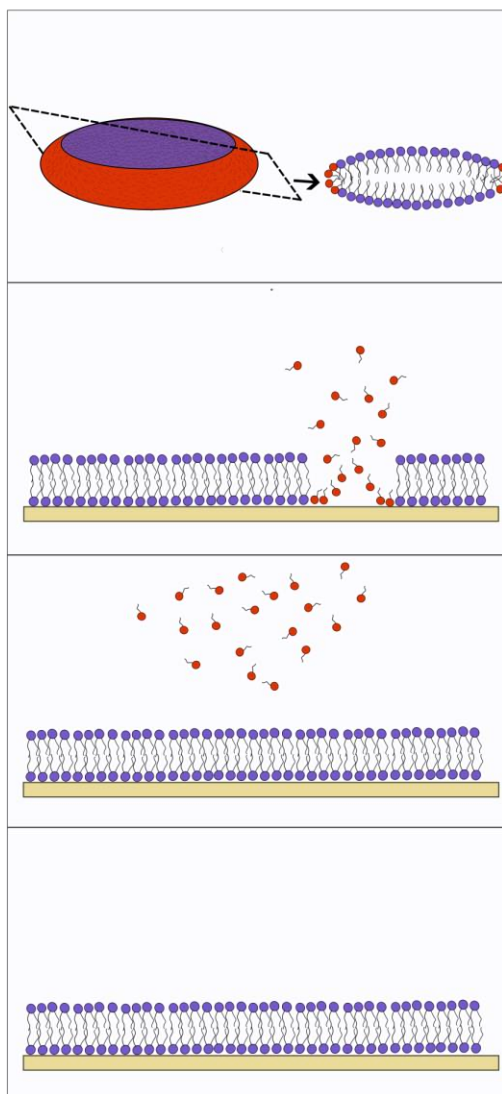
Figure 4. Comparison of the Solvent-assisted lipid bilayer (SALB) and bicelle mediated method for formation of SLBs. A) The SALB method begins when lipids are dissolved in a water-miscible organic solvent. The organic solvent is gradually exchanged with the aqueous solvent. During the solvent exchange, the lipids first assemble into inverted micelles and later into micelles and vesicles. These attach themselves to the surface and rupture to form an SLB. B) Bicelle mediated method. Bicelles are disk-like structures containing both long-chain (blue) and short-chain (red) lipids. If there is an attractive force between the substrate and the bicelles, they are adsorbed onto the surface and fuse together. Long-chain phospholipids remain attached to the substrate, and short-chain phospholipids are washed away in the form of monomers using a buffer. Figure taken from [21].

2.3 Giant unilamellar vesicles

GUVs are the most commonly used vesicle model for studying membrane physical properties and bilayer lateral organization. Their size is similar to the size of the eukaryotic cells (diameters greater than 1 μm), making them detectable using fluorescence microscopy. Reeves and Dowben made the first attempt to form GUVs in 1969 [44]. In their approach, a lipid mixture was applied to an electrode, dried to form a lipid film, and then rehydrated (gentle hydration). Osmotic pressure drives the aqueous solution between the lipid layers. Due to the amphiphilic nature of lipids, exposing their hydrophobic acyl chains to water is unfavourable, leading the lipid bilayers to enclose and form vesicles. Although simple to perform, this method yields a low number of GUVs, with many defects.

There are various methods for forming GUVs, but electroformation is the most widely used. Developed by Angelova and Dimitrova in 1986 [45], this method involves drying lipids on an electrode to form a dry lipid film. The electrode, coated with the lipid film, is used to create an electroformation chamber, which is filled with the desired aqueous solution and connected to an external alternating electric field. The electric field and osmotic pressure help detach lipids from the electrode, leading to the formation of GUVs [46]. Compared to the gentle hydration method, electroformation produces a higher yield of GUVs with fewer defects. When the electric field is optimised properly GUVs with high yield can be produced.

Although Angelova and Dimitrova originally used platinum wires, today, indium tin oxide (ITO)-coated glass is the most widely used electrode material [47–49]. The electroformation chamber setup is slightly different: one ITO-coated glass is coated with lipids and dried, while the second remains lipid-free. Additionally, fluorescent lipid analogs are mixed with the lipids in very small quantities to enable detection using fluorescence microscopy. After lipid deposition, the lipid-coated and lipid-free electrodes are used to assemble the electroformation chamber. The lipid-coated glass is sealed to a spacer using vacuum grease and the lipid-free electrode is sealed to the spacer on the opposite side. Copper tape is often attached to the electrodes to ensure better contact with the alternating electric field generator. The chamber is then filled with the desired solution and connected to the generator. The entire setup is placed in an incubator to maintain a temperature higher than the phase transition temperature of the deposited lipids. The electroformation process typically lasts 2 to 3 hours. Even though the protocol is straightforward, there are many factors that can influence GUVs formation.

2.4 Modification of traditional electroformation protocol

The electroformation method has evolved significantly since its introduction, with numerous modifications made to protocols to improve reproducibility and accommodate a broader range of lipid mixtures. Despite the apparent simplicity of this technique, various factors can influence the formation of GUVs, including lipid composition, deposition methods, temperature, electrode type, internal solution and the electric field used (alternating electric field with varying frequency and amplitude). Optimizing the electroformation protocol for different lipid mixtures is crucial for achieving a high yield of GUVs. Using ionic solutions as internal solution can produce electric field screening, where ions rearrange themselves in response to an external electric field, creating an opposing field that reduces the overall effect of the external field within the solution.

Currently, alongside platinum wires, ITO-coated glass is commonly used for electroformation. The ITO-coated glass provides a large flat surface that enable a high yield of GUVs. Additionally, its transparency makes it ideal for microscopy applications. Other electrode materials, such as steel syringes, copper, and titanium, have also been employed [50–52].

To prepare electrodes for lipid deposition, various cleaning methods are used, including sonication with organic solvents [47], repeated rinsing with organic solvents [53], and wiping with lint-free wipes [49]. Plasma cleaning has shown particularly good results. Exposing the electrode to plasma effectively cleans the surface [47]. Oxygen plasma is most often used, but argon or air can also be used. Plasma interacts with the surface of the electrode. Highly energetic particles such as ions, electrons, and radicals in the plasma react with the surface of the material. These interactions can result in the introduction of polar functional groups onto the surface, making it more hydrophilic. The hydrophilic surface created after plasma cleaning can promote the hydration of the solid lipid film, leading to the formation of lipid bilayers that eventually curve and form vesicles [47].

In the traditional electroformation protocol, lipids dissolved in an organic solvent are deposited onto the electrode by simply dropping the solution onto the surface, followed by solvent evaporation, which leaves behind a dry lipid film [26,54]. In our previous work using atomic force microscopy, we demonstrated that an optimal lipid film thickness of approximately 30-60 nm is required for the successful formation of GUVs [55]. However, the drop deposition method often results in a film of uneven thickness, with some areas being too thick or too thin, leading to low yield and poor reproducibility.

To improve the deposition process, researchers have tested various approaches. Some have used needles or rods to spread the lipid solution across the electrode surface after drop deposition

[47,56,57]. Dip coating, where the ITO-coated glass is immersed in the lipid solution, has also been explored. Variations in solvent evaporation rates during drying can cause non-uniform lipid films due to surface tension differences, temperature, or solvent concentration gradients. These variations can lead to the formation of an inhomogeneous lipid film [58].

Today, spin-coating is a widely used method for reproducible lipid deposition [58]. In this technique, the lipid solution is applied to a flat electrode, which is then spun at high speed to create a uniform lipid film. The uniformity of the lipid layer has been confirmed by atomic force microscopy and ellipsometry [55,58]. However, spin-coating requires a larger volume of lipid solution, as some material is lost during the process.

For complete drying of the lipid film, electrodes are usually placed under vacuum to evaporate the solvent. Alternatively, drying can be achieved using a flow of inert gas, such as nitrogen or argon. Lyophilization is another option for solvent removal [59].

Researchers have also modified the lipid deposition method by using an aqueous solution of LUVs or SUVs instead of lipids dissolved in an organic solvent [60–64]. This approach has been shown to improve GUV formation, likely due to the formation of well-oriented membrane stacks after water evaporation [60]. Although they completely removed the excess water from the deposits, an alternative approach was proposed in which the deposits were only partially dehydrated before the addition of the internal solution. Baykal-Caglar et al. further investigated the impact of using damp lipid films on the properties of GUV [31]. They concluded that a more uniform composition of GUVs was achieved in this way. This was explained by preventing lipid demixing, which can occur when the lipids are completely dried. Lipid demixing is particularly pronounced in lipid mixtures with a high Chol content (close to or above the CSAT) [65].

Using electroformation, electrical parameters must also be adjusted to achieve a high yield of GUVs. Most of the research groups chose voltage and frequency values from Angelova et al. or Veatch protocol, where voltage is adjusted between 1 to 10 V and frequency around 10 Hz [54,56]. The knowledge of the thickness of the electroformation chamber is essential for accuracy in electric field calculation. Commonly a spacer is positioned between electrodes and has thickness from 0.5 to 3 mm. In combination with ITO electrodes, polytetrafluoroethylene (Teflon) or silicon are used as spacers [47,49,52,54,56,61,62]. Some groups provide direct information on the electric field value instead of voltage [49,53,60].

In previous research our group tested various electric parameters for a binary mixture of 1-palmitoyl-2-oleoyl-sn-glycero-3-phosphocholine (POPC)/Chol and a ternary mixture of POPC/sphingomyelin/Chol. A broad range of frequency and voltage combinations was explored: 10–10,000 Hz and 1–15 V peak-to-peak for low and high Chol content [49,55]. The optimal

frequency and voltage combinations were found to be in the ranges of 2–6 V and 10–100 Hz, using a 1.6 mm spacer thickness.

When saline buffers are used as internal solution, higher frequency and voltage should be applied [47,60,66]. The high ionic strength of these solutions hinders the separation of lamellae and increases the normal forces needed for the lipid film to swell into liposomes [47]. Some groups have used 500 Hz frequency and successfully formed GUVs in saline solution [60,66]. Li et al. systematically tested electrical parameters, varying voltage from 1 to 20 V and frequency from 1 Hz to 100 kHz for different lipid compositions, finding that frequency of around 1 kHz was generally the most effective [47]. Frequencies in the kHz range are favoured for GUV formation in saline solutions as they help suppress the formation of the electric double layer.

Pot et al. proposed a gradual approach to alternate the voltage during electroformation [60]. Initially, the voltage is progressively increased to the maximum value at a fixed frequency. In the second step, the voltage and frequency are maintained at the maximum values, during which GUV swelling occurs. In the third step, the voltage is kept constant while the frequency is decreased to promote vesicle fusion and the detachment of lipids from the electrodes.

The traditional electroformation protocol encounters difficulties when forming GUVs with high Chol content. The most problematic step is during the lipid drying process. As the lipid film dries, Chol tends to form anhydrous crystals, which do not integrate into the bilayer during rehydration, resulting in a lower Chol content in the bilayers than in the initial mixture [12,65].

A study using confocal microscopy highlighted Chol demixing in GUVs formed from a Chol and POPC mixture using the traditional electroformation method, which involves a dry lipid film step. CBDs were observed only when the Chol content exceeded 75 mol%, rather than at the expected 50 mol% [12].

To address the issue of Chol demixing, Buboltz and Feigenson introduced a novel approach for vesicle preparation known as rapid solvent exchange (RSE) [67,68]. In this method, lipids dissolved in an organic solvent are mixed with an aqueous solution. The mixture is subjected to vortexing and a low-pressure environment that is sufficient to evaporate the organic solvent while water was not evaporated. During this process an inert gas flow can be applied to accelerate the evaporation of the organic solvent. Once the organic solvent is completely evaporated, an aqueous solution of MLVs is obtained. Our group confirmed, using attenuated total reflectance-Fourier transform infrared spectroscopy, that the resulting MLV solution contained no traces of organic solvent [61].
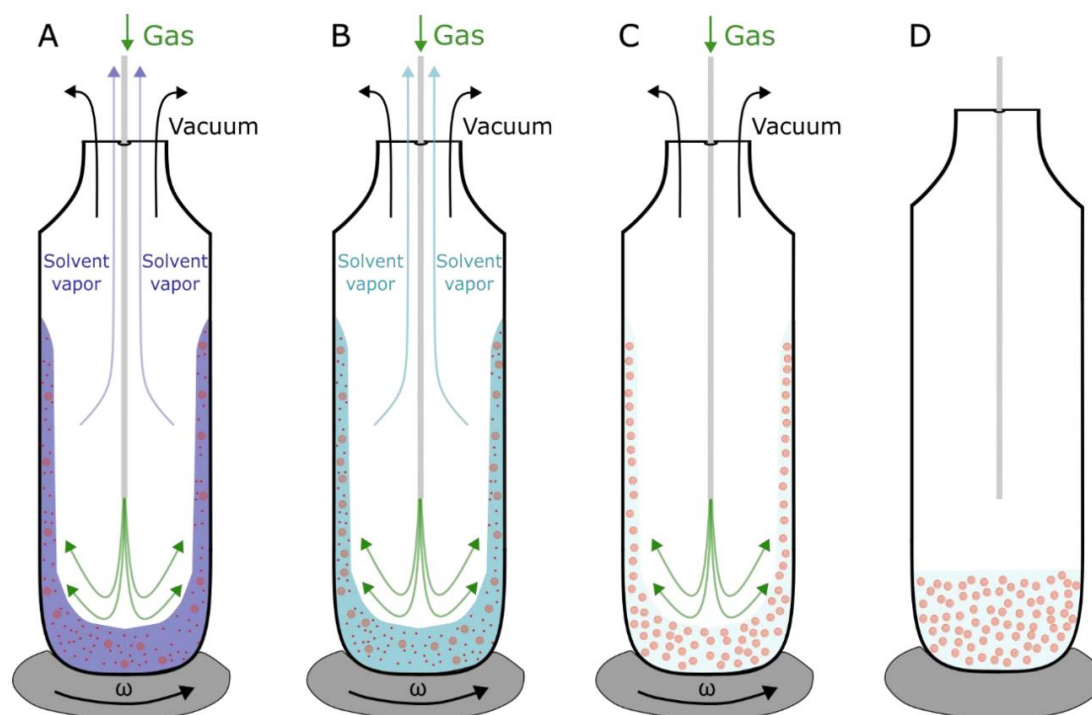
Figure 5. Schematic depiction of the rapid solvent exchange method. A) Organic solvent (blue) containing lipids (red) is mixed with an aqueous solution, and removal is achieved by vortexing the solution under vacuum. The process can be made more efficient by adding a flow of inert gas (green) pushing the organic solvent vapors out. B) MLVs start to form. The vacuum pressure is set below the organic solvent evaporation point, but higher than the evaporation point of water. C) Exchange is finished when all the organic solution is evaporated and only aqueous solution containing formed MLVs is left. D) When MLVs are formed vortex is turned off, and vacuum and gas flow pipes are closed. Figure taken from [21].

The RSE method effectively avoids Chol demixing. Electron paramagnetic resonance studies on MLVs prepared through RSE demonstrated that CBDs begin to form at 50 mol% Chol in a Chol/phospholipid mixture [22,69]. This finding contrasts the traditional methods, where the initial lipid mixture requires a higher Chol content to detect CBDs, highlighting the significant Chol demixing that occurs during the lipid film drying step.

AIMS AND SCOPES OF THE THESIS

The long term aim of this thesis is to investigate the properties of CBDs. We believe that unique structure and properties of CBDs are still underappreciated in membrane research. Motivated by this, we decided to conduct detailed literature search and write a review article about all membrane models and experimental methods suitable for studying properties of CBD domains.

Producing lipid membranes with high Chol content, as suitable models for this research, was challenging. In our first paper, we focused on protocols for producing various liposomes and SLBs that can provide insights into the key properties of CBDs. Additionally, we presented different experimental techniques that allow detection of CBDs in both model and intact membranes. For liposome research, saturation recovery electron paramagnetic resonance and fluorescence microscopy provided the most significant results regarding CBD properties. For detection of CBDs in SLBs, atomic force microscopy, fluorescence microscopy, and X-ray diffraction provided significant results. We listed all known properties of CBDs and their functions in biological membranes. The primary focus was on the beneficial roles of CBDs in fiber cell plasma membranes of the eye lens. The presence of CBDs enables the bilayer to become saturated with Chol, maintaining consistent physical properties of the eye lens despite the drastic changes in lipid composition that occur with aging. Another important function of CBDs is enhancing the membrane's hydrophobic and oxygen barrier, thereby reducing the likelihood of oxidative stress that enables cataract development. Finally, the smoothing of the membrane surface by the saturating content of Chol should decrease the light scattering and help to maintain the lens transparency. Most of these properties were also confirm by molecular dynamic simulations.

The goal of this thesis was to study the properties of the lipid portion of fiber cell plasma membranes of the eye lens. These membranes not only contain high Chol content, in which CBDs form, but also contain significant amounts of sphingolipids and some charged lipids. In order to produce a membrane model suitable for investigating these unique properties under controlled conditions, in our second and third paper, we optimized and modified the electroformation protocol for GUVs production. As a final result we achieved a high yield of vesicles by making several changes to the traditional protocol even when Chol content was high.

The first issue was the drop deposition method, which resulted in low reproducibility and a lower yield of GUVs. The second problem arose from drying the lipid film when using lipid mixtures with high Chol content. Complete evaporation of the lipid film led to the formation of Chol anhydrous crystals, which do not integrate into the bilayer, thereby reducing the Chol content in the bilayer compared to the initial lipid mixture. Additionally, producing GUVs with charged

lipids in ionic solutions proved problematic. Incorporating charged lipids can destabilize the membrane by reducing membrane edge tension, leading to vesicle collapse. Furthermore, using ionic solutions hinders the separation of lamellae and increases the value of forces required for the bilayers to swell and form vesicles from the lipid film.

To address these challenges, we modified the traditional electroformation protocol to reproducibly produce GUVs with high Chol content, charged lipids and in ionic solutions. Our modified protocol combines the traditional method with the use of damp lipid films (Figure 6). This protocol was developed by our group in previous research, but was not optimized. In first experimental article used in this thesis, we optimized protocol. We used a binary mixture of POPC and Chol. Chol/POPC mixing ratio ranged between 0 and 2.5. To prevent drying of the lipid film, we incorporated the RSE method to create an aqueous solution of MLVs. This solution was then extruded to produce LUVs. The electrode was plasma-treated to enhance hydrophilicity. Inspired by the vesicle fusion technique used for preparing SLBs, we deposited the LUV solution onto the electrode. During LUV deposition, we employed the spin-coating method in order to obtain homogeneous and damp lipid film. Various spin durations were tested. We found that 30 seconds at angular velocity of 600 rpm was optimal for mixtures of Chol and POPC. Shorter spin durations resulted in uneven film thickness or films that were too wet, leading to poor reproducibility. Longer spin durations risked drying the lipid film and inducing Chol demixing artifacts. After spin-coating, the electrode with the damp lipid film was used to assemble the electroformation chamber that was filled with aqueous solution. This chamber was connected to an alternating electric field generator. Under the influence of osmotic pressure and the electric field, the lipids detached from the electrode and formed GUVs.

Using this protocol, we tested the deposition of different vesicle types with high Chol content to maximize GUV yield. We compared MLVs formed using the RSE method, LUVs obtained by extruding MLVs through 100 nm membrane pores (LUV 100), and LUVs produced by an additional extrusion of LUV 100 through 50 nm pores (LUV 50). Although all vesicle types resulted in a high yield of GUVs, the deposition of LUV 100 provided the most reproducible results. We initially expected LUV 50 to yield the highest results, as smaller vesicles tend to rupture more easily. However, challenges arose with LUVs containing high Chol, as they were more rigid and exhibited higher flow resistance during extrusion, often resulting in the solution leakage. As anticipated, the deposition of MLVs resulted in lower reproducibility due to the variable sizes of the MLVs.
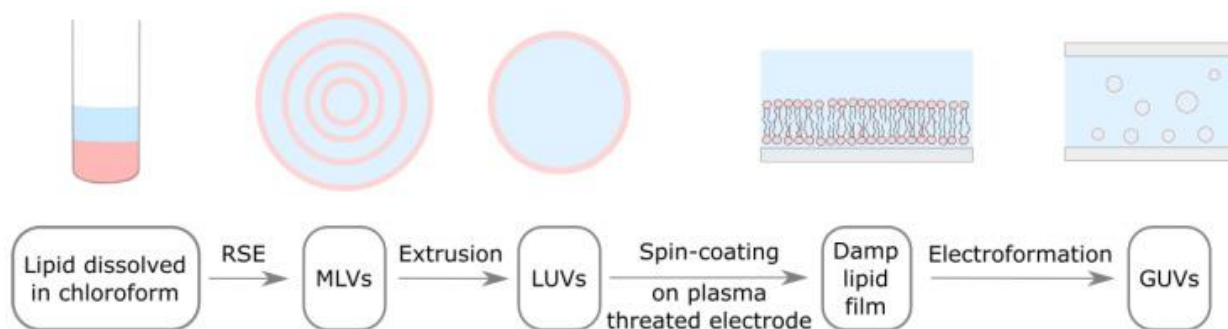
Figure 6. Adapted electroformation protocol. Lipids dissolved in organic solvent (pink) are mixed with an aqueous solution (light blue). MLVs are formed using the RSE method. MLV solution is extruded through a filter with membrane pores in order to obtain LUVs. LUV solution is spin-coated on a plasma threated electrode, where these vesicle rupture and form a damp lipid film. An electrode with damp lipid film is used to build an electroformation chamber, where lipid bilayers detach and form GUVs under the influence of osmotic pressure and an alternating electric field. Figure taken from [62].

The challenges encountered during the extrusion of vesicles with high Chol content led us to further modify the electroformation protocol. In the third article included in this thesis, we replaced the extrusion step with sonication (Figure 7) [70]. One of the primary advantages of sonication is its simplicity and convenience, requiring only one manual step: submerging a sonicator tip into the MLV suspension. Additionally, sonication is more cost-effective in the long run, as it eliminates the need for disposable filters required in the extrusion process.

We first optimized the sonication process for vesicles with high Chol content. After fine-tuning the sonication conditions, we tested the modified protocol using lipid mixtures with very high Chol content, charged lipids 1-palmitoyl-2-oleoyl-sn-glycero-3-phospho-L-serine (POPS), and saline solutions (NaCl solution). Our results were comparable to, or even better than, those reported in other studies that have tested GUV electroformation under similar conditions.
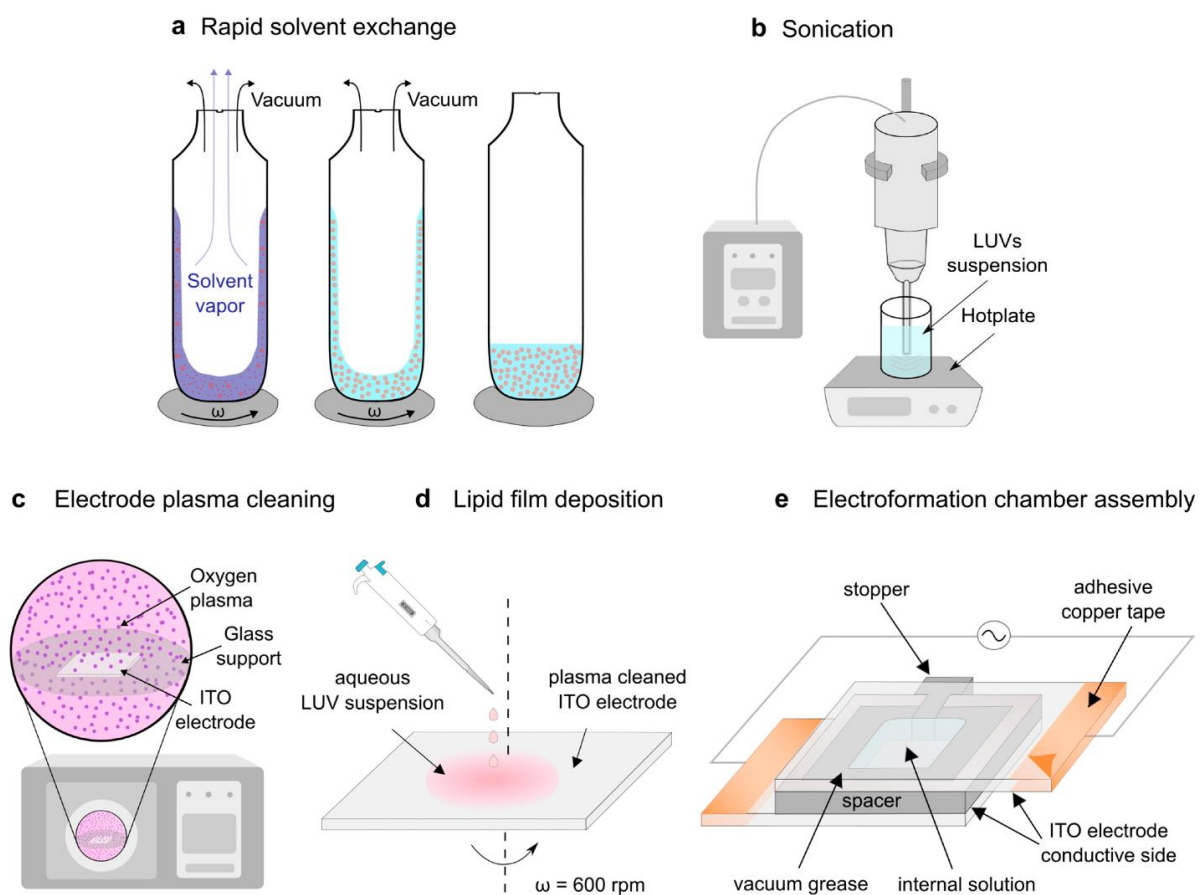
Figure 7. The modified protocol of electroformation of GUVs from a damp lipid film. (a) The RSE method is used to produce an MLV solution. An organic solvent (blue) containing lipids (red) is mixed with an aqueous solution (tube 1). The organic solvent is removed by vortexing the solution under vacuum in order to form MLVs (tube 3). (b) The suspension of MLVs is sonicated to produce LUVs. (c) A plasma cleaner is used to hydrophilize the ITO electrode. (d) The LUV suspension is deposited onto a plasma-cleaned ITO-coated glass and spin-coated to obtain a damp lipid film. (e) The coated electrode is used to assemble the electroformation chamber and connected to a voltage source to enable the growth of GUVs. Figure taken from [70].

This newly improved electroformation protocol will enable the effective study of fiber cell plasma membranes of the eye lens, which are known for their exceptionally high Chol content and significant amounts of sphingomyelin and some charged lipids. Additionally, by eliminating the drying phase, our protocol is expected to be more suitable for incorporating proteins into GUVs, while also minimizing the risk of protein denaturation [63].

REFERENCE

1. Harayama, T.; Riezman, H. Understanding the Diversity of Membrane Lipid Composition. *Nat. Rev. Mol. Cell Biol.* **2018**, *19*, 281–296, doi:10.1038/nrm.2017.138.

2. Nicolson, G.L. The Fluid—Mosaic Model of Membrane Structure: Still Relevant to Understanding the Structure, Function and Dynamics of Biological Membranes after More than 40years. *Biochim. Biophys. Acta - Biomembr.* **2014**, *1838*, 1451–1466, doi:10.1016/j.bbamem.2013.10.019.

3. Casares, D.; Escribá, P. V.; Rosselló, C.A. Membrane Lipid Composition: Effect on Membrane and Organelle Structure, Function and Compartmentalization and Therapeutic Avenues. *Int. J. Mol. Sci.* **2019**, *20*, 2167, doi:10.3390/ijms20092167.

4. Harder, T. Formation of Functional Cell Membrane Domains: The Interplay of Lipid– and Protein–Mediated Interactions. *Philos. Trans. R. Soc. London. Ser. B Biol. Sci.* **2003**, *358*, 863–868, doi:10.1098/rstb.2003.1274.

5. Gupta, A.; Phang, I.Y.; Wohland, T. To Hop or Not to Hop: Exceptions in the FCS Diffusion Law. *Biophys. J.* **2020**, *118*, 2434–2447, doi:10.1016/j.bpj.2020.04.004.

6. Incardona, J.P.; Eaton, S. Cholesterol in Signal Transduction. *Curr. Opin. Cell Biol.* **2000**, *12*, 193–203, doi:10.1016/S0955-0674(99)00076-9.

7. Róg, T.; Pasenkiewicz-Gierula, M.; Vattulainen, I.; Karttunen, M. Ordering Effects of Cholesterol and Its Analogues. *Biochim. Biophys. Acta - Biomembr.* **2009**, *1788*, 97–121, doi:10.1016/j.bbamem.2008.08.022.

8. Simons, K.; Toomre, D. Lipid Rafts and Signal Transduction. *Nat. Rev. Mol. Cell Biol.* **2000**, *1*, 31–39, doi:10.1038/35036052.

9. Viola, A. The Amplification of TCR Signaling by Dynamic Membrane Microdomains. *Trends Immunol.* **2001**, *22*, 322–327, doi:10.1016/S1471-4906(01)01938-X.

10. Simons, K.; Ikonen, E. Functional Rafts in Cell Membranes. *Nature* **1997**, *387*, 569–572, doi:10.1038/42408.

11. Kusumi, A.; Fujiwara, T.K.; Tsunoyama, T.A.; Kasai, R.S.; Liu, A.; Hirosawa, K.M.; Kinoshita, M.; Matsumori, N.; Komura, N.; Ando, H.; et al. Defining Raft Domains in the Plasma Membrane. *Traffic* **2020**, *21*, 106–137, doi:10.1111/tra.12718.

12. Raguz, M.; Kumar, S.N.; Zareba, M.; Ilic, N.; Mainali, L.; Subczynski, W.K. Confocal Microscopy Confirmed That in Phosphatidylcholine Giant Unilamellar Vesicles with Very

High Cholesterol Content Pure Cholesterol Bilayer Domains Form. *Cell Biochem. Biophys.* **2019**, *77*, 309–317, doi:10.1007/s12013-019-00889-y.

13. Widomska, J.; Subczynski, W.K.; Mainali, L.; Raguz, M. Cholesterol Bilayer Domains in the Eye Lens Health: A Review. *Cell Biochem. Biophys.* **2017**, *75*, 387–398, doi:10.1007/s12013-017-0812-7.

14. Widomska, J.; Subczynski, W.K. Why Is Very High Cholesterol Content Beneficial for the Eye Lens but Negative for Other Organs? *Nutrients* **2019**, *11*, 1083, doi:10.3390/nu11051083.

15. Mainali, L.; Raguz, M.; O'Brien, W.J.; Subczynski, W.K. Properties of Membranes Derived from the Total Lipids Extracted from the Human Lens Cortex and Nucleus. *Biochim. Biophys. Acta - Biomembr.* **2013**, *1828*, 1432–1440, doi:10.1016/j.bbamem.2013.02.006.

16. Subczynski, W.K.; Pasenkiewicz-Gierula, M.; Widomska, J.; Mainali, L.; Raguz, M. High Cholesterol/Low Cholesterol: Effects in Biological Membranes: A Review. *Cell Biochem. Biophys.* **2017**, *75*, 369–385, doi:10.1007/s12013-017-0792-7.

17. Subczynski, W.K.; Raguz, M.; Widomska, J.; Mainali, L.; Konovalov, A. Functions of Cholesterol and the Cholesterol Bilayer Domain Specific to the Fiber-Cell Plasma Membrane of the Eye Lens. *J. Membr. Biol.* **2012**, *245*, 51–68, doi:10.1007/s00232-011-9412-4.

18. Plesnar, E.; Subczynski, W.K.; Pasenkiewicz-Gierula, M. Saturation with Cholesterol Increases Vertical Order and Smoothes the Surface of the Phosphatidylcholine Bilayer: A Molecular Simulation Study. *Biochim. Biophys. Acta - Biomembr.* **2012**, *1818*, 520–529, doi:10.1016/j.bbamem.2011.10.023.

19. Preston Mason, R.; Tulenko, T.N.; Jacob, R.F. Direct Evidence for Cholesterol Crystalline Domains in Biological Membranes: Role in Human Pathobiology. *Biochim. Biophys. Acta - Biomembr.* **2003**, *1610*, 198–207, doi:10.1016/S0005-2736(03)00018-X.

20. Mainali, L.; Raguz, M.; O'Brien, W.J.; Subczynski, W.K. Properties of Membranes Derived from the Total Lipids Extracted from Clear and Cataractous Lenses of 61–70-Year-Old Human Donors. *Eur. Biophys. J.* **2015**, *44*, 91–102, doi:10.1007/s00249-014-1004-7.

21. Mardešić, I.; Boban, Z.; Subczynski, W.K.; Raguz, M. Membrane Models and Experiments Suitable for Studies of the Cholesterol Bilayer Domains. *Membranes (Basel).* **2023**, *13*, doi:10.3390/membranes13030320.

22. Mainali, L.; Raguz, M.; Subczynski, W.K. Formation of Cholesterol Bilayer Domains

Precedes Formation of Cholesterol Crystals in
Cholesterol/Dimyristoylphosphatidylcholine Membranes: EPR and DSC Studies. *J. Phys. Chem. B* **2013**, *117*, 8994–9003, doi:10.1021/jp402394m.

23. Deeley, J.M.; Mitchell, T.W.; Wei, X.; Korth, J.; Nealon, J.R.; Blanksby, S.J.; Truscott, R.J.W. Human Lens Lipids Differ Markedly from Those of Commonly Used Experimental Animals. *Biochim. Biophys. Acta - Mol. Cell Biol. Lipids* **2008**, *1781*, 288–298, doi:10.1016/j.bbalip.2008.04.002.

24. Ertel, A.; Marangoni, A.G.; Marsh, J.; Hallett, F.R.; Wood, J.M. Mechanical Properties of Vesicles. I. Coordinated Analysis of Osmotic Swelling and Lysis. *Biophys. J.* **1993**, *64*, 426–434, doi:10.1016/S0006-3495(93)81383-3.

25. Buzás, E.I.; Tóth, E.Á.; Sódar, B.W.; Szabó-Taylor, K.É. Molecular Interactions at the Surface of Extracellular Vesicles. *Semin. Immunopathol.* **2018**, *40*, 453–464, doi:10.1007/s00281-018-0682-0.

26. Menger, F.M.; Angelova, M.I. Giant Vesicles: Imitating the Cytological Processes of Cell Membranes. *Acc. Chem. Res.* **1998**, *31*, 789–797, doi:10.1021/ar970103v.

27. Chacko, I.A.; Ghate, V.M.; Dsouza, L.; Lewis, S.A. Lipid Vesicles: A Versatile Drug Delivery Platform for Dermal and Transdermal Applications. *Colloids Surfaces B Biointerfaces* **2020**, *195*, 111262, doi:10.1016/j.colsurfb.2020.111262.

28. Mihailescu, M.; Krepkiy, D.; Milescu, M.; Gawrisch, K.; Swartz, K.J.; White, S. Structural Interactions of a Voltage Sensor Toxin with Lipid Membranes. *Proc. Natl. Acad. Sci.* **2014**, *111*, 5463–5470, doi:10.1073/pnas.1415324111.

29. Karal, M.A.S.; Ahammed, S.; Levadny, V.; Belaya, M.; Ahamed, M.K.; Ahmed, M.; Mahbub, Z. Bin; Ullah, A.K.M.A. Deformation and Poration of Giant Unilamellar Vesicles Induced by Anionic Nanoparticles. *Chem. Phys. Lipids* **2020**, *230*, 104916, doi:10.1016/j.chemphyslip.2020.104916.

30. Akbarzadeh, A.; Rezaei-Sadabady, R.; Davaran, S.; Joo, S.W.; Zarghami, N.; Hanifehpour, Y.; Samiei, M.; Kouhi, M.; Nejati-Koshki, K. Liposome: Classification, Preparation, and Applications. *Nanoscale Res. Lett.* **2013**, *8*, 102, doi:10.1186/1556-276X-8-102.

31. Baykal-Caglar, E.; Hassan-Zadeh, E.; Saremi, B.; Huang, J. Preparation of Giant Unilamellar Vesicles from Damp Lipid Film for Better Lipid Compositional Uniformity. *Biochim. Biophys. Acta - Biomembr.* **2012**, *1818*, 2598–2604, doi:10.1016/j.bbamem.2012.05.023.

32. Lind, T.K.; Cárdenas, M. Understanding the Formation of Supported Lipid Bilayers via

Vesicle Fusion—A Case That Exemplifies the Need for the Complementary Method Approach (Review). *Biointerphases* **2016**, *11*, 020801, doi:10.1116/1.4944830.

33. Tero, R. Substrate Effects on the Formation Process, Structure and Physicochemical Properties of Supported Lipid Bilayers. *Materials (Basel).* **2012**, *5*, 2658–2680, doi:10.3390/ma5122658.

34. Richter, R.P.; Bérat, R.; Brisson, A.R. Formation of Solid-Supported Lipid Bilayers: An Integrated View. *Langmuir* **2006**, *22*, 3497–3505, doi:10.1021/la052687c.

35. Khadka, N.K.; Timsina, R.; Rowe, E.; O'Dell, M.; Mainali, L. Mechanical Properties of the High Cholesterol-Containing Membrane: An AFM Study. *Biochim. Biophys. Acta - Biomembr.* **2021**, *1863*, 183625, doi:10.1016/j.bbamem.2021.183625.

36. Ziblat, R.; Fargion, I.; Leiserowitz, L.; Addadi, L. Spontaneous Formation of Two-Dimensional and Three-Dimensional Cholesterol Crystals in Single Hydrated Lipid Bilayers. *Biophys. J.* **2012**, *103*, 255–264, doi:10.1016/j.bpj.2012.05.025.

37. Ziblat, R.; Leiserowitz, L.; Addadi, L. Crystalline Lipid Domains: Characterization by X-Ray Diffraction and Their Relation to Biology. *Angew. Chemie Int. Ed.* **2011**, *50*, 3620–3629, doi:10.1002/anie.201004470.

38. Litz, J.P.; Thakkar, N.; Portet, T.; Keller, S.L. Depletion with Cyclodextrin Reveals Two Populations of Cholesterol in Model Lipid Membranes. *Biophys. J.* **2016**, *110*, 635–645, doi:10.1016/j.bpj.2015.11.021.

39. Cho, N.J.; Frank, C.W.; Kasemo, B.; Höök, F. Quartz Crystal Microbalance with Dissipation Monitoring of Supported Lipid Bilayers on Various Substrates. *Nat. Protoc.* **2010**, *5*, 1096–1106, doi:10.1038/nprot.2010.65.

40. Jackman, J.A.; Cho, N.-J. Supported Lipid Bilayer Formation: Beyond Vesicle Fusion. *Langmuir* **2020**, *36*, 1387–1400, doi:10.1021/acs.langmuir.9b03706.

41. Lind, T.K.; Cárdenas, M.; Wacklin, H.P. Formation of Supported Lipid Bilayers by Vesicle Fusion: Effect of Deposition Temperature. *Langmuir* **2014**, *30*, 7259–7263, doi:10.1021/la500897x.

42. Tabaei, S.R.; Choi, J.; Haw Zan, G.; Zhdanov, V.P.; Cho, N. Solvent-Assisted Lipid Bilayer Formation on Silicon Dioxide and Gold. *Langmuir* **2014**, *30*, 10363–10373, doi:10.1021/la501534f.

43. Tabaei, S.R.; Jackman, J.A.; Kim, S.-O.; Liedberg, B.; Knoll, W.; Parikh, A.N.; Cho, N. Formation of Cholesterol-Rich Supported Membranes Using Solvent-Assisted Lipid Self-Assembly. *Langmuir* **2014**, *30*, 13345–13352, doi:10.1021/la5034433.

44. Reeves, J.P.; Dowben, R.M. Formation and Properties of Thin-Walled Phospholipid

Vesicles. *J. Cell. Physiol.* **1969**, *73*, 49–60, doi:10.1002/jcp.1040730108.

45. Angelova, M.I.; Dimitrov, D.S. Liposome Electroformation. *Faraday Discuss. Chem. Soc.* **1986**, *81*, 303, doi:10.1039/dc9868100303.

46. Dimitrov, D.S.; Angelova, M.I. Lipid Swelling and Liposome Formation on Solid Surfaces in External Electric Fields. In *New Trends in Colloid Science*; Steinkopff: Darmstadt, 1987; Vol. 56, pp. 48–56.

47. Li, Q.; Wang, X.; Ma, S.; Zhang, Y.; Han, X. Electroformation of Giant Unilamellar Vesicles in Saline Solution. *Colloids Surfaces B Biointerfaces* **2016**, *147*, 368–375, doi:10.1016/j.colsurfb.2016.08.018.

48. Herold, C.; Chwastek, G.; Schwille, P.; Petrov, E.P. Efficient Electroformation of Supergiant Unilamellar Vesicles Containing Cationic Lipids on ITO-Coated Electrodes. *Langmuir* **2012**, *28*, 5518–5521, doi:10.1021/la3005807.

49. Boban, Z.; Puljas, A.; Kovač, D.; Subczynski, W.K.; Raguz, M. Effect of Electrical Parameters and Cholesterol Concentration on Giant Unilamellar Vesicles Electroformation. *Cell Biochem. Biophys.* **2020**, *78*, 157–164, doi:10.1007/s12013-020-00910-9.

50. Pereno, V.; Carugo, D.; Bau, L.; Sezgin, E.; Bernardino De La Serna, J.; Eggeling, C.; Stride, E. Electroformation of Giant Unilamellar Vesicles on Stainless Steel Electrodes. **2017**, doi:10.1021/acsomega.6b00395.

51. Behuria, H.G.; Biswal, B.K.; Sahu, S.K. Electroformation of Liposomes and Phytosomes Using Copper Electrode. *J. Liposome Res.* **2021**, *31*, 255–266, doi:10.1080/08982104.2020.1800729.

52. Ayuyan, A.G.; Cohen, F.S. Lipid Peroxides Promote Large Rafts: Effects of Excitation of Probes in Fluorescence Microscopy and Electrochemical Reactions during Vesicle Formation. *Biophys. J.* **2006**, *91*, 2172–2183, doi:10.1529/biophysj.106.087387.

53. Politano, T.J.; Froude, V.E.; Jing, B.; Zhu, Y. AC-Electric Field Dependent Electroformation of Giant Lipid Vesicles. *Colloids Surfaces B Biointerfaces* **2010**, *79*, 75–82, doi:10.1016/j.colsurfb.2010.03.032.

54. Angelova, M.I.; Dimitrov, D.S. Liposome Electro Formation. **1986**, 303–311.

55. Boban, Z.; Mardešić, I.; Subczynski, W.K.; Jozić, D.; Raguz, M. Optimization of Giant Unilamellar Vesicle Electroformation for Phosphatidylcholine/Sphingomyelin/Cholesterol Ternary Mixtures. *Membranes (Basel).* **2022**, *12*, 525, doi:10.3390/membranes12050525.

56. Veatch, S.L. Electro-Formation and Fluorescence Microscopy of Giant Vesicles With Coexisting Liquid Phases. In; 2007; Vol. 398, pp. 59–72.

57. Ghellab, S.E.; Mu, W.; Li, Q.; Han, X. Prediction of the Size of Electroformed Giant Unilamellar Vesicle Using Response Surface Methodology. *Biophys. Chem.* **2019**, doi:10.1016/j.bpc.2019.106217.

58. Estes, D.J.; Mayer, M. Electroformation of Giant Liposomes from Spin-Coated Films of Lipids. *Colloids Surfaces B Biointerfaces* **2005**, *42*, 115–123, doi:10.1016/j.colsurfb.2005.01.016.

59. Bagatolli, L.A.; Parasassi, T.; Gratton, E. Giant Phospholipid Vesicles: Comparison among the Whole Lipid Sample Characteristics Using Different Preparation Methods - A Two Photon Fluorescence Microscopy Study. *Chem. Phys. Lipids* **2000**, *105*, 135–147, doi:10.1016/S0009-3084(00)00118-3.

60. Pott, T.; Bouvrais, H.; Méléard, P. Giant Unilamellar Vesicle Formation under Physiologically Relevant Conditions. *Chem. Phys. Lipids* **2008**, *154*, 115–119, doi:10.1016/j.chemphyslip.2008.03.008.

61. Boban, Z.; Mardešić, I.; Jozić, S.P.; Šumanovac, J.; Subczynski, W.K.; Raguz, M. Electroformation of Giant Unilamellar Vesicles from Damp Lipid Films Formed by Vesicle Fusion. *Membranes (Basel).* **2023**, *13*, 352, doi:10.3390/membranes13030352.

62. Mardešić, I.; Boban, Z.; Raguz, M. Electroformation of Giant Unilamellar Vesicles from Damp Lipid Films with a Focus on Vesicles with High Cholesterol Content. *Membranes (Basel).* **2024**, *14*, 79, doi:10.3390/membranes14040079.

63. Girard, P.; Pécréaux, J.; Lenoir, G.; Falson, P.; Rigaud, J.L.; Bassereau, P. A New Method for the Reconstitution of Membrane Proteins into Giant Unilamellar Vesicles. *Biophys. J.* **2004**, *87*, 419–429, doi:10.1529/biophysj.104.040360.

64. Oropeza-Guzman, E.; Riós-Ramírez, M.; Ruiz-Suárez, J.C. Leveraging the Coffee Ring Effect for a Defect-Free Electroformation of Giant Unilamellar Vesicles. *Langmuir* **2019**, *35*, 16528–16535, doi:10.1021/acs.langmuir.9b02488.

65. Huang, J.; Feigenson, G.W. A Microscopic Interaction Model of Maximum Solubility of Cholesterol in Lipid Bilayers. *Biophys. J.* **1999**, *76*, 2142–2157, doi:10.1016/S0006-3495(99)77369-8.

66. Lefrançois, P.; Goudeau, B.; Arbault, S. Electroformation of Phospholipid Giant Unilamellar Vesicles in Physiological Phosphate Buffer. *Integr. Biol. (United Kingdom)* **2018**, *10*, 429–434, doi:10.1039/c8ib00074c.

67. Buboltz, J.T.; Feigenson, G.W. A Novel Strategy for the Preparation of Liposomes : Rapid Solvent Exchange. *Biochim. Biophys. Acta - Biomembr.* **1999**, *1417*, 232–245.

68. Buboltz, J.T. A More Efficient Device for Preparing Model-Membrane Liposomes by the

Rapid Solvent Exchange Method. *Rev. Sci. Instrum.* **2009**, *80*, 124301, doi:10.1063/1.3264073.

69. Mainali, L.; Pasenkiewicz-Gierula, M.; Subczynski, W.K. Formation of Cholesterol Bilayer Domains Precedes Formation of Cholesterol Crystals in Membranes Made of the Major Phospholipids of Human Eye Lens Fiber Cell Plasma Membranes. *Curr. Eye Res.* **2020**, *45*, 162–172, doi:10.1080/02713683.2019.1662058.

70. Mardešić, I.; Boban, Z.; Raguz, M. Electroformation of Giant Unilamellar Vesicles from Damp Films in Conditions Involving High Cholesterol Contents, Charged Lipids, and Saline Solutions. Membranes 2024, 14, 215. https://doi.org/10.3390/membranes14100215

5. Membrane Models and Experiments Suitable for Studies of the Cholesterol Bilayer Domains

Membrane Models and Experiments Suitable for Studies of the Cholesterol Bilayer Domains

Ivan Mardešić [1,2], Zvonimir Boban [1,2], Witold Karol Subczynski [3] and Marija Raguz [1,*]

1 Department of Medical Physics and Biophysics, University of Split School of Medicine, 21000 Split, Croatia; imardesi@mefst.hr (I.M.); zvonimir.boban@mefst.hr (Z.B.)
2 Faculty of Science, University of Split, Doctoral Study of Biophysics, 21000 Split, Croatia
3 Department of Biophysics, Medical College of Wisconsin, Milwaukee, WI 53226, USA; subczyn@mcw.edu
* Correspondence: marija.raguz@mefst.hr; Tel.: +385-9876-8819

Abstract: Cholesterol (Chol) is an essential component of animal cell membranes and is most abundant in plasma membranes (PMs) where its concentration typically ranges from 10 to 30 mol%. However, in red blood cells and Schwann cells, PMs Chol content is as high as 50 mol%, and in the PMs of the eye lens fiber cells, it can reach up to 66 mol%. Being amphiphilic, Chol molecules are easily incorporated into the lipid bilayer where they affect the membrane lateral organization and transmembrane physical properties. In the aqueous phase, Chol cannot form free bilayers by itself. However, pure Chol bilayer domains (CBDs) can form in lipid bilayer membranes with the Chol content exceeding 50 mol%. The range of Chol concentrations surpassing 50 mol% is less frequent in biological membranes and is consequently less investigated. Nevertheless, it is significant for the normal functioning of the eye lens and understanding how Chol plaques form in atherosclerosis. The most commonly used membrane models are unilamellar and multilamellar vesicles (MLVs) and supported lipid bilayers (SLBs). CBDs have been observed directly using confocal microscopy, X-ray reflectometry and saturation recovery electron paramagnetic resonance (SR EPR). Indirect evidence of CBDs has also been reported by using atomic force microscopy (AFM) and fluorescence recovery after photobleaching (FRAP) experiments. The overall goal of this review is to demonstrate the advantages and limitations of the various membrane models and experimental techniques suitable for the detection and investigation of the lateral organization, function and physical properties of CBDs.

Keywords: plasma membrane; cholesterol; phospholipids; liposomes; supported lipid bilayer; cholesterol bilayer domains; cholesterol crystals; saturation recovery electron paramagnetic resonance; atomic force microscopy; X-ray diffraction

1. Introduction

A plasma membrane (PM) is a complex structure that separates the cell from its environment. It contains different lipids, mostly phospholipids (PLs), sphingolipids and cholesterol (Chol), but also membrane proteins and carbohydrates [1,2]. PLs differ with respect to the headgroup, hydrocarbon chain length and degree of unsaturation. The properties of PMs change depending on the type of PLs they contain and the differences in the Chol content [3]. Chol plays many roles in PMs, influencing the membrane thickness and rigidity [4,5], domain formation [6,7] and cell signaling [8]. Chol is an amphiphilic molecule consisting of a large, nonpolar rigid planar fused ring structure with a smooth and a rough side, a short flexible isooctyl tail and a small hydroxyl (−H) hydrophilic moiety [4] (Figure 1). With such a structure, the Chol molecule naturally orients itself vertically in the PL bilayer, with its head among the polar heads of other PLs and the fused ring structure tugged inside the acyl chain region of the lipids. This enables the Chol molecule to regulate the lateral organization of PLs and influence the membrane physical properties at different membrane depths. These regulatory functions include

altering the bilayer transition temperature [9] and the formation of certain membrane phases and domains [10–12]. In the last few decades, raft domains (domains that are rich in Chol and sphingolipids and span both bilayer leaflets) attracted researchers' attention. Raft domains control many complex functions of PMs, such as signal transduction, protein sorting and lipid trafficking [13–17]. This research is well documented and reviewed [17]. PMs are a more complex system compared to model membranes due to the heterogeneous distribution of proteins and the interactions of lipid components with proteins and the cytoskeleton [18]. The properties of Chol differ in PMs compared to model membranes. Recent studies indicate that Chol moves 1.2 times faster in model membranes compared to the PLs and sphingomyelin (SM) and 2 times faster in live cells compared to the PLs and SM [19]. The same study showed two-component diffusion in PMs, the fast one and one similar to PLs. When the Chol analog was localized in the outer leaflet, the fast diffusion disappeared. This suggests asymmetric Chol diffusion and localization in PMs.
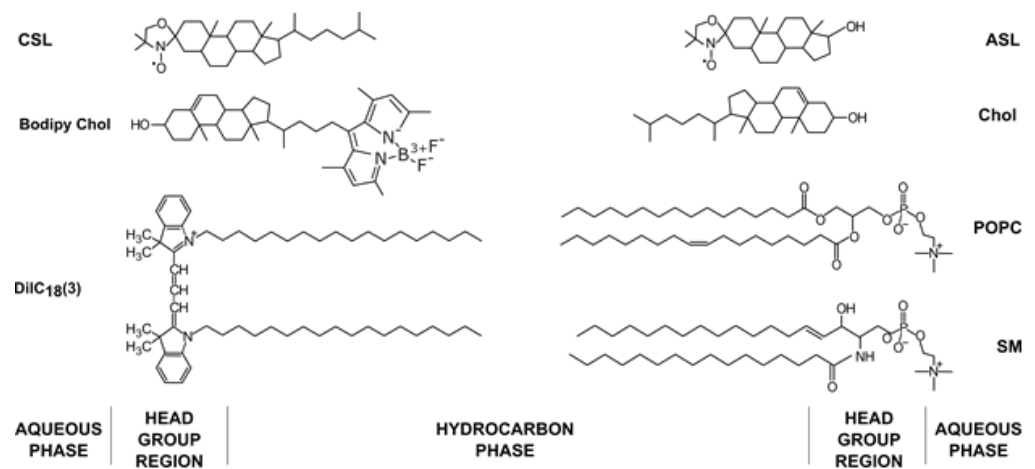
Figure 1. Chemical structures of lipids (1-palmitoyl-2-oleoyl-glycero-3-phosphocholine (POPC), SM and Chol), fluorescent dyes (Bodipy Chol and 1,1′-dioctadecyl-3,3,3′,3′-tetramethylindocarbocyanine (DiIC$_{18}$(3))) and spin labels (androstane spin label (ASL) and cholestane spin label (CSL)) used in the membrane model experiments with their approximate locations in the membrane bilayer.

When the Chol content in the lipid bilayer exceeds a Chol saturation threshold (CSAT) (around 50 mol% Chol), pure Chol bilayer domains (CBDs) are formed within the bulk bilayer. CBDs span both membrane leaflets [20] and are stabilized by the surrounding PL bilayer saturated with Chol [21] (Figure 2). Contrary to lipid rafts, these domains and their functions are less investigated and documented. The eye lens fiber cells contain large amounts of Chol, and it was shown that CBDs are present in the lens lipid membranes [22], forming the buffering capacity, which ensures that these membranes are always saturated with Chol. Because of that, it is argued that CBDs guarantee the homeostasis of the fiber cell PMs, fiber cells themselves and the entire eye lens [23–26].
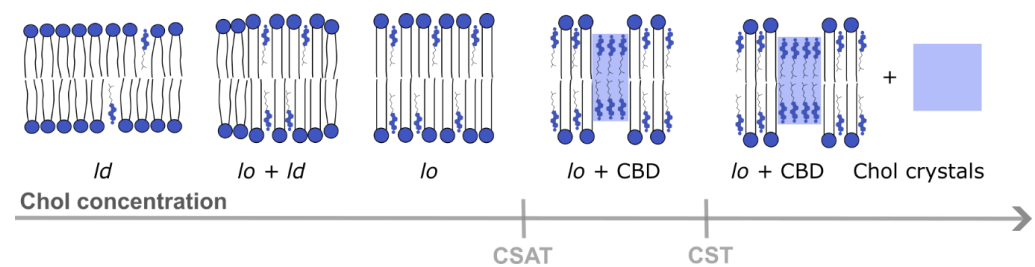

Figure 2. Different membrane domains (l_d—liquid-disordered domain, l_o—liquid-ordered domain) formed in a lipid bilayer at different Chol concentrations from lower to higher content. CBDs start to form above the CSAT, and Chol precipitates in the form of Chol crystals above the CST level [21].

A further increase in the Chol content in the lipid bilayer (above the Chol solubility threshold (CST), ~66 mol%, (Figure 2) induces the formation of Chol crystals which can activate an inflammatory cascade, leading to the development of atherosclerosis. The CST is a total amount of Chol that can be accommodated by the lipid bilayer membrane, both in the PL bilayer saturated with Chol and in CBDs. Thus, the appearance of CBDs in biological membranes other than the eye lens fiber cell membranes is usually treated as a sign of pathology [27].

In this review, we will present different techniques which allow the discrimination of CBDs in model and intact membranes. We will focus on membrane models which can provide information on the major CBD properties. Finally, we will discuss the future direction of CBD research.

2. Liposomes with High Chol Content

Liposomes (lipid vesicles) are structures with at least one lipid bilayer enclosing an aqueous solution. Because they enable research under controlled conditions, they are often used as biological membrane models for investigating the physical properties of membranes [28,29], mimicking cell interactions [30–32], drug delivery [33], interactions with toxins [34] and nanoparticles [35]. In addition, a possible application of liposomes is to use them to build cell-like systems that form whole-cellular models [36]. Depending on their lamellarity, lipid vesicles can be unilamellar (single bilayer), multilamellar (MLVs, more than one concentric bilayer), oligolamellar (OLVs, smaller vesicles within a larger one) or multivesicular vesicles (MVVs, bilayers within other bilayers that are not concentric). Unilamellar vesicles are further classified according to their size into small (SUV) (<100 nm), large (LUV) (>100 nm and <1 μm) and giant (GUV) (>1 μm) unilamellar vesicles. Depending on the target vesicle type, different methods are used to produce them (electroformation, hydration, sonication, extrusion, etc.) (Figure 3) [37,38]. In the following sections, we will first discuss the protocols for the preparation of lipid vesicles with Chol content above the CSAT and, later, the experimental techniques used to study these models.
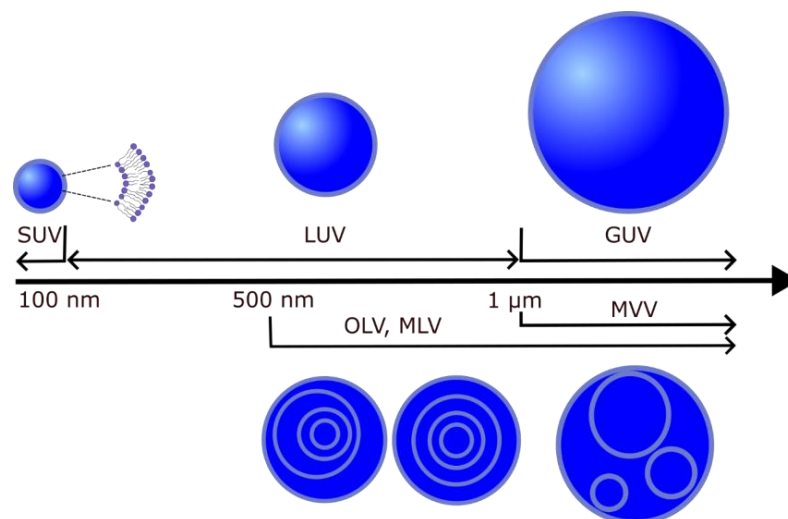
Figure 3. Different types of lipid vesicles depending on their size and structure.

2.1. Liposome Preparation

2.1.1. MLVs, SUVs and LUVs

In order to form MLVs, lipids are usually first dissolved in an organic solvent (chloroform or chloroform/methanol). The lipid mixture is deposited in the test tube or on the substrate and dried using inert gas, rotary evaporation or lyophilization until the lipid film is formed. A vacuum is used to remove the residual organic solvent. The lipid film is then hydrated with an aqueous solution at a temperature above the highest transition temperature of lipids in the mixture. During hydration, the lipid sheets start swelling and

detach to form MLVs. Shaking, vortexing or stirring is needed to enhance the liposome formation [37]. The problem with this approach is the appearance of artificial Chol crystals during the drying process, especially for a Chol concentration above the CSAT. Consequently, the amount of Chol incorporated into the vesicle bilayer is lower than intended because a portion of Chol from the mixture forms Chol crystals which do not participate in the following vesicle formation. In order to differentiate between these two values, we introduced the terms mixing and molar Chol ratios. The mixing ratio defines the ratio of Chol to other lipids dissolved in the organic solution, and the molar ratio is the ratio of the actual amount of Chol to other lipids incorporated into the vesicle bilayer. Using these terms, it follows that Chol demixing causes problems in the sample preparation because the molar ratio in the bilayer is lower than the mixing ratio.

In order to avoid the Chol demixing artifact, a method called the rapid solvent exchange (RSE) can be utilized for the production of MLVs (Figure 4) [39,40]. This method bypasses the dry phase by mixing the lipids dissolved in an organic solvent with an aqueous solution. Applying a vacuum in combination with inert gas flow, the organic solvent is gradually evaporated, leaving only MLVs in an aqueous solution. To confirm the advantages of the RSE method over the film deposition method, differential scanning calorimetry experiments were performed on MLV dispersions for various Chol contents, including those above the CST. We showed that using the RSE for the production of MLVs with Chol contents below the CST, no transition peaks were recorded. A single broad transition peak at 86 °C, representing a transition of a monohydrate to an anhydrous crystal, is observed only for mixtures with Chol content above the CST. Conversely, the dispersions obtained using the film deposition method displayed two peaks. Aside from the broad peak at 86 °C, an additional peak appeared at ~36 °C, representing transformations of one form of anhydrous crystal to another. This is attributed to artificial Chol demixing, resulting in Chol crystals that do not participate in a further vesicle formation. Consequently, the experiments confirm the usefulness of the RSE in terms of bypassing the Chol demixing artifact [21].
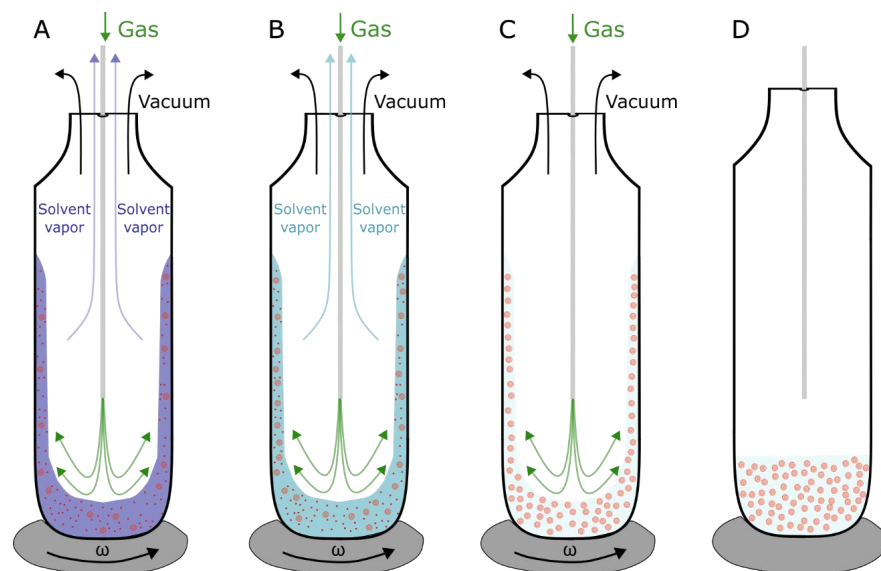
Figure 4. Schematic depiction of the RSE method. (**A**) Organic solvent (chloroform) (blue) containing lipids (red) is mixed with aqueous solution, and removal of organic solvent is achieved by vortexing the solution under vacuum. The process is made more efficient by adding a flow of inert gas (argon) (green) pushing the organic solvent vapors out. (**B**) MLVs start to form. The vacuum pressure is set below the organic solvent evaporation point but higher than the evaporation point of water. (**C**) Exchange is finished when all the organic solution is evaporated and only aqueous solution containing formed MLVs is left. (**D**) When MLVs are formed, vortex is turned off, and vacuum and gas flow pipes are closed. As reported in [40], the whole process takes less than a minute.

SUVs and LUVs are used as intermediate steps in protocols for GUVs production [41] or the formation of supported lipid bilayers (SLBs) [42]. In order to form SUVs and LUVs, MLVs are usually produced first. The sonication of the MLV suspension produces SUVs with diameters in the range of 15 to 50 nm. During extrusion, the MLVs suspension is passed through a polycarbonate filter and a membrane with pores of different sizes. The extruder is positioned on a hot plate, with the temperature set above the highest transition temperature of all the lipids in the mixture. To achieve a homogeneous unilamellar vesicles population, the MLV suspension has to be passed through the pores around 15 times. The final vesicle diameters are determined by the size of the membrane pores. It should be noted that formed vesicles usually have a somewhat larger average diameter than the pores, if the pore size is smaller than 200 nm [43]. This is due to the elasticity of the vesicle membranes, allowing them to squeeze through pores narrower than their nominal diameter. The size distribution of produced unilamellar vesicles can be verified using dynamic light scattering. Although less common, the freeze–thaw and the hand-shaking methods can also be used for SUV and LUV formation [37].

2.1.2. GUVs

GUVs are widely used for the investigation of membrane properties due to their size being similar to the sizes of eukaryotic cells. Most often, they are analyzed using optical microscopy techniques. Different approaches have been attempted for GUV production [37,44–47]. One of the first attempts was reported by Reeves and Dowben in 1969 [29]. The lipid mixture was deposited onto the surface and dried to form a lipid film. The lipid film is then rehydrated, and the solution is stirred to form GUVs. Due to osmotic pressure, the aqueous solution is driven between the lipid bilayer stacks. It is energetically unfavorable for the hydrophobic chains of lipids to be exposed to an aqueous solution, so lipid bilayers spontaneously close into spherical vesicles. Although simple and straightforward, the method produces a low GUVs yield, with lots of defects and a high proportion of MLVs [48]. To address these shortcomings, Angelova and Dimitrov invented the electroformation method which is the most common method used today. In addition to hydration due to osmosis, the method also involves an external electric field applied to the lipid film to promote swelling and vesicle formation [49]. The exact theoretical mechanism of electroformation is not yet completely understood, but it is believed that the electric field affects the lipid swelling through direct electrostatic interactions, the redistribution of counterions, changes in the membrane surface and line tension, and electroosmotic flow effects [50].

The electroformation protocol starts with a mixture of lipids dissolved in an organic solvent. The mixture is spread on conductive electrodes and the bulk of the solvent evaporates shortly after. The remaining traces of the solvent are removed using a vacuum or a flow of inert gas. To form an electroformation chamber (Figure 5), a spacer is attached to the electrodes using vacuum grease.
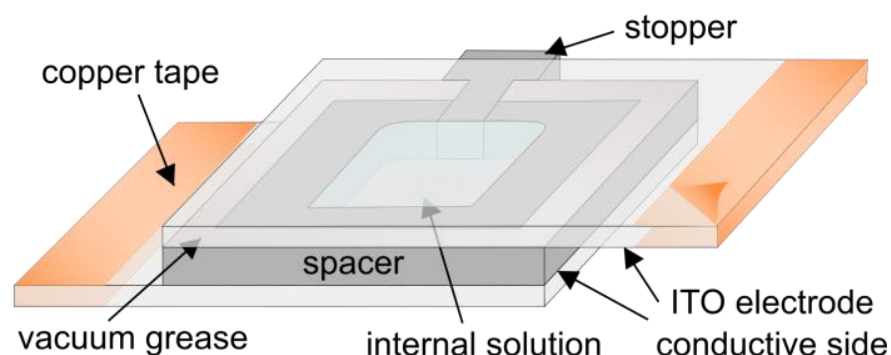
Figure 5. Schematic drawing of a chamber used in electroformation experiments.

After being assembled, the chamber filled with an internal solution is connected to an alternating current waveform generator in order to produce an alternating electric field inside the chamber. Copper tape is often attached to the edges of the electrodes in order to provide better contact with the wires leading to the function generator. The successfulness of the final electroformation depends on lots of factors, such as the choice of electrode material, the film deposition method, the procedure for solvent removal, the lipid composition and internal solution, the choice of electrical parameters, the temperature and the duration of electroformation. The influence of the electroformation parameters on the final result is covered in more detail in a previous review by our group [51].

In order to achieve the best electroformation results, our group conducted experiments in the Chol regime above the CSAT using binary and ternary mixtures of POPC/Chol and POPC/SM/Chol [52,53]. The optimal voltage was found to be in the range of 2 to 6 V and the frequency in the range from 10 to 100 Hz. Lipid thickness is also a parameter that needs to be considered for optimal GUV electroformation. Using spin-coating to achieve reproducible lipid film thicknesses, the highest GUVs successfulness was achieved for thicknesses of approximately 30 nm [53].

Protocols containing steps involving a dry phase result in a lipid film containing Chol crystals formed due to the Chol demixing artifact. Unfortunately, the RSE method cannot be directly used in this case because it produces a solution of multilamellar vesicles. A possible solution was offered by Baykal-Caglar et al. who spread the RSE suspension on an electrode and then placed it in a chamber with a humidity of 55% for 22–25 h to obtain a damp lipid film. Because the lipid film was never completely dry, the Chol demixing artifact was significantly reduced [41].

2.2. Experimental Techniques Utilizing Liposome Models with Particular Focus on CBDs

2.2.1. X-ray Diffraction

Barrett et al. used a specific type of MLVs called highly oriented multilamellar membranes to identify pure Chol domains by X-ray diffraction [54]. 1,2-Dimyristoyl-*sn*-glycero-3-phosphocholine/Chol mixtures with a Chol content ranging from 0 to 60 mol% were used. Highly ordered Chol domains were observed when the Chol content exceeded 40 mol%. These domains were not referred to as CBDs in the article but as immiscible cholesterol plaques. One out-of-plane Bragg peak was observed for Chol concentrations up to 40 mol% and an additional one for concentrations above 40 mol%. The second peak indicates the presence of a Chol bilayer coexisting with the lamellar membrane structure. The in-plane signals were used to infer the type of the Chol structure. At 40 mol% Chol, the pattern was fitted to a monoclinic structure. At a Chol content of 60 mol%, a triclinic structure was observed. The height of the pure Chol domain was estimated to be 26.5 to 32.5 Å. The Chol molecule is 17 Å long, so these values are compatible with the Chol bilayer (the CBDs may be tilted). An important aspect to mention is that all measurements were performed in a humidity chamber with 50% relative humidity. When the humidity was increased, the signal corresponding to pure Chol domains disappeared at a Chol concentration of 40 mol%.

2.2.2. SR EPR Spin Labeling

Using EPR techniques, the CBD as a pure Chol domain can be detected only with Chol analogs, such as an ASL and a CSL (see Figure 1 for spin labels structures). However, conventional and saturation recovery EPR spectroscopy alone cannot discriminate CBDs from the surrounding PL bilayer containing Chol because the spectral characteristics of the Chol analogs are very close (undistinguished) in these two environments [55,56]. Fortunately, a paramagnetic relaxation agent, hydrophobic (dissolved in membranes) molecular oxygen and polar water soluble Ni(II) diethylene diamine diacetic acid exist. The effect of these relaxation agents is especially pronounced on the spin lattice relaxation time of the ASL and CSL and is proportional to the bimolecular collision rate between the relaxation agent and the nitroxide moiety of these spin labels. In turn, bimolecular collisions depend on the local relaxation agent concentration and the diffusion coefficient around the

nitroxide fragment, and thus the local product of the relaxation agent concentration and diffusion. Because these two components can be very different in the different environments surrounding the nitroxide moieties of the ASL and CSL, the observed EPR saturation signal is giving two separated components (which can be fitted by two exponential functions) [55]. In our discrimination approach, the effect of molecular oxygen on the spin lattice relaxation time of the nitroxide moiety of the ASL (located in the membrane center) is very strong and different in CBDs and the surrounding PL bilayer, allowing to discriminate the CBD. The surface-located nitroxide moiety of the CSL is strongly affected by water-soluble Ni(II) diethylene diamine diacetic acid but differently when CSL is present in CBDs and in the surrounding PL bilayer. These two methodological approaches are described in detail in [55] and were used to discriminate CBDs in model [57], lens lipid [22,23,58] and intact membranes [59].

2.2.3. Fluorescence Microscopy

The Chol demixing artifact was encountered by our group as well while using confocal microscopy to detect CBDs in GUVs formed of POPC/Chol mixtures. CBDs were detected only when the Chol concentration in the mixture was equal to or greater than 75% (Figure 6) [20].
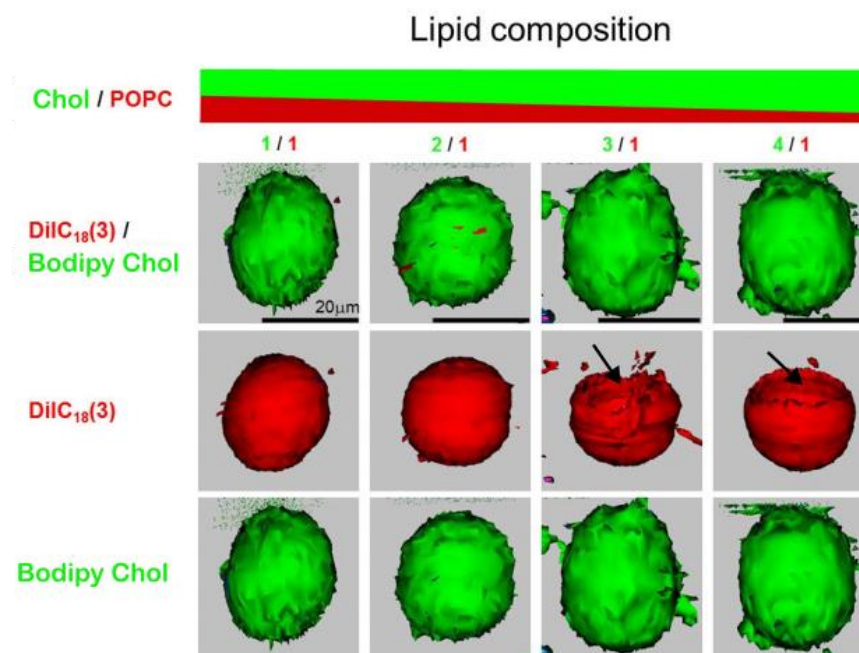
Figure 6. Confocal fluorescence images of GUVs made of Chol/POPC mixtures, with mixing ratios from 1 to 4 and recorded at 22 °C. Each vesicle contains PL and Chol analog probes, DiIC$_{18}$(3) (red) and Bodipy Chol (green), respectively. In the upper row, each image is an overlay of two simultaneously acquired fluorescence signals from DiIC$_{18}$(3) and Bodipy Chol. These same data are presented in the middle and bottom rows, but fluorescence signals originate from DiIC$_{18}$(3) in the middle row and Bodipy Chol in the bottom row, respectively. We collected green and red signals in an independent mode. Each fluorophore was excited by its own individual excitation wavelength, and the resultant emission was collected, first for Bodipy Chol (green) and then for DiIC$_{18}$(3) (red) data. This sequence was repeated over different Z-levels. This enables each fluorophore to be captured independently and in microseconds apart from each other. To gain a three-dimensional distribution of DiIC$_{18}$(3) and Bodipy Chol in the GUV, Z-scan images were converted into surface-rendered images. Three-dimensional renderings of the Z-stack images were performed under the same settings, including threshold (lower limit set at 0.05 for both green and red) orientation, projected image brightness, etc. Arrows show the lack of fluorophore in certain parts of the vesicles. Data for Figure 6 are reproduced with permission from [20]. Copyright 2023, Springer nature BV.

DiIC$_{18}$(3) (PL analog) and Bodipy Chol (Chol analog) fluorescent probes were used for the labeling (see Figure 1 for their structures). From our previous studies on MLVs produced by the RSE method, we know that CBDs should appear at a 50 mol% Chol concentration [21]. This indicates significant Chol demixing when producing GUVs using electroformation protocols containing a dry lipid film step during preparation. Interestingly, confocal microscopy images of GUVs revealed very large CBDs [20]. This is in contrast with evaluations suggesting that the CBDs discriminated by EPR are rather small [60]. This discrepancy could possibly be assigned to different systems used for observation, as EPR measurements were performed on MLVs with a curvature much greater than that of GUVs. We assume that in GUVs, smaller individual CBDs coalesce to form a single large CBD. Another unexpected observation is that the CBDs were always detected on the top of GUVs in what is indicated as a lack of a fluorescence signal originating from the DiIC$_{18}$(3) probe that is presented in the middle row of Figure 6, when the Chol/POPC mixing ratio is higher than 3. We proposed that this occurs due to gravitational forces. Because the surface area density of the CBD is ~25% lower than that of the l_o, the gravitation force will orient GUVs with the less dense surface on the top. When we flipped the sample upside down, the GUVs reoriented so that the CBDs could be found on the top again [20].

## 3. SLBs with High Chol Concentrations

3.1. SLBs Preparation

3.1.1. Vesicle Fusion SLBs

The advantage of using monolayers is the ability to control the lipid coverage, and a disadvantage is that it only contains one membrane leaflet, so it does not adequately represent the PM. The SLBs contain two lipid leaflets on a solid support, with a 1–2 nm water layer between the surface and the membrane. Different substrates can be used for the fabrication of SLBs, but not all substrates are compatible with all lipid compositions. Substrates that are used the most are silica and glass, but mica, gold, silicon, titanium oxide and others have also been experimented with [61].

Different methods can be used for the formation of SLBs. The most widely used method today is vesicle fusion, pioneered by McConnell et al. (Figure 7). The method involves spreading SUVs or LUVs on a hydrophilic surface and their subsequent rupturing in order to form an SLB [62]. It is a fast and easy method but depends on different aspects, such as the vesicle size (a smaller size leads to easier vesicle rupturing), lipid composition (charge of lipids, Chol concentration and saturation degree of the lipids), temperature, the type of substrate and ionic strength [61,63–65]. Plasma treatment is most commonly used for surface hydrophilization to promote the rupture of vesicles. Vesicles are adsorbed onto the surface until a critical concentration is achieved, after which the vesicle rupture occurs. Around 1 h is needed for this process to occur [66]. Lipids are then reorganized into a bilayer that is separated from the surface by a thin layer of water. The sample is washed with a buffer to remove unadsorbed vesicles.

It has been shown that using vesicles containing more than 20 mol% Chol makes it harder for the vesicle rupture to occur due to the vesicle heterogeneity and increased rigidity [61]. Some reagents and buffers can be used to alleviate this problem and promote vesicle rupture. NaCl ions and divalent CaCl$_2$ cations are often used to promote vesicle rupture [64,67] for SLBs with a Chol content above 20 mol% [67–69]. Furthermore, the vesicle lipid composition does not have to be equal to that in the SLB. To quantify the cholesterol fraction in the SLBs, sterol removal by methyl-β-cyclodextrin can be performed and quantified using the Sauerbrey relationship on the quartz crystal microbalance with dissipation monitoring (QCM-d) data [70]. Tabai et al. showed that SLBs had a lower Chol concentration compared to vesicles (20 mol% in vesicles compared to ~10 mol% in the SLB) [71].
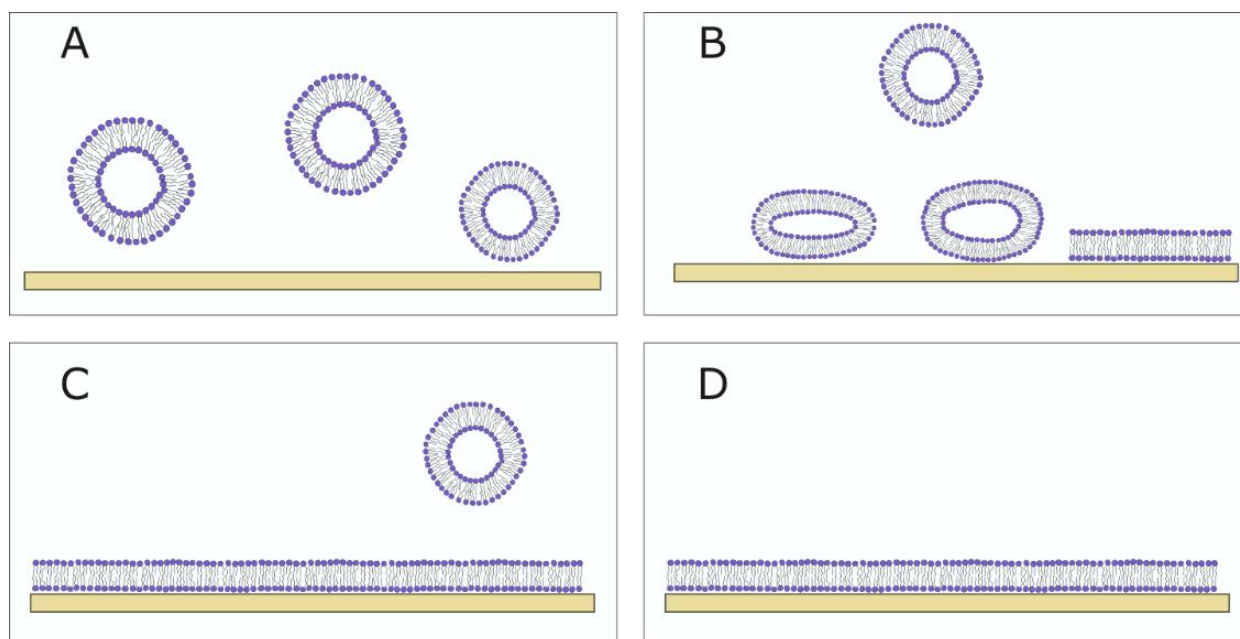
Figure 7. The SLB formation using vesicle fusion method. (**A**) Vesicles float in the bulk solution. (**B**) If the vesicle–substrate interaction is sufficiently strong, the adsorbed vesicles rupture on the substrate. (**C**) The SLB forms, and the unadsorbed vesicles are washed away using a buffer. (**D**) The fully formed SLB.

3.1.2. Solvent-Assisted and Bicelle-Mediated SLBs

Two methods suitable for the formation of SLBs with high Chol content are the solvent-assisted lipid bilayer (SALB, Figure 8A) method and the bicelle-mediated method (Figure 8B). The SALB method incorporates a step principally similar to the one used in the RSE as it involves a gradual exchange of organic and aqueous solutions. Hohner et al. first created a phospholipid SLB using the SALB method by dissolving the PLs in isopropanol and gradually increasing the water content [72]. Depending on the lipid composition, temperature and water content, different lipid structures were formed (micelle, inverted micelle, unilamellar and multilamellar vesicles). During the micelle-to-vesicle transition, the lipid bilayer is formed on a solid substrate. Various protocol parameters (flow, total lipid concentration, lipid content, etc.) need to be regulated for successful SLB production [70]. The solvent exchange velocity needs to be compatible with the velocity of the SLB formation. The total lipid concentration needs to be controlled as well. An overly low amount of lipids leads to incomplete surface coverage ("islands" can be detected), and a surplus of lipids leads to the formation of more than one lipid bilayer. Moreover, just like in vesicle fusion, a surface treatment is recommended for better SLB formation. Using the above approach, a 1,2-dioleoyl-*sn*-glycero-3-phosphocholine/Chol SLB with different Chol concentrations up to ~50 mol% was created successfully [68]. The SLBs were labeled with the rhodamine-modified 1,2-dihexadecanoyl-*sn*-glycero-3-phosphoethanolamine (Rhodamine-DHPE) fluorescent probe which prefers the fluid phase. Using epifluorescence microscopy, dark spots were visible. Considering the fluorescence dye preferences, and the fact that increasing the Chol concentration led to an increase in the area of the dark spots, these spots were hypothesized to be cholesterol-enriched phases. The FRAP experiments showed a near-complete recovery 1 min after the photobleaching, proving that the Chol-depleted phase is laterally fluid. The AFM experiments showed a 1.5 nm difference in height between the phospholipid-rich domain (~4.5 nm) and the dark spots (~3 nm). This value is consistent with the values obtained using X-ray diffraction on highly ordered MLVs [54].
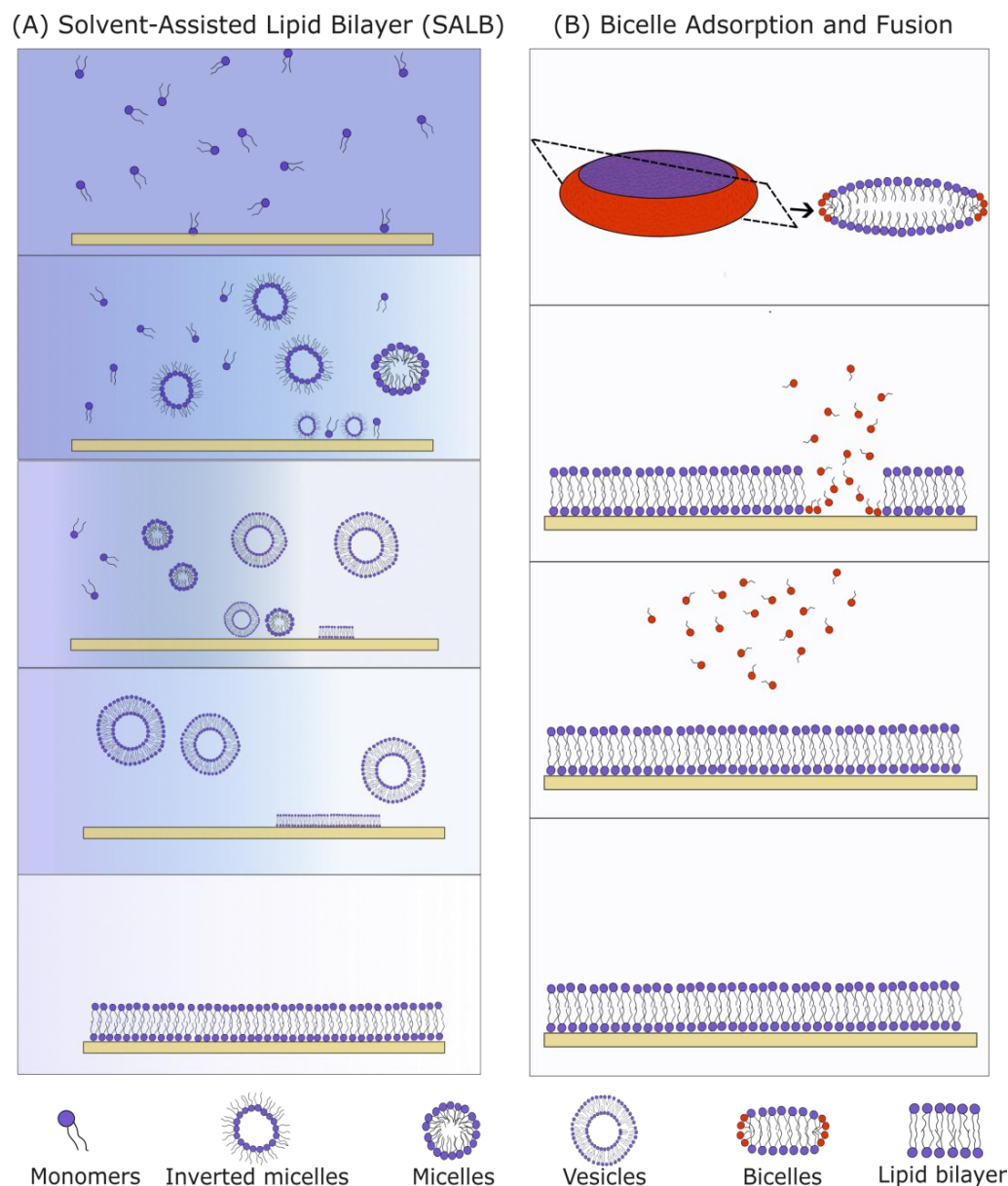
Figure 8. Comparison of the SALB (**A**) and bicelle method (**B**) for formation of SLBs. (**A**) The SALB method begins when long-chain PLs are dissolved in a water-miscible organic solvent. The organic solvent is gradually exchanged with the aqueous solvent. During the solvent exchange, the lipids first assemble into inverted micelles and later into micelles and vesicles. These attach themselves to the surface and rupture to form an SLB. (**B**) Bicelles are disk-like structures containing both long-chain (blue) and short-chain (red) lipids. If there is an attractive force between the substrate and the bicelles, they are adsorbed onto the surface and fuse together. Long-chain PLs remain attached to the substrate, and short-chain PLs are washed away in the form of monomers using a buffer.

Bicelle-mediated SLB formation is another approach that can be used for the fabrication of SLBs with a high Chol content. Bicelles are lipid structures with a disc-like shape, containing a mixture of long-chain and short-chain lipids (Figure 8B). The first publication on bicelle-mediated SLBs was conducted by Zeineldin et al. in 2006, using 1,2-dipalmitoyl-*sn*-glycero-3-phosphocholine (DPPC) and 1,2-dihexanoyl-*sn*-glycero-3-phosphocholine lipids [73]. The main advantage of the method is the ease of the bicelles preparation. A dry lipid film containing a mixture of long-chain and short-chain PLs is hydrated in an aqueous solution and then vortexed. After mixing, the solution is frozen in liquid nitrogen, heated in a water bath at around 60 °C and then vortexed again. Usually, five cycles are

needed for the fabrication of bicelles. The obtained suspension is subsequently deposited onto a hydrophilized substrate. Bicelles get adsorbed, they rupture and then a buffer is used to wash away the short-chain lipids and unadsorbed bicelles. The short-chain PLs make bicelles softer compared to vesicles, so they rupture more easily.

The QCM-d is often used to control the SLB formation. It is a surface-sensitive technique for the determination of the material mass on a piezoelectric crystal quartz sensor. Resonance is achieved when the thickness of the quartz crystal is an odd integer of the half-wavelength of the induced wave, so different overtones (n) can be measured. Changing the frequency gives us information about the mass adsorbed to the crystal. For a successful SLB formation, the change in frequency should be $\Delta f/n = -25$ Hz. The energy loss (dissipation) can also be measured using the QCM-d. It is quantified by measuring the oscillation decay time of the quartz crystal after the alternating potential is turned off and depends on the viscoelastic properties of the mass on the crystal. The dissipation for a successful SLB formation should be $\Delta D/n = 1 \times 10^{-6}$. A combination of Δf and ΔD from measurements of several overtones can be extracted through data modeling. Parameters such as the adsorbed mass, film thickness and viscoelastic properties can be calculated. For a better understanding of the QCM-d, we recommend a detailed review by Allasi et al. [74].

The successfulness of the SLB formation using bicelles depends on the ratio of the long/short-chain PLs (q-ratio), total lipid concentration, lipid composition, type of substrate and NaCl concentration [73,75,76]. Using epifluorescence microscopy, it has been shown that bicelle-mediated SLBs with high Chol content form homogenous SLBs, unlike the SALB method where there are regions with no signal. Although QCM-d results imply the existence of unruptured bicelles on the surface of SLBs containing 40–60 mol% Chol, epifluorescence microscopy could not confirm the same result. On the contrary, regions with unruptured vesicles are seen as bright spots using epifluorescence microscopy. The inability to detect unruptured bicelles is explained by their disk-like shape which allows them to blend in better with the SLB patches.

### 3.2. Experimental Techniques Utilizing SLBs with Particular Focus on CBDs

3.2.1. X-ray Diffraction

Ziblat et al. have examined the formation of CBDs on a polymer-cushioned lipid bilayer using grazing-incidence X-ray diffraction measurements. They introduced a new humidity control method for grazing-incidence X-ray diffraction experiments (Figure 9). In short, using the Langmuir–Blodgett/Langmuir–Schaeffer method, they deposited the bilayer in the chamber and evaporated the sample to 42% relative humidity. The relative humidity was increased by cooling the sample to 6.7 °C, and in these conditions, the relative humidity above the sample was 95.7%. The bilayer was sandwiched with two thin layers of polyethyleneimine. The purpose of the polymer is to keep the bilayer hydrated and allow bilayer components for free diffusion, thus better reproducing biological conditions. A different composition of the lipid bilayer has been investigated with Chol, SM, DPPC or ceramide. The Chol concentration at which they detected CBDs for the SM/Chol mixture was 38 ± 3 mol%; for DPPC/Chol, it was 54 ± 3 mol%; and for Ceramide/Chol, it was 45 ± 5 mol% [77–79].

3.2.2. Atomic Force Microscopy

Khadka et al. [67] used AFM to investigate the mechanical properties of POPC/Chol SLBs with Chol concentrations ranging from 0 to 75 mol%. The SLBs were made using the vesicle fusion of SUVs which were prepared using the RSE method. No direct AFM detection of CBDs was made in SLBs with a Chol content higher than 50 mol%. This was probably due to the AFM tip having a larger area than the CBD. The surface roughness of the SLBs was decreasing until a Chol content of 60 mol%, and it started to increase above that level. The increase above 60 mol% is explained by the possible formation of CBDs [67]. Using force spectroscopy, a single puncture event was obtained for SLBs with Chol concentrations up to 50 mol% and for two events above that concentration. The first puncture event represents the

coexisting l_o and CBDs and the second one is thought to represent the "CBD water pocket" formed on the water layer above the surface. Because of the difference in height between the CBD and l_o, an additional buffer thickness, which acts as an additional resistance for the AFM tip, should be present between the CBD and the surface [67].
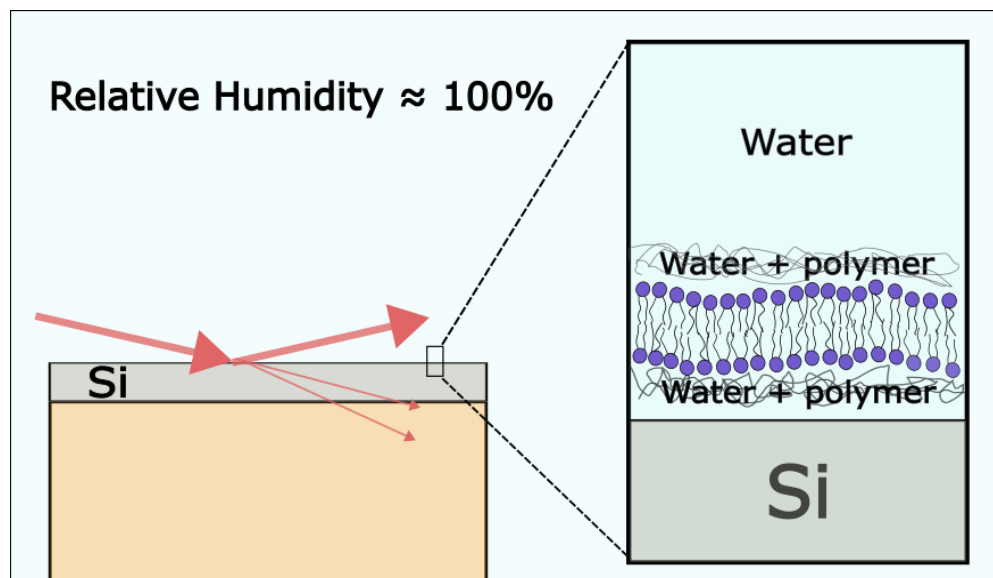
Figure 9. Schematic drawing of grazing-incidence X-ray diffraction measurements of a highly hydrated polymer-cushioned SLB. The figure is based on an image from ref. [78].

3.2.3. Fluorescence Microscopy

FRAP is a technique used for the investigation of lateral mobility and the distribution of lipids in an artificial membrane [80]. Litz et al. [81] made SLBs with a high Chol content (30–66 mol%) using vesicle fusion. Most commonly, SUVs or LUVs are used for the vesicle fusion method, but in their experiment, they used GUVs to form the SLBs. The methyl-β-cyclodextrin was used for the removal of Chol from the SLBs. Two populations of Chol with different properties were found, first with low and the second with high surface accessibility. This finding is consistent with the prediction of the CBD model of the cholesterol–phospholipid interaction in the lipid bilayer. The Chol inside the CBDs would be less shielded from the aqueous phase compared to those inside the l_o. The characteristic Chol fraction at which Chol accessibility begins to increase is in correspondence to the CSAT [81].

3.2.4. QCM-D

FRAP and the QCM-d are often-used methods for controlling the formation of SLBs. Sut at al. [82] have successfully formed SLBs using bicelles with mixtures containing up to a 30 mol% Chol concentration. However, when increasing the Chol content further, some bicelles did not rupture, so incomplete SLBs formed with adsorbed unruptured bicelles. The QCM-d data show a successful SLB formation for 10 and 20 mol% of Chol. At 30–60 mol% of Chol, the QCM-d data indicated incomplete SLB formation. Interestingly, the results showed a smaller Δf for 60 mol% compared to 50 mol% with the same ΔD shifts. The authors suggest that this is due to the formation of CBDs which have a different local thickness, causing a change in the Δf without changing the global viscoelasticity of the membrane (determined by ΔD) [83].

4. Properties of CBDs

The Gibbs phase rule, $f = c - P + 1$ (f, degree of freedom, i.e., the largest number of thermodynamic parameters such as temperature and pressure that can be varied simultaneously; c, the number of components; P, the number of phases, assuming that in all phases the membrane is under the same pressure), must be obeyed for all the regions of the phase

diagram and in all the indicated phase boundaries. The Gibbs phase rule has imposed a few immediate consequences (limitations) regarding the effects of Chol on the physical properties of the fluid-phase membrane. One of them is that the Chol concentration that can be accommodated within a certain phase has an upper limit. For the l_o phase, this limit is 50 mol% Chol. The addition of Chol above this concentration leads to the formation of pure CBDs within the l_o phase. However, the newly formed CBD within the l_o phase cannot be considered as a new phase because it would break the Gibbs phase rule. The single-phase region (l_o phase with CBDs) is called a structured [84], or a dispersed [85], l_o phase. We define the Chol concentration (limit) at which the l_o phase is saturated with Chol as the CSAT (or at which the CBDs start to form). The total amount of Chol that can be accommodated by the structured l_o phase (both in the PL bilayer saturated with Chol and in CBDs) is defined as the CST. This limit occurs at 66 mol% of Chol [86]. Above this limit, Chol crystals are formed as a new phase in the Chol/PL mixture. Thus, above this limit, two phases coexist, a structured l_o phase and Chol crystals [87]. It was shown that in model membranes, the CSAT as well as the CST are decreased by the presence of polyunsaturated chains in the phospholipid bilayer [88]. The peroxidation of phospholipid unsaturated acyl chains has also been linked to a decrease in the CSAT [89,90] and CST [91].

Chronologically, about two decades ago, the first reports appeared that the pure bilayers of Chol were detected using X-ray diffraction and supported bilayer membranes formed from distinct mammalian cell types: arterial smooth muscle cells and ocular lens fiber cells [27,92]. According to the authors, these domains were formed by anhydrous Chol molecules, and all the domains possessed a structure as rigid as the bilayers in Chol crystals. Because of that, they named these domains "cholesterol crystalline domains". Ten years later, the authors of this review detected pure CBDs in membranes oversaturated with Chol by using the saturation recovery EPR method and multilamellar liposomes. The results showed that the rigid cholesterol crystalline domains are not the same as highly fluid CBDs [57]. This highly dynamic structure of the CBD was additionally confirmed by molecular dynamic simulations [88]. Furthermore, both approaches indicated that the Chol–OH groups in CBDs are highly accessible to water molecules; thus, this bilayer cannot be formed by anhydrous Chol molecules. Finally, using fluorescence probe molecules and GUVs, it was unambiguously confirmed that CBDs are transmembrane structures and not separately formed in each bilayer leaflet [20].

We think that the CBD with its unique structure and properties is not yet appreciated enough in membrane research. Additionally, of those properties indicated above, the most significant one is that the presence of the CBD ensures that the surrounding PL bilayer is always saturated with Chol. We can state that the CBD forms the buffering capacity for Chol in the surrounding phospholipid bilayer. Most significantly, the saturation of PL bilayers with Chol ensures that the membrane physical properties of these bilayers (including profiles of the acyl chain order, membrane fluidity, hydrophobicity and oxygen diffusion-concentration product) become consistent and independent of the compositions. It is observed for a membrane made of a single PL, PL mixtures and membranes made of total lipid extracts from intact membranes. The saturation with Chol smooths the bilayer surface. Moreover, the CBD itself forms a significant barrier to oxygen transport [57]. Due to the presence of CBDs in all human fiber cell membranes, the Chol content in these membranes is always high enough to saturate the lens fiber cell membranes regardless of the age of the cell [60]. This ensures the homeostasis of the PMs, fiber cells themselves and entire eye lens [24–26]

Using the RSE method for the formation of multilamellar liposomes (Section 2), we were able to show that the formation of CBDs precedes the formation of Chol crystals [21,93]. These results allowed us to extend the phase diagram for Chol/1,2-dimyristoyl-*sn*-glycero-3-phosphocholine mixtures presented by Almeida et al. [87] to greater Chol contents in the bilayer [21]. Moreover, based on these results, a phase diagram was proposed, showing how a mixture of different PLs can affect the CSAT and CST, and it was hypothesized that CBDs, at a further increase in the Chol content in the bilayer, can collapse to form Chol

seed crystals which further grow to Chol microcrystals [94]. Below, we will discuss how the effects of these CBD properties and the CBDs themselves affect the surrounding PL bilayer and the functions of the different membranes in the human organism.

5. Understanding of CBD Functions in Model Membranes Helps to Understand Its Functions in Biological Membranes

In Section 4, we summarized the properties of CBDs obtained with the different membrane models and techniques described in Sections 2 and 3. Here, we will only indicate the membrane properties which are significant for understanding the CBD's function and high (saturating) Chol content in a human organism. To the best of our knowledge, the extremely high Chol content and appearance of CBDs plays a positive role only in the eye lens fiber cell plasma membranes. There, CBDs support the normal physiological function by helping to maintain lens transparency and preventing the development of a cataract [24]. In membranes of other organs and tissues, the appearance of CBDs is treated as a sign of pathology [25,94].

The positive functions of CBDs in fiber cell plasma membranes are already discussed in detail in [24]. Here, we emphasize these functions which were obtained using appropriate membrane models and techniques. We think that the application of SR EPR spin labeling with the use of multilamellar liposomes gave very significant results. It enabled the measurement of physical properties of the PL bilayer surrounding the CBDs (and thus saturated with Chol). (1) The results show that the physical properties of these PL bilayers surrounding the membrane-integral proteins are consistent and independent of the PL composition of the bilayer. These properties ensure the proper functioning of the eye lens fiber cell membranes (ensure their homeostasis) through drastic changes in the PL composition that occurs with age. It is especially significant because human fiber cells undergo minimal cell turnover, so the same membrane-integral proteins are immersed in the lipid bilayer with drastic changes in the PL composition occurring throughout the human life. Thanks to the presence of CBDs and the saturation of this bilayer with Chol, the effects of these drastic changes are minimized, and proteins are always surrounded by a lipid bilayer with consistent physical properties. (2) Another significant function of CBDs is maximizing the membrane hydrophobic barrier. That way, the permeation of polar molecules in and out of fiber cells can be tightly controlled through gap junctions built of connexins Cx43, Cx46 and Cx50 [95] and water channels built of AQP0 [90]. The saturation of the PL bilayer with Chol is necessary to fulfill this condition. These membranes are built mainly by saturated sphingolipids and dihydrosphingolipids, and without Chol, they would display a very low hydrophobic barrier. (3) It is known that any increase in the oxygen partial pressure inside the lens often results in cataract development. One of the mechanisms helping to keep low oxygen partial pressure inside the lens is the formation of barriers to oxygen permeation across the layers of fiber cells. By saturating the PL bilayer with Chol, CBDs significantly increase the barrier to oxygen permeation. Additionally, the CBD itself has very low oxygen permeability. All these factors indicate that high Chol content and CBDs are needed, and even necessary, to protect the lens against oxidative stress (4). Furthermore, the smoothing of the membrane surface by the saturating content of Chol should decrease the light scattering and help to maintain the lens transparency. These conclusions were made from the results obtained with SR EPR spin labeling using multilamellar liposomes. Most of them were confirmed by molecular dynamic simulations of PL bilayers and CBDs properties [88].

α-crystallin, the major protein found in the human eye lens cytoplasm, works as a molecular chaperone by preventing the aggregation of proteins and thus maintaining lens transparency [96]. With age, the content of membrane-bound α-crystallin increases at the expense of its decrease in the cytoplasm. These processes are accompanied by increased light scattering which compromises lens transparency. Using continuous wave EPR spin labeling and SUVs as a membrane model, Mainali's group showed that high Chol content and the presence of CBDs inhibits the binding of α-crystallin to membranes

made of the major PLs of the eye lens fiber cell plasma membranes. They showed that the same conclusion is valid for membranes (SUV) made of the total lipids extracted from bovine cortical and nuclear lenses [97]. These results present another mechanism through which high Chol and CBDs protect the eye lens against age-related cataract development. However, it should be noted that the SUVs used in these investigations were made using the RSE method followed by probe-tip sonication, and it was not yet confirmed that CBDs can be formed in SUVs with their high curvature. This is an open problem that is significant for the use of SUVs prepared from lipid mixtures with a high Chol/PL mixing ratio.

The formation of CBDs and Chol crystals in membranes of most organs and tissues is considered a sign of pathology [22,27]. Thanks to the application of the RSE method for the formation of multilamellar liposomes and with the use of SR EPR and differential scanning calorimetry techniques, we were able to show that when the Chol content in the phospholipid bilayer exceeds the CST [24,25,27] Chol crystals form, presumably outside the membrane [21,93]. Additionally, the peroxidation of PLs lowers the amount of Chol needed for CBDs and Chol crystals to start to form [89,90]. These are the conditions driving the development of atherosclerosis (high-Chol level and oxidative stress) in which membranes oversaturated with Chol are no longer able to support some of the CBDs. Consequently, the CBDs detach from the membrane and collapse outside of the membranes in the form of Chol aggregates that can become crystal nuclei and, in time, convert into Chol microcrystals. Chol microcrystals activate inflammasomes, thereby stimulating immune responses and initiating inflammation that may lead to the development of atherosclerosis.

In the eye lens, the presence of CBDs is beneficial, and the appearance of Chol crystals in lenses at old age does not compromise lens transparency [22]. The lens is avascular and, soon after formation, its fiber cells lose their intracellular organelles [98,99]. These factors protect the lens from the harmful induction of inflammasomes by Chol crystals as well as from the initiation of the inflammatory cascade. Thus, inflammation does not appear to be involved in cataract formation in the eye lens.

6. Conclusions and Perspectives

We presented the protocols for the preparation of membrane models at Chol concentrations above the CSAT and discussed the problems that may be encountered. GUVs, MLVs and SLBs have been used in CBD studies. The most commonly used method for GUVs production is electroformation. The traditional electroformation protocol contains a step where the lipid film is in a dry state. This induces Chol precipitation in the form of crystals—an issue known as the Chol demixing artifact. These crystals are not incorporated into the GUV bilayer, resulting in a decreased Chol concentration compared to the initial mixture. The dry phase can be bypassed using the RSE method. However, the resulting solution contains only MLVs and not GUVs. Baykal-Caglar et al. have succeeded in reconciling these two approaches to produce GUVs using electroformation without the dry lipid film step. They achieved this using the RSE solution to produce damp lipid films which were used in electroformation.

SLB formation at high Chol contents is also challenging. Vesicle fusion is the most commonly used method but can be problematic at Chol concentrations above 20 mol%. Recent studies suggest that specific ions and buffers can be used to promote a vesicle rupture, potentially solving this issue. The RSE method can be very useful for the production of SLBs, especially as a part of the vesicle fusion protocol. As previously stated, this method of preparation is required to form vesicles with high Chol content. The SALB and bicelle methods can be used as alternatives for SLB formation with Chol contents near and above the CSAT. Using fluorescence microscopy, dark and bright spots could be seen in SLBs prepared by the SALB method, whereas no dark spots could be detected when the bicelle method was used.

CBDs were detected using different techniques applied to different model systems. They were directly detected using confocal microscopy of electroformed GUVs, EPR studies on MLVs and intact membranes and X-ray measurements of polymer-cushioned SLBs and

highly oriented MLVs. Measurements indirectly implying CBD formation have also been obtained using AFM and QCM-d on SLBs.

Using confocal microscopy on GUVs with a Chol concentration above the CSAT, large CBDs were observed. This is in contrast with much smaller CBDs discriminated by the EPR. It is suggested that the difference appears due to EPR studies being performed on MLVs which have a much higher curvature compared to GUVs. EPR studies provide information about the lateral organization of the lipid bilayer. The order of the PL acyl chains, fluidity and hydrophobicity of the bilayer were obtained as a function of the bilayer depth on the model, the lens lipid and intact membranes. At Chol concentrations higher than the CSAT, two domains were observed within the bilayer, representing the l_o phase and CBD, respectively. X-ray diffraction methods were also used to measure the properties of pure Chol domains but were unable to explain the Chol molecular dynamics within the bilayer. These experiments have been performed on highly oriented MLVs and polymer-cushioned SLBs.

Because CBDs appear at very high Chol concentrations (above ~50 mol% in PLs), the existing techniques for the preparation of model membranes are usually not equipped to handle such conditions. Although CBDs were already detected in GUVs, that study used traditional electroformation, resulting in the Chol demixing artifact. Consequently, CBDs could not be detected below a Chol concentration of 75 mol% in the initial mixture. Although not tested on Chol concentrations above the CSAT, modifications of the electroformation protocol by Baykal-Caglar et al. should enable the production of GUVs with well-controlled Chol contents. This should allow for a comparison of CSATs with different membrane models (for example, MLVs). The bicelle and SALB methods look the most promising for the production of SLBs with a high Chol concentration. These new methods can be utilized to study CBD properties in order to further elucidate its role in the membrane.

Regarding the biological function of CBDs in PMs, the presence of CBDs in the eye lens membrane has been shown to be beneficial. l_o surrounded by CBDs have consistent physical properties regardless of the PL composition. This is important for the homeostasis of the eye lens, whose PL composition changes with aging. The proteins in the fiber cells of the eye lens are always surrounded by the PLs with constant physical properties. Another beneficial property of CBDs is the maximization of the hydrophobic barrier of the membrane, so that the movement of polar molecules within the fiber cells is regulated by gap junctions and water channels. Increased oxygen partial pressure also promotes cataract formation, and CBDs saturate l_o to keep the oxygen barrier high during aging. The smoothing of the membrane surface by saturation with Chol reduces light scattering. In other membranes and tissues, CBDs and Chol crystals are indicative of a pathological condition.

Abbreviations

AFM	Atomic force microscopy
ASL	Androstane spin label
CBD	Cholesterol bilayer domain
Chol	Cholesterol
CSL	Cholestane spin label
CST	Cholesterol solubility threshold
CSAT	Cholesterol saturation threshold
DPPC	1,2-dipalmitoyl-*sn*-glycero-3-phosphocholine
DiIC$_{18}$(3)	1,1′-dioctadecyl-3,3,3′,3′-tetramethylindocarbocyanine
FRAP	Fluorescence recovery after photobleaching
GUV	Giant unilamellar vesicle
l_d	Liquid-disordered domain
l_o	Liquid-ordered domain
LUV	Large unilamellar vesicle
MLV	Multilamellar vesicle
MVV	Multivesicular vesicle
OLV	Oligolamellar vesicle
PL	Phospholipid
PM	Plasma membrane
POPC	1-palmitoyl-2-oleoyl-glycero-3-phosphocholine
QCM-d	Quartz crystal microbalance with dissipation monitoring
RSE	Rapid solvent exchange
SALB	Solvent-assisted lipid bilayer
SM	Sphingomyelin
SLB	Supported lipid bilayer
SR EPR	Saturation recovery electron paramagnetic resonance
SUV	Small unilamellar vesicle

References

1. Harayama, T.; Riezman, H. Understanding the Diversity of Membrane Lipid Composition. *Nat. Rev. Mol. Cell Biol.* **2018**, *19*, 281–296. [CrossRef] [PubMed]
2. Nicolson, G.L. The Fluid—Mosaic Model of Membrane Structure: Still Relevant to Understanding the Structure, Function and Dynamics of Biological Membranes after More than 40 years. *Biochim. Biophys. Acta Biomembr.* **2014**, *1838*, 1451–1466. [CrossRef] [PubMed]
3. Casares, D.; Escribá, P.V.; Rosselló, C.A. Membrane Lipid Composition: Effect on Membrane and Organelle Structure, Function and Compartmentalization and Therapeutic Avenues. *Int. J. Mol. Sci.* **2019**, *20*, 2167. [CrossRef] [PubMed]
4. Róg, T.; Pasenkiewicz-Gierula, M.; Vattulainen, I.; Karttunen, M. Ordering Effects of Cholesterol and Its Analogues. *Biochim. Biophys. Acta Biomembr.* **2009**, *1788*, 97–121. [CrossRef] [PubMed]
5. Gumí-Audenis, B.; Costa, L.; Carlá, F.; Comin, F.; Sanz, F.; Giannotti, M. Structure and Nanomechanics of Model Membranes by Atomic Force Microscopy and Spectroscopy: Insights into the Role of Cholesterol and Sphingolipids. *Membranes* **2016**, *6*, 58. [CrossRef]
6. Harder, T. Formation of Functional Cell Membrane Domains: The Interplay of Lipid– and Protein–Mediated Interactions. *Philos. Trans. R. Soc. London. Ser. B Biol. Sci.* **2003**, *358*, 863–868. [CrossRef]
7. Gupta, A.; Phang, I.Y.; Wohland, T. To Hop or Not to Hop: Exceptions in the FCS Diffusion Law. *Biophys. J.* **2020**, *118*, 2434–2447. [CrossRef]
8. Incardona, J.P.; Eaton, S. Cholesterol in Signal Transduction. *Curr. Opin. Cell Biol.* **2000**, *12*, 193–203. [CrossRef]
9. Redondo-Morata, L.; Giannotti, M.I.; Sanz, F. Influence of Cholesterol on the Phase Transition of Lipid Bilayers: A Temperature-Controlled Force Spectroscopy Study. *Langmuir* **2012**, *28*, 12851–12860. [CrossRef]
10. Kotenkov, S.A.; Gnezdilov, O.I.; Khaliullina, A.V.; Antzutkin, O.N.; Gimatdinov, R.S.; Filippov, A.V. Effect of Cholesterol and Curcumin on Ordering of DMPC Bilayers. *Appl. Magn. Reson.* **2019**, *50*, 511–520. [CrossRef]
11. Rabinovich, A.L.; Kornilov, V.V.; Balabaev, N.K.; Leermakers, F.A.M.; Filippov, A.V. Properties of Unsaturated Phospholipid Bilayers: Effect of Cholesterol. *Biol. Membr.* **2007**, *24*, 490–505. [CrossRef]
12. Filippov, A.V.; Rudakova, M.A.; Oradd, G.; Lindblom, G. Lateral Diffusion of Saturated Phosphatidylcholines in Cholesterol-Containing Bilayers. *Biophysics* **2007**, *52*, 307–314. [CrossRef]
13. Simons, K.; Ikonen, E. Functional Rafts in Cell Membranes. *Nature* **1997**, *387*, 569–572. [CrossRef] [PubMed]

14. Viola, A. The Amplification of TCR Signaling by Dynamic Membrane Microdomains. *Trends Immunol.* **2001**, *22*, 322–327. [CrossRef]

15. Kusumi, A.; Fujiwara, T.K.; Chadda, R.; Xie, M.; Tsunoyama, T.A.; Kalay, Z.; Kasai, R.S.; Suzuki, K.G.N. Dynamic Organizing Principles of the Plasma Membrane That Regulate Signal Transduction: Commemorating the Fortieth Anniversary of Singer and Nicolson's Fluid-Mosaic Model. *Annu. Rev. Cell Dev. Biol.* **2012**, *28*, 215–250. [CrossRef]

16. Simons, K.; Toomre, D. Lipid Rafts and Signal Transduction. *Nat. Rev. Mol. Cell Biol.* **2000**, *1*, 31–39. [CrossRef] [PubMed]

17. Kusumi, A.; Fujiwara, T.K.; Tsunoyama, T.A.; Kasai, R.S.; Liu, A.; Hirosawa, K.M.; Kinoshita, M.; Matsumori, N.; Komura, N.; Ando, H.; et al. Defining Raft Domains in the Plasma Membrane. *Traffic* **2020**, *21*, 106–137. [CrossRef]

18. Huang, S.; Lim, S.Y.; Gupta, A.; Bag, N.; Wohland, T. Plasma Membrane Organization and Dynamics Is Probe and Cell Line Dependent. *Biochim. Biophys. Acta Biomembr.* **2017**, *1859*, 1483–1492. [CrossRef]

19. Pinkwart, K.; Schneider, F.; Lukoseviciute, M.; Sauka-Spengler, T.; Lyman, E.; Eggeling, C.; Sezgin, E. Nanoscale Dynamics of Cholesterol in the Cell Membrane. *J. Biol. Chem.* **2019**, *294*, 12599–12609. [CrossRef]

20. Raguz, M.; Kumar, S.N.; Zareba, M.; Ilic, N.; Mainali, L.; Subczynski, W.K. Confocal Microscopy Confirmed That in Phosphatidyl-choline Giant Unilamellar Vesicles with Very High Cholesterol Content Pure Cholesterol Bilayer Domains Form. *Cell Biochem. Biophys.* **2019**, *77*, 309–317. [CrossRef]

21. Mainali, L.; Raguz, M.; Subczynski, W.K. Formation of Cholesterol Bilayer Domains Precedes Formation of Cholesterol Crystals in Cholesterol/Dimyristoylphosphatidylcholine Membranes: EPR and DSC Studies. *J. Phys. Chem. B* **2013**, *117*, 8994–9003. [CrossRef] [PubMed]

22. Mainali, L.; Raguz, M.; O'Brien, W.J.; Subczynski, W.K. Properties of Membranes Derived from the Total Lipids Extracted from Clear and Cataractous Lenses of 61–70-Year-Old Human Donors. *Eur. Biophys. J.* **2015**, *44*, 91–102. [CrossRef] [PubMed]

23. Subczynski, W.K.; Pasenkiewicz-Gierula, M.; Widomska, J.; Mainali, L.; Raguz, M. High Cholesterol/Low Cholesterol: Effects in Biological Membranes: A Review. *Cell Biochem. Biophys.* **2017**, *75*, 369–385. [CrossRef] [PubMed]

24. Subczynski, W.K.; Raguz, M.; Widomska, J.; Mainali, L.; Konovalov, A. Functions of Cholesterol and the Cholesterol Bilayer Domain Specific to the Fiber-Cell Plasma Membrane of the Eye Lens. *J. Membr. Biol.* **2012**, *245*, 51–68. [CrossRef] [PubMed]

25. Widomska, J.; Subczynski, W.K. Why Is Very High Cholesterol Content Beneficial for the Eye Lens but Negative for Other Organs? *Nutrients* **2019**, *11*, 1083. [CrossRef] [PubMed]

26. Subczynski, W.K.; Mainali, L.; Raguz, M.; O'Brien, W.J. Organization of Lipids in Fiber-Cell Plasma Membranes of the Eye Lens. *Exp. Eye Res.* **2017**, *156*, 79–86. [CrossRef]

27. Preston Mason, R.; Tulenko, T.N.; Jacob, R.F. Direct Evidence for Cholesterol Crystalline Domains in Biological Membranes: Role in Human Pathobiology. *Biochim. Biophys. Acta Biomembr.* **2003**, *1610*, 198–207. [CrossRef]

28. Ertel, A.; Marangoni, A.G.; Marsh, J.; Hallett, F.R.; Wood, J.M. Mechanical Properties of Vesicles. I. Coordinated Analysis of Osmotic Swelling and Lysis. *Biophys. J.* **1993**, *64*, 426–434. [CrossRef]

29. Reeves, J.P.; Dowben, R.M. Formation and Properties of Thin-Walled Phospholipid Vesicles. *J. Cell. Physiol.* **1969**, *73*, 49–60. [CrossRef]

30. Buzás, E.I.; Tóth, E.Á.; Sódar, B.W.; Szabó-Taylor, K.É. Molecular Interactions at the Surface of Extracellular Vesicles. *Semin. Immunopathol.* **2018**, *40*, 453–464. [CrossRef]

31. Menger, F.M.; Angelova, M.I. Giant Vesicles: Imitating the Cytological Processes of Cell Membranes. *Acc. Chem. Res.* **1998**, *31*, 789–797. [CrossRef]

32. Valkenier, H.; López Mora, N.; Kros, A.; Davis, A.P. Visualization and Quantification of Transmembrane Ion Transport into Giant Unilamellar Vesicles. *Angew. Chemie Int. Ed.* **2015**, *54*, 2137–2141. [CrossRef]

33. Chacko, I.A.; Ghate, V.M.; Dsouza, L.; Lewis, S.A. Lipid Vesicles: A Versatile Drug Delivery Platform for Dermal and Transdermal Applications. *Colloids Surf. B Biointerfaces* **2020**, *195*, 111262. [CrossRef] [PubMed]

34. Mihailescu, M.; Krepkiy, D.; Milescu, M.; Gawrisch, K.; Swartz, K.J.; White, S. Structural Interactions of a Voltage Sensor Toxin with Lipid Membranes. *Proc. Natl. Acad. Sci. USA* **2014**, *111*, 5463–5470. [CrossRef] [PubMed]

35. Karal, M.A.S.; Ahammed, S.; Levadny, V.; Belaya, M.; Ahamed, M.K.; Ahmed, M.; Bin Mahbub, Z.; Ullah, A.K.M.A. Deformation and Poration of Giant Unilamellar Vesicles Induced by Anionic Nanoparticles. *Chem. Phys. Lipids* **2020**, *230*, 104916. [CrossRef]

36. Luisi, P.L. Toward the Engineering of Minimal Living Cells. *Anat. Rec.* **2002**, *268*, 208–214. [CrossRef]

37. Akbarzadeh, A.; Rezaei-Sadabady, R.; Davaran, S.; Joo, S.W.; Zarghami, N.; Hanifehpour, Y.; Samiei, M.; Kouhi, M.; Nejati-Koshki, K. Liposome: Classification, Preparation, and Applications. *Nanoscale Res. Lett.* **2013**, *8*, 102. [CrossRef]

38. Walde, P. Preparation of Vesicles (Liposomes). *Encycl. Nanosci. Nanotechnol.* **2004**, *8*, 43–79.

39. Buboltz, J.T.; Feigenson, G.W. A Novel Strategy for the Preparation of Liposomes: Rapid Solvent Exchange. *Biochim. Biophys. Acta Biomembr.* **1999**, *1417*, 232–245. [CrossRef]

40. Buboltz, J.T. A More Efficient Device for Preparing Model-Membrane Liposomes by the Rapid Solvent Exchange Method. *Rev. Sci. Instrum.* **2009**, *80*, 124301. [CrossRef]

41. Baykal-Caglar, E.; Hassan-Zadeh, E.; Saremi, B.; Huang, J. Preparation of Giant Unilamellar Vesicles from Damp Lipid Film for Better Lipid Compositional Uniformity. *Biochim. Biophys. Acta Biomembr.* **2012**, *1818*, 2598–2604. [CrossRef] [PubMed]

42. Lind, T.K.; Cárdenas, M. Understanding the Formation of Supported Lipid Bilayers via Vesicle Fusion—A Case That Exemplifies the Need for the Complementary Method Approach (Review). *Biointerphases* **2016**, *11*, 020801. [CrossRef] [PubMed]

43. Ong, S.; Chitneni, M.; Lee, K.; Ming, L.; Yuen, K. Evaluation of Extrusion Technique for Nanosizing Liposomes. *Pharmaceutics* **2016**, *8*, 36. [CrossRef] [PubMed]

44. Beales, P.A.; Ciani, B.; Cleasby, A.J. Nature's Lessons in Design: Nanomachines to Scaffold, Remodel and Shape Membrane Compartments. *Phys. Chem. Chem. Phys.* **2015**, *17*, 15489–15507. [CrossRef] [PubMed]

45. Walde, P.; Cosentino, K.; Engel, H.; Stano, P. Giant Vesicles: Preparations and Applications. *ChemBioChem* **2010**, *11*, 848–865. [CrossRef]

46. van Swaay, D.; DeMello, A. Microfluidic Methods for Forming Liposomes. *Lab Chip* **2013**, *13*, 752. [CrossRef]

47. Patil, Y.P.; Jadhav, S. Novel Methods for Liposome Preparation. *Chem. Phys. Lipids* **2014**, *177*, 8–18. [CrossRef]

48. Rodriguez, N.; Pincet, F.; Cribier, S. Giant Vesicles Formed by Gentle Hydration and Electroformation: A Comparison by Fluorescence Microscopy. *Colloids Surf. B Biointerfaces* **2005**, *42*, 125–130. [CrossRef]

49. Angelova, M.I.; Dimitrov, D.S. Liposome Electroformation. *Faraday Discuss. Chem. Soc.* **1986**, *81*, 303. [CrossRef]

50. Dimitrov, D.S.; Angelova, M.I. Lipid Swelling and Liposome Formation on Solid Surfaces in External Electric Fields. In *New Trends in Colloid Science*; Steinkopff: Darmstadt, Germany, 1987; Volume 56, pp. 48–56.

51. Boban, Z.; Mardešić, I.; Subczynski, W.K.; Raguz, M. Giant Unilamellar Vesicle Electroformation: What to Use, What to Avoid, and How to Quantify the Results. *Membranes* **2021**, *11*, 860. [CrossRef]

52. Boban, Z.; Puljas, A.; Kovač, D.; Subczynski, W.K.; Raguz, M. Effect of Electrical Parameters and Cholesterol Concentration on Giant Unilamellar Vesicles Electroformation. *Cell Biochem. Biophys.* **2020**, *78*, 157–164. [CrossRef]

53. Boban, Z.; Mardešić, I.; Subczynski, W.K.; Jozić, D.; Raguz, M. Optimization of Giant Unilamellar Vesicle Electroformation for Phosphatidylcholine/Sphingomyelin/Cholesterol Ternary Mixtures. *Membranes* **2022**, *12*, 525. [CrossRef] [PubMed]

54. Barrett, M.A.; Zheng, S.; Toppozini, L.A.; Alsop, R.J.; Dies, H.; Wang, A.; Jago, N.; Moore, M.; Rheinstädter, M.C. Solubility of Cholesterol in Lipid Membranes and the Formation of Immiscible Cholesterol Plaques at High Cholesterol Concentrations. *Soft Matter* **2013**, *9*, 9342. [CrossRef]

55. Raguz, M.; Mainali, L.; Widomska, J.; Subczynski, W.K. Using Spin-Label Electron Paramagnetic Resonance (EPR) to Discriminate and Characterize the Cholesterol Bilayer Domain. *Chem. Phys. Lipids* **2011**, *164*, 819–829. [CrossRef] [PubMed]

56. Raguz, M.; Widomska, J.; Dillon, J.; Gaillard, E.R.; Subczynski, W.K. Characterization of Lipid Domains in Reconstituted Porcine Lens Membranes Using EPR Spin-Labeling Approaches. *Biochim. Biophys. Acta Biomembr.* **2008**, *1778*, 1079–1090. [CrossRef] [PubMed]

57. Raguz, M.; Mainali, L.; Widomska, J.; Subczynski, W.K. The Immiscible Cholesterol Bilayer Domain Exists as an Integral Part of Phospholipid Bilayer Membranes. *Biochim. Biophys. Acta Biomembr.* **2011**, *1808*, 1072–1080. [CrossRef]

58. Mainali, L.; Raguz, M.; O'Brien, W.J.; Subczynski, W.K. Properties of Membranes Derived from the Total Lipids Extracted from the Human Lens Cortex and Nucleus. *Biochim. Biophys. Acta Biomembr.* **2013**, *1828*, 1432–1440. [CrossRef]

59. Mainali, L.; O'Brien, W.J.; Subczynski, W.K. Detection of Cholesterol Bilayer Domains in Intact Biological Membranes: Methodology Development and Its Application to Studies of Eye Lens Fiber Cell Plasma Membranes. *Exp. Eye Res.* **2019**, *178*, 72–81. [CrossRef]

60. Mainali, L.; Raguz, M.; O'Brien, W.J.; Subczynski, W.K. Changes in the Properties and Organization of Human Lens Lipid Membranes Occurring with Age. *Curr. Eye Res.* **2017**, *42*, 721–731. [CrossRef]

61. Richter, R.P.; Bérat, R.; Brisson, A.R. Formation of Solid-Supported Lipid Bilayers: An Integrated View. *Langmuir* **2006**, *22*, 3497–3505. [CrossRef]

62. Brian, A.A.; McConnell, H.M. Allogeneic Stimulation of Cytotoxic T Cells by Supported Planar Membranes. *Proc. Natl. Acad. Sci. USA* **1984**, *81*, 6159–6163. [CrossRef] [PubMed]

63. Lind, T.K.; Cárdenas, M.; Wacklin, H.P. Formation of Supported Lipid Bilayers by Vesicle Fusion: Effect of Deposition Temperature. *Langmuir* **2014**, *30*, 7259–7263. [CrossRef] [PubMed]

64. Jackman, J.A.; Cho, N.-J. Supported Lipid Bilayer Formation: Beyond Vesicle Fusion. *Langmuir* **2020**, *36*, 1387–1400. [CrossRef] [PubMed]

65. Tero, R. Substrate Effects on the Formation Process, Structure and Physicochemical Properties of Supported Lipid Bilayers. *Materials* **2012**, *5*, 2658–2680. [CrossRef]

66. Koenig, B.W.; Krueger, S.; Orts, W.J.; Majkrzak, C.F.; Berk, N.F.; Silverton, J.V.; Gawrisch, K. Neutron Reflectivity and Atomic Force Microscopy Studies of a Lipid Bilayer in Water Adsorbed to the Surface of a Silicon Single Crystal. *Langmuir* **1996**, *12*, 1343–1350. [CrossRef]

67. Khadka, N.K.; Timsina, R.; Rowe, E.; O'Dell, M.; Mainali, L. Mechanical Properties of the High Cholesterol-Containing Membrane: An AFM Study. *Biochim. Biophys. Acta Biomembr.* **2021**, *1863*, 183625. [CrossRef]

68. Waldie, S.; Moulin, M.; Porcar, L.; Pichler, H.; Strohmeier, G.A.; Skoda, M.; Forsyth, V.T.; Haertlein, M.; Maric, S.; Cárdenas, M. The Production of Matchout-Deuterated Cholesterol and the Study of Bilayer-Cholesterol Interactions. *Sci. Rep.* **2019**, *9*, 5118. [CrossRef]

69. Waldie, S.; Lind, T.K.; Browning, K.; Moulin, M.; Haertlein, M.; Forsyth, V.T.; Luchini, A.; Strohmeier, G.A.; Pichler, H.; Maric, S.; et al. Localization of Cholesterol within Supported Lipid Bilayers Made of a Natural Extract of Tailor-Deuterated Phosphatidylcholine. *Langmuir* **2018**, *34*, 472–479. [CrossRef]

70. Tabaei, S.R.; Choi, J.; Haw Zan, G.; Zhdanov, V.P.; Cho, N. Solvent-Assisted Lipid Bilayer Formation on Silicon Dioxide and Gold. *Langmuir* **2014**, *30*, 10363–10373. [CrossRef]

71. Tabaei, S.R.; Jackman, J.A.; Kim, S.-O.; Liedberg, B.; Knoll, W.; Parikh, A.N.; Cho, N. Formation of Cholesterol-Rich Supported Membranes Using Solvent-Assisted Lipid Self-Assembly. *Langmuir* **2014**, *30*, 13345–13352. [CrossRef]

72. Hohner, A.O.; David, M.P.C.; Rädler, J.O. Controlled Solvent-Exchange Deposition of Phospholipid Membranes onto Solid Surfaces. *Biointerphases* **2010**, *5*, 1. [CrossRef] [PubMed]

73. Zeineldin, R.; Last, J.A.; Slade, A.L.; Ista, L.K.; Bisong, P.; O'Brien, M.J.; Brueck, S.R.J.; Sasaki, D.Y.; Lopez, G.P. Using Bicellar Mixtures To Form Supported and Suspended Lipid Bilayers on Silicon Chips. *Langmuir* **2006**, *22*, 8163–8168. [CrossRef] [PubMed]

74. Alassi, A.; Benammar, M.; Brett, D. Quartz Crystal Microbalance Electronic Interfacing Systems: A Review. *Sensors* **2017**, *17*, 2799. [CrossRef] [PubMed]

75. Sut, T.N.; Jackman, J.A.; Yoon, B.K.; Park, S.; Kolahdouzan, K.; Ma, G.J.; Zhdanov, V.P.; Cho, N. Influence of NaCl Concentration on Bicelle-Mediated SLB Formation. *Langmuir* **2019**, *35*, 10658–10666. [CrossRef]

76. Dudás, E.F.; Wacha, A.; Bóta, A.; Bodor, A. Peptide-Bicelle Interaction: Following Variations in Size and Morphology by a Combined NMR-SAXS Approach. *Biochim. Biophys. Acta Biomembr.* **2020**, *1862*, 183095. [CrossRef]

77. Ziblat, R.; Fargion, I.; Leiserowitz, L.; Addadi, L. Spontaneous Formation of Two-Dimensional and Three-Dimensional Cholesterol Crystals in Single Hydrated Lipid Bilayers. *Biophys. J.* **2012**, *103*, 255–264. [CrossRef]

78. Ziblat, R.; Leiserowitz, L.; Addadi, L. Crystalline Lipid Domains: Characterization by X-Ray Diffraction and Their Relation to Biology. *Angew. Chemie Int. Ed.* **2011**, *50*, 3620–3629. [CrossRef]

79. Ziblat, R.; Leiserowitz, L.; Addadi, L. Crystalline Domain Structure and Cholesterol Crystal Nucleation in Single Hydrated DPPC:Cholesterol:POPC Bilayers. *J. Am. Chem. Soc.* **2010**, *132*, 9920–9927. [CrossRef]

80. Pincet, F.; Adrien, V.; Yang, R.; Delacotte, J.; Rothman, J.E.; Urbach, W.; Tareste, D. FRAP to Characterize Molecular Diffusion and Interaction in Various Membrane Environments. *PLoS ONE* **2016**, *11*, e0158457. [CrossRef]

81. Litz, J.P.; Thakkar, N.; Portet, T.; Keller, S.L. Depletion with Cyclodextrin Reveals Two Populations of Cholesterol in Model Lipid Membranes. *Biophys. J.* **2016**, *110*, 635–645. [CrossRef]

82. Sut, T.N.; Yoon, B.K.; Park, S.; Jackman, J.A. Versatile Formation of Supported Lipid Bilayers from Bicellar Mixtures of Phospholipids and Capric Acid. *Sci. Rep.* **2020**, 1–10. [CrossRef] [PubMed]

83. Sut, T.N.; Park, S.; Choe, Y.; Cho, N.-J. Characterizing the Supported Lipid Membrane Formation from Cholesterol-Rich Bicelles. *Langmuir* **2019**, *35*, 15063–15070. [CrossRef] [PubMed]

84. Heberle, F.A.; Feigenson, G.W. Phase Separation in Lipid Membranes. *Cold Spring Harb. Perspect. Biol.* **2011**, *3*, a004630. [CrossRef]

85. Simons, K.; Vaz, W.L.C. Model Systems, Lipid Rafts, and Cell Membranes. *Annu. Rev. Biophys. Biomol. Struct.* **2004**, *33*, 269–295. [CrossRef]

86. Huang, J.; Feigenson, G.W. A Microscopic Interaction Model of Maximum Solubility of Cholesterol in Lipid Bilayers. *Biophys. J.* **1999**, *76*, 2142–2157. [CrossRef]

87. Almeida, P.F.F.; Pokorny, A.; Hinderliter, A. Thermodynamics of Membrane Domains. *Biochim. Biophys. Acta Biomembr.* **2005**, *1720*, 1–13. [CrossRef]

88. Plesnar, E.; Subczynski, W.K.; Pasenkiewicz-Gierula, M. Saturation with Cholesterol Increases Vertical Order and Smoothes the Surface of the Phosphatidylcholine Bilayer: A Molecular Simulation Study. *Biochim. Biophys. Acta Biomembr.* **2012**, *1818*, 520–529. [CrossRef] [PubMed]

89. Brzustowicz, M.R.; Cherezov, V.; Caffrey, M.; Stillwell, W.; Wassall, S.R. Molecular Organization of Cholesterol in Polyunsaturated Membranes: Microdomain Formation. *Biophys. J.* **2002**, *82*, 285–298. [CrossRef]

90. Buzhynskyy, N.; Sens, P.; Behar-Cohen, F.; Scheuring, S. Eye Lens Membrane Junctional Microdomains: A Comparison between Healthy and Pathological Cases. *New J. Phys.* **2011**, *13*, 085016. [CrossRef]

91. Tulenko, T.N.; Chen, M.; Mason, P.E.; Mason, R.P. Physical Effects of Cholesterol on Arterial Smooth Muscle Membranes: Evidence of Immiscible Cholesterol Domains and Alterations in Bilayer Width during Atherogenesis. *J. Lipid Res.* **1998**, *39*, 947–956. [CrossRef]

92. Jacob, R.F.; Cenedella, R.J.; Mason, R.P. Direct Evidence for Immiscible Cholesterol Domains in Human Ocular Lens Fiber Cell Plasma Membranes. *J. Biol. Chem.* **1999**, *274*, 31613–31618. [CrossRef] [PubMed]

93. Mainali, L.; Pasenkiewicz-Gierula, M.; Subczynski, W.K. Formation of Cholesterol Bilayer Domains Precedes Formation of Cholesterol Crystals in Membranes Made of the Major Phospholipids of Human Eye Lens Fiber Cell Plasma Membranes. *Curr. Eye Res.* **2020**, *45*, 162–172. [CrossRef] [PubMed]

94. Subczynski, W.K.; Pasenkiewicz-Gierula, M. Hypothetical Pathway for Formation of Cholesterol Microcrystals Initiating the Atherosclerotic Process. *Cell Biochem. Biophys.* **2020**, *78*, 241–247. [CrossRef] [PubMed]

95. Kar, R.; Batra, N.; Riquelme, M.A.; Jiang, J.X. Biological Role of Connexin Intercellular Channels and Hemichannels. *Arch. Biochem. Biophys.* **2012**, *524*, 2–15. [CrossRef] [PubMed]

96. Timsina, R.; Mainali, L. Association of Alpha-Crystallin with Fiber Cell Plasma Membrane of the Eye Lens Accompanied by Light Scattering and Cataract Formation. *Membranes* **2021**, *11*, 447. [CrossRef]

97. Timsina, R.; Wellisch, S.; Haemmerle, D.; Mainali, L. Binding of Alpha-Crystallin to Cortical and Nuclear Lens Lipid Membranes Derived from a Single Lens. *Int. J. Mol. Sci.* **2022**, *23*, 11295. [CrossRef]

98. Bassnett, S. Lens Organelle Degradation. *Exp. Eye Res.* **2002**, *74*, 1–6. [CrossRef]
99. Wride, M.A. Lens Fibre Cell Differentiation and Organelle Loss: Many Paths Lead to Clarity. *Philos. Trans. R. Soc. B Biol. Sci.* **2011**, *366*, 1219–1233. [CrossRef]

6. Electroformation of Giant Unilamellar Vesicles from Damp Lipid Films with a Focus on Vesicles with High Cholesterol Content

Electroformation of Giant Unilamellar Vesicles from Damp Lipid Films with a Focus on Vesicles with High Cholesterol Content

Ivan Mardešić [1,2] , Zvonimir Boban [1] and Marija Raguz [1,*]

1 Department of Medical Physics and Biophysics, University of Split School of Medicine, 21000 Split, Croatia; imardesi@mefst.hr (I.M.); zvonimir.boban@mefst.hr (Z.B.)
2 Doctoral Study of Biophysics, Faculty of Science, University of Split, 21000 Split, Croatia
* Correspondence: marija.raguz@mefst.hr; Tel.: +385-9876-8819

Abstract: Giant unilamellar vesicles (GUVs) are membrane models used to study membrane properties. Electroformation is one of the methods used to produce GUVs. During electroformation protocol, dry lipid film is formed. The drying of the lipid film induces the cholesterol (Chol) demixing artifact, in which Chol forms anhydrous crystals which do not participate in the formation of vesicles. This leads to a lower Chol concentration in the vesicle bilayers compared to the Chol concentration in the initial lipid solution. To address this problem, we propose a novel electroformation protocol that includes rapid solvent exchange (RSE), plasma cleaning, and spin-coating methods to produce GUVs. We tested the protocol, focusing on vesicles with a high Chol content using different spin-coating durations and vesicle type deposition. Additionally, we compared the novel protocol using completely dry lipid film. The optimal spin-coating duration for vesicles created from the phosphatidylcholine/Chol mixture was 30 s. Multilamellar vesicles (MLVs), large unilamellar vesicles (LUVs) obtained by the extrusion of MLVs through 100 nm membrane pores and LUVs obtained by extrusion of previously obtained LUVs through 50 nm membrane pores, were deposited on an electrode for 1.5/1 Chol/phosphatidylcholine (POPC) lipid mixture, and the results were compared. Electroformation using all three deposited vesicle types resulted in a high GUV yield, but the deposition of LUVs obtained by the extrusion of MLVs through 100 nm membrane pores provided the most reproducible results. Using the deposition of these LUVs, we produced high yield GUVs for six different Chol concentrations (from 0% to 71.4%). Using a protocol that included dry lipid film GUVs resulted in lower yields and induced the Chol demixing artifact, proving that the lipid film should never be subjected to drying when the Chol content is high.

Keywords: GUV; electroformation; cholesterol; damp lipid film; lipid film deposition; cholesterol demixing artifact

1. Introduction

Vesicles are membrane models consisting of one or more lipid bilayers filled with aqueous solution. They are commonly used to investigate membrane properties under controlled conditions [1,2]. Depending on their structure, lipid vesicles can be unilamellar, multilamellar, or oligolamellar. Unilamellar vesicles have only a single lipid bilayer, multilamellar vesicles (MLVs) contain multiple lipid bilayers arranged in concentric circles, and oligolamellar vesicles contain smaller vesicles within the outer bilayer. With respect to their size, unilamellar vesicles are usually divided into three groups: small (SUVs) (<100 nm), large (LUVs) (100 nm–1 μm), and giant (GUVs) (>1 μm). SUVs and LUVs are the most common type of unilamellar vesicles produced by extrusion, and they are often used for drug delivery studies or in protocols for the formation of GUVs [3] or supported lipid bilayers [4]. Among these three groups, researchers studying membrane properties and organization are most interested in GUVs, as their size is similar to that of eukaryotic cells.

The first attempt to form GUVs was performed by Reeves and Dowben [2]. In their approach, the lipid mixture is deposited onto the electrode, dried to form a dry lipid film that is then rehydrated, and the aqueous solution is driven between the lipid stacks due to osmotic pressure (gentle hydration). Because of the amphiphilic nature of lipids, it is unfavorable for their hydrophobic acyl chains to be exposed to the aqueous solution, so the lipid bilayers enclose, forming vesicles. Even though this method is straightforward and simple, it results in a low GUVs yield, with many defects [5].

One of the most commonly common currently used methods for the production of GUVs is electroformation, which was developed by Angelova and Dimitrov in 1986 [6]. This method improved the previous approach by applying an external electric field to the lipid film, in addition to the use of hydration. In their protocol, lipids are dissolved in an organic solvent and deposited on an electrode. The organic solvent is then evaporated using a stream of inert gas and a vacuum. The electrode with the lipid film is used to construct an electroformation chamber, which is filled with a desired aqueous solution and connected to an external alternating electric field. The electric field and osmotic pressure promote the detachment of the lipids from the electrode, leading to the formation of GUVs [7]. Compared to samples obtained using the gentle hydration method, the vesicles formed by electroformation exhibit a higher yield, a lower number of defects, and a higher proportion of unilamellar vesicles [5].

The electroformation method has evolved significantly since its inception, with various modifications made to the tested protocols [8–10] in order to improve the method's reproducibility and enable its compatibility with a wider range of lipid mixtures. Some groups attempted to improve the method by replacing the lipids dissolved in an organic solvent with an aqueous solution of SUVs or LUVs [11]. It was concluded that the use of a unilamellar vesicle aqueous solution improved the efficiency of GUVs formation compared to the deposition of lipids dissolved in an organic solvent. It was also shown that the formation of GUVs, with buffers as internal solutions, is easier when using buffer-loaded SUVs or LUVs compared to the previous approach, in which the buffer would be applied to a dry lipid film [11]. Another advantage of this modification is the possibility of improved proteoliposome formation, due to reduced protein denaturation when the organic solvent is removed from the protocol [11–13].

Another issue with the traditional protocol was the use of the drop-deposition method for lipid film deposition [6,7,9]. The problem with this approach is the formation of lipid films of nonuniform thickness, resulting in high vesicle heterogeneity in the sample and low experimental reproducibility. Various alternative approaches have been tested to address this issue [14–16]. The one we found to be optimal in terms of ease of use and quality of the final result is the spin-coating technique, in which uniform lipid films are obtained by depositing the lipid solution onto a flat surface and spinning it at a high angular velocity [15,17–20].

The initial electroformation protocol also turned out to be incompatible with lipid mixtures containing a high cholesterol (Chol) concentration. This is due to the precipitation of Chol into anhydrous Chol crystals during the lipid film drying phase [21]. When the film is rehydrated, these anhydrous Chol crystals do not participate in the bilayer formation, resulting in a lower Chol concentration in the vesicle bilayers compared to the Chol concentration in the initial lipid solution. Chol demixing can be avoided by using the rapid solvent exchange (RSE) method [22,23]. In this method, lipids dissolved in an organic solvent are first mixed with an aqueous solution. By suddenly decreasing the pressure, the organic solvent is evaporated, leaving behind an aqueous solution of MLVs. In order to avoid Chol demixing artifact during GUVs preparation, Baykal-Caglar et al. tested the use of electroformation from a damp lipid film formed by depositing MLVs, produced using the RSE method, onto the electrode [3]. The final results were positive, indicating a higher Chol content in the formed GUVs compared to that of the GUVs obtained using the original protocol. However, the described protocol is very time consuming, due to the long

lipid film drying time (22–25 h), and the MLVs were deposited using the drop-deposition method, inevitably resulting in a non-uniform film.

In addition to the deposition techniques and the properties of the lipid mixtures, the cleanliness of the electrodes has also been shown to influence the electroformation results. Pretreatment of the electrodes with plasma improved the efficiency of the formation of GUVs containing buffers with physiological charge levels. This is probably due to the fact that the plasma makes the electrode surface more hydrophilic, facilitating the hydration of the lipid film and the subsequent formation of the lipid bilayers [24].

In our previous study, we adapted the traditional electroformation protocol to incorporate all of the aforementioned improvements, allowing us to bypass the dry lipid film phase and produce a uniform damp lipid film (Figure 1) [25]. Inspired by the vesicle fusion method for the preparation of supported lipid bilayers [4,26,27], the adapted protocol uses spin-coating to deposit an aqueous solution of LUVs onto a plasma-treated electrode. The hydrophilized surface induces LUV rupturing and the formation of lipid bilayers on the electrode surface. The bilayers later detach and form GUVs under the influence of osmotic pressure and an alternating electric field. With respect to the approach of Baykal-Caglar et al., these modifications significantly shorten the duration of the protocol, while also increasing the experiment reproducibility. In order to make the protocol compatible with high Chol concentrations, the deposited LUVs were obtained by extruding a solution of MLVs, produced using the RSE method, and the lipid film was not dried after spin-coating.
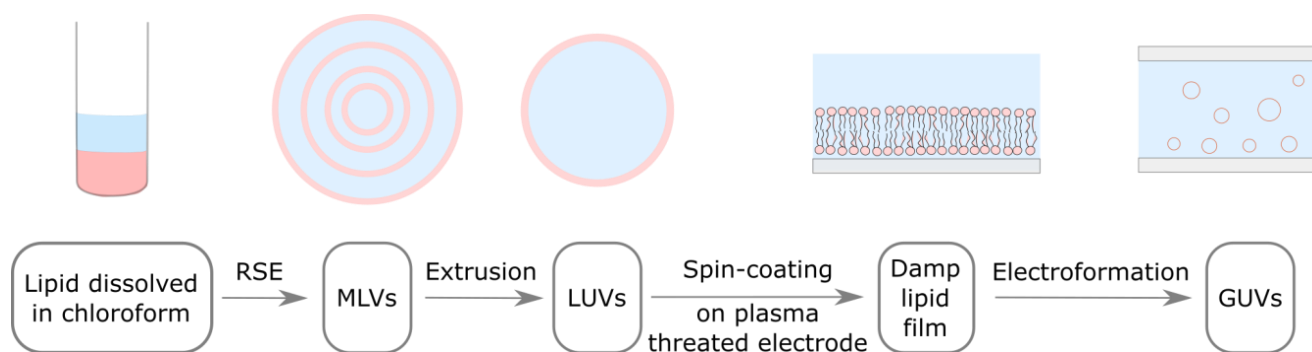
Figure 1. Adapted electroformation protocol. Lipids dissolved in organic solvent (pink) are mixed with an aqueous solution (light blue). MLVs are formed using the RSE method. MLV solution is extruded through a filter with membrane pores in order to obtain LUVs. LUV solution is spin-coated on a plasma threated electrode, where these vesicle rupture and form a damp lipid film. An electrode with damp lipid film is used to build an electroformation chamber, where lipid bilayers detach and form GUVs under the influence of osmotic pressure and an alternating electric field.

The efficiency of the protocol was tested using 1/1 Chol/1-palmitoyl-2-oleoyl-glycero-3-phosphocholine (POPC) and 1/1/1 Chol/POPC/sphingomyelin lipid mixtures [25]. This ternary mixture was selected because these three lipid types are highly prevalent in biological membranes. Particularly noteworthy is the phenomenon of liquid order–liquid disorder phase separation, which plays a crucial role in the development of lipid rafts [28–31]. Furthermore, recent research has also shown the possibility of the coexistence of three phases of similar composition in GUVs [32].

Compared to the protocol involving a drying step, the new protocol resulted in a similar or better GUV yield, while exhibiting the potential to significantly reduce the Chol demixing artifact [25]. In order to further increase the reproducibility and yield of the obtained samples, this study will focus on the further optimization of the new protocol.

Special focus is placed on GUVs with a high Chol content, for which the Chol demixing issue is more pronounced. Chol plays diverse roles in phospholipid membranes, impacting membrane thickness and rigidity [33–35], domain formation [36,37], cell signaling [38], and bending modulus [39]. Positioned vertically within the phospholipid bilayer, its polar head

aligns with other phospholipid heads, while its fused ring structure resides within the acyl chain region. This orientation enables cholesterol to modulate the lateral organization of phospholipids, affecting membrane properties across various depths. These regulatory actions include changes in the bilayer transition temperature [40] and the emergence of specific membrane phases and domains. For vesicles with a Chol content lower than ~15 mol%, the lipid bilayer is in a liquid disordered phase. At 30–50 mol%, it is in a liquid ordered phase. Cholesterol bilayer domains (CBDs), containing only Chol molecules with no phospholipids, start forming when the Chol content is greater than 50 mol%. After reaching the Chol solubility limit at ~66 mol%, excess Chol precipitates in the form of Chol crystals [41].

Modeling membranes with such a high Chol concentration is important for groups such as ours that study the properties of the eye lens plasma membranes [21,42,43] or for groups performing atherosclerosis research [44]. The protocol may also be beneficial for the formation of proteoliposomes by reducing the denaturation of proteins that occurs during the preparation of GUVs from lipids dissolved in an organic solvent or during film drying.

2. Materials and Methods

2.1. Materials

POPC and Chol were purchased from Avanti Polar Lipids Inc. (Alabaster, AL, USA), while the fluorescent dye 1,1-dioctadecyl-3,3,3,3-tetramethylindocarbocyanine Perchlorate (DiIC$_{18}$(3)) was acquired from Invitrogen, Thermo Fisher Scientific (Waltham, MA, USA). Lipids were stored at -20 °C when not in use. Indium tin oxide (ITO) coated glass (ICG-90 INS 115, resistance 70–100 Ω), measuring $25 \times 75 \times 1.1$ mm, was procured from Delta Technologies (Loveland, LO, USA). Fresh ITO-coated glass was employed for each preparation to ensure the efficient formation of GUVs [45]. Mili-Q deionized water (Merck, Rahway, NJ, USA), preheated to 60 °C, served as the internal chamber solution.

2.2. Preparation of Multilamellar Vesicles Using the Rapid Solvent Exchange Method

Initially, multilamellar vesicles (MLVs) were generated using a home-built RSE device to circumvent the cholesterol demixing issue. A lipid mixture dissolved in chloroform was prepared by blending 25 mg/mL of POPC, 20 mg/mL of cholesterol (Chol), and 1 mg/mL of DiIC$_{18}$(3), in appropriate proportions. The Chol/POPC mixing ratios were maintained between 0 and 2.5 (Chol mixing concentration of 0% to 71.4%), while the DiIC$_{18}$(3)/POPC mixing ratio was fixed at 1/500. The total lipid mass amounted to 2.1 mg. Subsequently, 400 μL of Mili-Q water was introduced into the solution, and the mixture was vortexed (Vortex IR, Star Lab, Blakelands, UK) at an angular velocity of 2200 rpm. Throughout the vortexing process, the pressure was regulated to approximately 0.05 bar using a vacuum pump (HiScroll 6, Pfeiffer Vacuum, Asslar, Germany). The sample was maintained at the specified pressure for 90 s to ensure the complete removal of residual organic solvent.

2.3. Preparation of Large Unilamellar Vesicles

The MLVs solution was extruded utilizing an Avanti Mini Extruder (Avanti Polar Lipids, Inc, Alabaster, AL, USA), passing through either a 50 or a 100 nm pore diameter polycarbonate filter (Nuclepore Track-Etch Membrane, Whatman, UK) 15 times to achieve a uniform LUV suspension. To prevent the loss of the lipid suspension, the filters and membranes were pre-wetted with Mili-Q water. Additional Mili-Q water was added to the LUV solution to reach a lipid concentration of 3.5 mg/mL.

2.4. Preparation of the Damp Lipid Film

Prior to conducting the experiments, the ITO-coated glass was submerged in Mili-Q deionized water. Subsequently, the glass was wiped using lint-free cloths saturated with 70% ethanol. Following this, the glass underwent treatment with oxygen plasma for a duration of 1 min utilizing a plasma cleaner (PDC-002-HPCE with the PLASMAFLO

PDC-FMG-2 attachment, Harrick Plasma, Ithaca, NY, USA) connected to a vacuum pump (HiScroll 6, Pfeiffer Vacuum, Assler, Germany).

Unless specified otherwise, a volume of 550 μL of LUV suspension was applied onto the hydrophilic plasma-treated ITO-coated glass electrode and promptly spin-coated using a spin-coater (SM-150, Sawatec, Sax, Switzerland). The electrode was spun at 600 rpm, achieving the final speed within 1 s. The duration of spin-coating, unless specified otherwise, was maintained at 30 s to guarantee the formation of a damp, uniform lipid film. To prevent unintended evaporation, the coated ITO-coated glass was transferred into a Petri dish and promptly utilized to form an electroformation chamber.

2.5. Electroformation Protocol

The electroformation chamber was constructed by sandwiching two 25×37.5 mm ITO-coated glasses with a 1.6 mm thick Teflon spacer in between. The electrodes were created by slicing a 25×75 mm ITO-coated glass using a diamond pen cutter. To form the electroformation chamber, the lipid-coated glass was sealed to the Teflon spacer with vacuum grease. Following the addition of 280 μL of Mili-Q water, the stopper was sealed using vacuum grease, ensuring that there was no contact between the grease and water to prevent any detrimental effects of grease contamination on GUV formation [9]. The chamber was secured with clamps at three points along the electrodes, two adjacent to the stopper and one opposite it. Subsequently, the chamber was connected to a pulse generator (UTG9005C, UNI–T, Dongguan City, China or PSG 9080, Joy-IT, Neukirchen-Vluyn, Germany) and placed in an incubator set to a temperature of 60 °C. Copper tape was applied to the outer edges of the electrode to enhance wire–electrode contact. Consistent with previous experiments [17,18,25], a voltage of 2 V and a frequency of 10 Hz were maintained. After 2 h, the pulse generator was turned off, and the chamber remained in the incubator for an additional hour.

2.6. Dynamic Light Scattering

Dynamic light scattering (DLS) was utilized to determine the hydrodynamic diameter and polydispersity index of the liposome suspensions (Litesizer 500, Anton Paar, Graz, Austria).

2.7. Fluorescence Imaging and Data Analysis

To cover the entire volume of the chamber, images were captured from 16 different regions of the sample. A total of 100 vesicles were then randomly selected from these images. In cases where the images did not contain 100 vesicles, all observed vesicles were included in the analysis. Imaging was conducted utilizing a fluorescence microscope (Olympus BX51, Olympus, Tokyo, Japan), and the vesicle diameters were measured using the line tool within Fiji software [46].

Unless specifically indicated otherwise, the numerical results are presented as the mean ± standard deviation. All data analysis and visualization were carried out using the R programming language [47].

3. Results and Discussion

In order to further improve our newly developed protocol, we performed experiments to test the effect of using different vesicle types during lipid film deposition, the effect of spin-coating duration, and the effect of different Chol concentrations. To confirm the utility of the optimized protocol, our samples were also compared to those obtained from fully dried lipid films.

3.1. Optimization of the Protocol

#### 3.1.1. The Spin-Coating Duration for Formation of Damp Lipid Film

We tested various coating durations ranging from 15 s to 60 s at an angular speed of 600 rpm. The deposited liquid was an aqueous suspension of LUVs obtained by extruding

MLVs through a 100 nm pore diameter filter. We concluded that 30 s is the optimal duration when using the aforementioned lipid mixtures. A shorter duration of spin-coating resulted in an uneven film thickness or a film that was too wet, leading to the low reproducibility of the experiment and high GUV heterogeneity within the successful samples. As shown in our previous study, for a spin-coating duration of 30 s, the lipid film remained damp, with high GUV electroformation yield [25]. At a duration of 30 s, water-dissolved lipid droplets can still be seen on the electrode, which assures us that the lipid film is still damp. Longer spin-coating durations were avoided due to the risk of excessive drying of the lipid film and the induction of the Chol demixing artifact. To prevent additional drying of the film due to water evaporation, the electrode was immediately used to build an electroformation chamber.

3.1.2. Comparison of MLVs and LUVs Deposition on the Electrode

Since the film in our protocol is kept damp, we rely on the fact that the vesicles to rupture when they come into contact with a hydrophilized electrode surface to obtain a lipid film [26,48,49]. However, how easily the vesicles rupture depends strongly upon the vesicle type and size [50]. Therefore, we compared the GUVs prepared from lipid films obtained with three different types of vesicles—MLVs formed using the RSE method, LUVs obtained by the extrusion of MLVs through 100 nm membrane pores (LUV 100), and LUVs formed by the additional extrusion of LUV 100 vesicles through 50 nm membrane pores (LUV 50). The Chol/POPC mixing ratio was maintained at 1.5 in all these experiments. DLS was used to determine the size distribution of the suspensions of each vesicle type. The average hydrodynamic diameter and polydispersity index were 761.1 nm and 0.29 for MLVs, 141.9 nm and 0.1 for LUV 100 vesicles, and 96.2 nm, and 0.12 for LUV 50 vesicles, respectively.

The deposition of the lipid film from all three vesicle types resulted in a high GUV yield (Figure 2a), with average diameters and standard deviations when using MLVs, LUV 50, and LUV 100 vesicles being 28.5 ± 3.71 μm, 33.9 ± 5.27 μm, and 24.5 ± 1.39 μm, respectively (Figure 2b). Although the average diameter of the GUVs obtained from LUV 100 vesicles deposition was the smallest, this method resulted in the highest reproducibility among the samples (smallest error bars in Figure 2b). In addition, the widths of the sample diameter distributions were also the smallest for this method, indicating the highest uniformity of GUV size compared to the other two protocols (Figure 2c). The advantage of depositing MLVs instead of LUVs is the shorter protocol duration, as the conversion to LUVs is skipped. However, the samples made from the MLV deposits displayed a lower reproducibility (Figure 2b) and a more heterogeneous GUV size distribution (Figure 2c) compared to samples obtained by depositing the LUV 100 vesicles. This could be due to the larger average diameter and polydispersity index of MLVs compared to those of LUVs, as smaller vesicles rupture more easily compared to larger ones. The average diameter of the GUVs was the largest when the LUV 50 vesicles were used. Since smaller vesicles rupture more easily, we expected the reproducibility to be the highest for the LUV 50 vesicles, but this was not the case (Figure 2c). This is probably a side effect of the additional extrusion compared to that of the LUV 100 vesicles. We tried to produce LUV 50 vesicles directly from MLVs, but the flow resistance was too great, especially at higher Chol concentrations. Consequently, we first produced LUV 100 vesicles and then passed them through a 50 nm filter, as LUV 100 vesicles offered less resistance compared to the MLVs. Due to the additional extrusion, the duration of the protocol was even longer, causing a greater loss of final suspension volume, as part of the lipid suspension is always lost during the extrusion process due to fluid leakage. Consequently, the GUV distributions we obtained after the deposition of such suspensions were less reproducible (Figure 2b,c), as a different total lipid amount was deposited on the electrode. We also tried extruding the vesicles through a 30 nm filter, but this only exacerbated the problem of high resistance, so we decided to exclude such suspensions from the comparison.
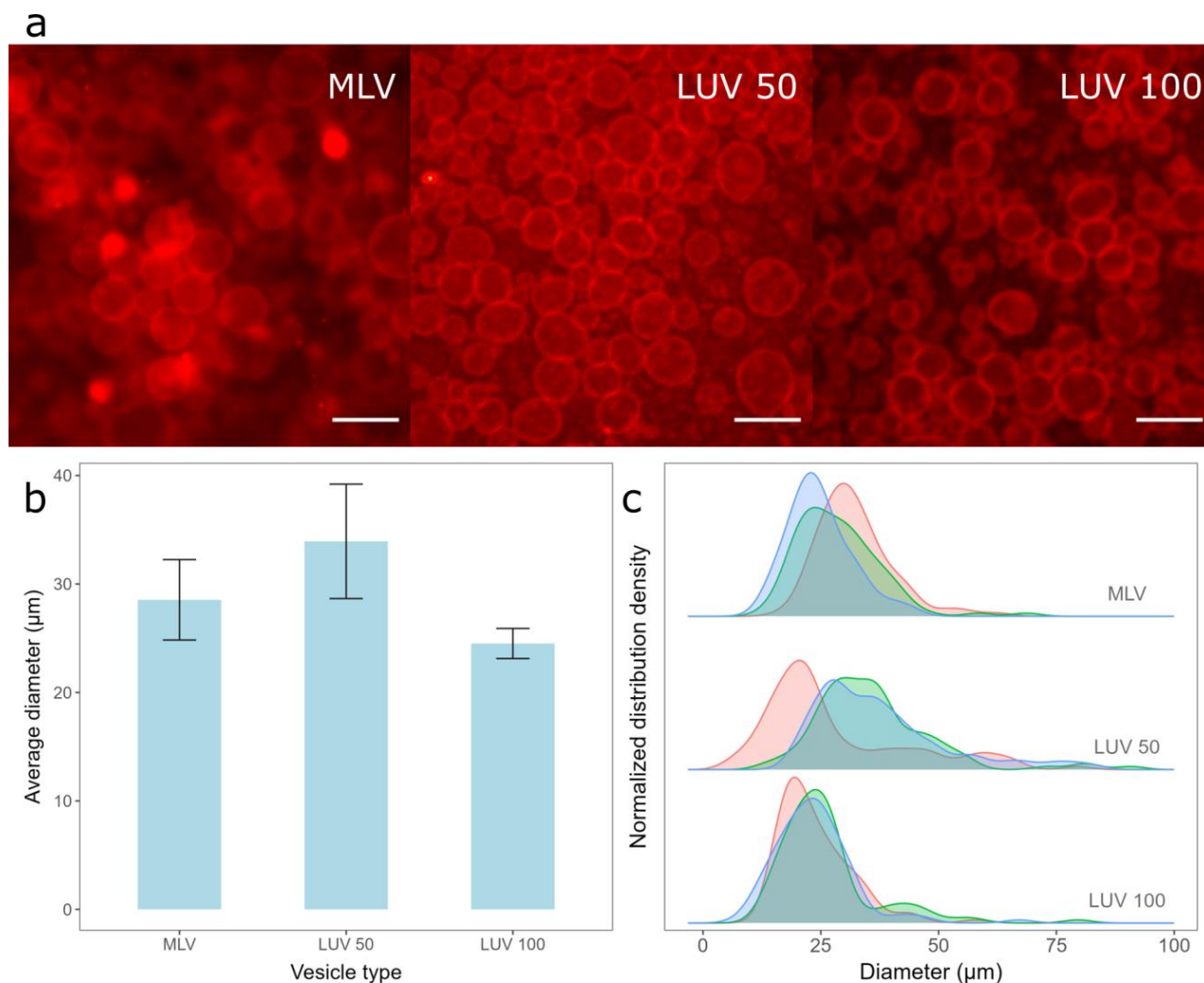
Figure 2. Electroformation of GUVs for deposition of different vesicle types. (**a**) Fluorescence microscopic images of GUVs formed when different vesicle types were deposited. MLV represents the deposition of MLVs on the electrode, LUV 100 represents the deposition of LUVs formed by extruding MLVs through 100 nm membrane pores, and LUV 50 represents the deposition of LUVs formed by extruding LUV 100 vesicles through 50 nm membrane pores. The scale bar represents 50 μm. (**b**) Comparison of average diameters and standard deviations of GUVs for preparations from three different vesicle types. The averages and standard deviations were calculated by averaging the mean diameters from three independent samples for each condition. (**c**) Size distribution densities of GUVs for deposition of different vesicle types for each sample. Each distribution density represents one independent sample (100 vesicles).

3.2. The Effect of Chol Content

After deciding on the duration of spin-coating and the vesicle type to be used for deposition, we tested the effect of Chol content on GUV electroformation. The mean diameter and standard errors of the formed GUVs were 45.5 ± 5 μm, 41.13 ± 1.68 μm, 32.67 ± 1.28 μm, 24.51 ± 0.8 μm, 29.18 ± 0.08 μm, and 26.97 ± 2.95 μm, respectively, for a Chol/POPC mixing ratio between 0 and 2.5 (Figure 3a). As expected, the distribution of the vesicle diameters shifted to lower values with increasing Chol content (Figure 3b) [18]. This could be due to decreasing membrane elasticity and increasing rigidity when more Chol is added, making vesicle formation more difficult. For Chol/POPC mixing ratios greater than 1.5 (more than 60% of Chol in the mixture), where the GUVs may contain CBDs, a significant decrease in the average GUV diameter is measured. It is about 40% lower compared to that of the pure POPC bilayer.
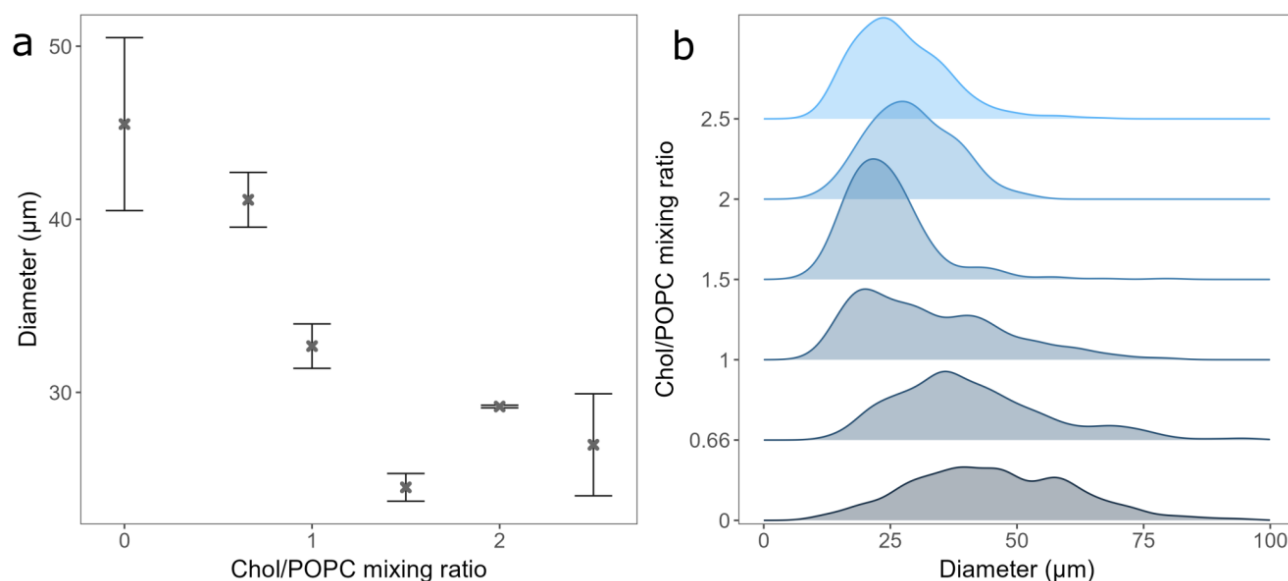
Figure 3. (**a**) GUVs mean diameters for different Chol/POPC mixing ratios. Points and bars represent mean values and their standard errors. (**b**) Size distribution densities of GUVs for different Chol/POPC mixing ratios. All experiments were performed using the deposition of LUV 100 vesicles spin-coated onto electrode for 30 s.

For Chol/POPC mixing ratios of 2 and lower, we found only a couple of small anhydrous Chol crystals per sample. This is probably due to small dry patches forming on the electrode during spin-coating. However, compared to electroformation samples made using a completely dry lipid film, this amount was negligible.

3.3. Comparison with Samples Obtained from Completely Dry Lipid Films

Finally, the samples prepared using the optimized protocol were compared with those obtained from fully dried lipid films. These additional samples were made by spin-coating the aqueous lipid suspension for either 30 s or 240 s and then placing the coated electrodes in a desiccator for 30 min to ensure that any residual water was removed from the sample (Figure 4a). Drying not only increased the number of Chol crystals, but also decreased the GUV yield (Figure 4b,c). At a low Chol content, a negligible number of GUVs were found in the samples. For the high Chol content, the GUV yield was much lower compared to that obtained in the equivalent damp lipid film scenario, with many defects and anhydrous Chol crystals.
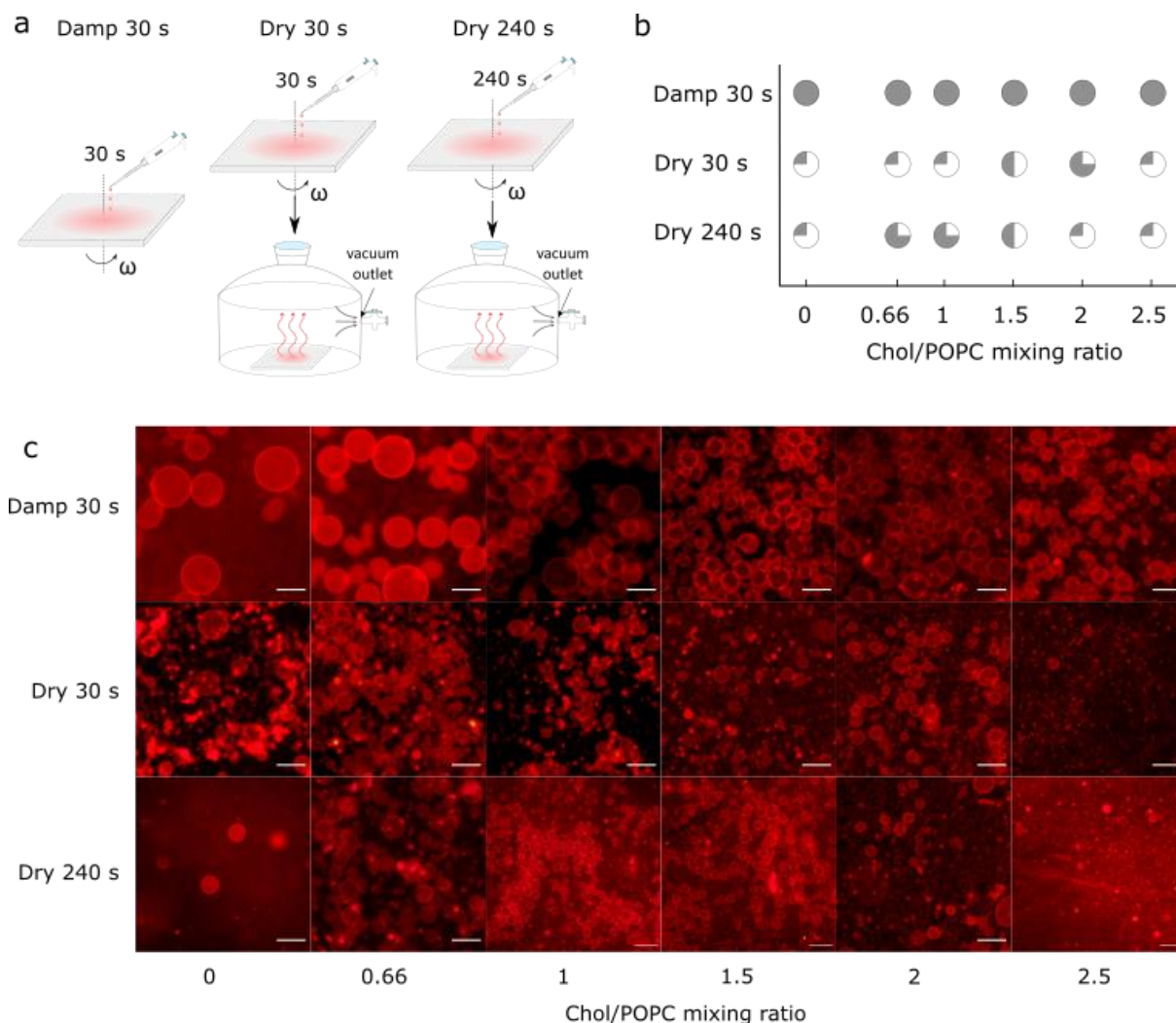
Figure 4. (**a**) Schematic depiction of differences obtained using our novel protocol for three different experiments. In the first experiment, damp lipid film was formed by depositing LUV 100 vesicles on an electrode and spinning it for 30 s at 600 rpm angular velocity (Damp 30 s). In the second experiment, Damp 30 s lipid film was held under vacuum for 30 min (Dry 30 s). In the third experiment, instead of spinning for 30 s, the electrode was spun for 240 s, and afterwards held under vacuum for 30 min (Dry 240 s). (**b**) Success of electroformation using Damp 30 s, Dry 30 s, and Dry 240 s protocols for obtaining lipid films, depending on different Chol/POPC mixing ratios. Success is based on the population homogeneity, yield, and number of defects. It is displayed through circle fullness, where a fuller circle indicates greater success. Empty circles (white circle) denote that no GUVs were formed or that their number was negligible; quarter circles represent low, half and three-quarter circles indicate medium, and full circles (gray circle) indicate high success. (**c**) Fluorescence microscopy images of GUVs for the different Chol/POPC mixing ratios using three different approaches for obtaining lipid films. The scale bar represents 50 μm.

4. Conclusions

In this study, we optimized an improved electroformation protocol that bypasses the dry lipid film phase of the traditional electroformation method and combines the RSE method, plasma cleaning, and spin-coating techniques to obtain a damp lipid film. To further optimize the protocol, we conducted additional experiments to test the effect of using different vesicle types during lipid film deposition, the effect of spin-coating duration, and the effect of different Chol concentrations. In order to confirm the utility of

the optimized protocol, our samples were also compared to those obtained from fully dried lipid films.

A spin-coating duration of 30 s was found to be optimal in terms of the balance between electroformation successfulness and lipid film dampness. A longer spin-coating duration would dry out the lipid film and exacerbate Chol demixing artifact. Compared to previous protocols that used damp lipid films, such as that employed by Baykal-Caglar et al., our method significantly shortened the preparation time by eliminating the 22–25 h high-humidity drying phase and replacing it with 30 s of spin-coating [3].

In terms of the vesicle type used for film deposition, the LUV 100 vesicles provided the best results in terms of reproducibility, even though the average diameter was smaller compared to that of the MLVs and the LUV 50 vesicles. The advantage of depositing MLVs instead of LUVs is the shorter protocol duration. However, samples made from MLV deposits displayed lower reproducibility and a more heterogeneous GUV size distribution. This is probably due to a larger average diameter and polydispersity index of the MLVs compared to the LUVs, as smaller vesicles rupture more easily compared to larger ones. The average diameter of the GUVs was the greatest when the LUV 50 vesicles were used, but the reproducibility of the samples was the lowest. This is probably a side effect of the additional extrusion performed compared to that used for the LUV 100 vesicles. Due to high flow resistance through a 50 nm filter, we could not directly extrude MLVs. We first produced LUV 100 vesicles and then passed them through a 50 nm filter. The additional extrusion step extends the duration of the protocol even further and causes a greater loss of final suspension volume, as part of the lipid suspension is always lost through liquid leakage during the extrusion process. This problem was even greater in our case, as the resistance increased along with the increasing Chol/POPC mixing ratio.

Finally, our samples were also compared with those obtained from fully dried lipid films. Drying increased the amount of Chol crystals found, which proves that the lipid film should never be subjected to a drying phase when using mixtures with a high Chol content.

This protocol allows us to successfully prepare GUVs and study the physical properties, lateral organization, and domain function of lipid membranes with a very high Chol content, such as the fiber cell plasma membrane of the eye lens. Furthermore, the avoidance of organic solutions and plasma cleaning of the electrode have been shown to be advantageous for the preparation of GUVs containing charged lipids and buffer solutions. Consequently, we believe that our protocol might also prove successful in those cases as well. Additionally, the protocol could also be adapted for protein–membrane interaction studies because protein denaturation is reduced by avoiding the dry film phase and due to the absence of organic solvents [11–13].

Author Contributions: Conceptualization, I.M. and M.R.; methodology, I.M. and Z.B.; software, I.M. and Z.B.; validation, I.M. and Z.B.; formal analysis, I.M. and Z.B.; investigation, I.M. and Z.B.; resources, M.R.; data curation, I.M. and Z.B.; writing—original draft preparation, I.M.; writing—review and editing, I.M., Z.B. and M.R.; visualization, I.M. and Z.B.; supervision, M.R.; project administration, M.R.; funding acquisition, M.R. All authors have read and agreed to the published version of the manuscript.

Institutional Review Board Statement: Not applicable.

Data Availability Statement: The data presented in this study are available upon reasonable request from the corresponding author.

Conflicts of Interest: The authors declare no conflicts of interest.

References

1. Ertel, A.; Marangoni, A.G.; Marsh, J.; Hallett, F.R.; Wood, J.M. Mechanical Properties of Vesicles. I. Coordinated Analysis of Osmotic Swelling and Lysis. *Biophys. J.* **1993**, *64*, 426–434. [CrossRef] [PubMed]
2. Reeves, J.P.; Dowben, R.M. Formation and Properties of Thin-Walled Phospholipid Vesicles. *J. Cell. Physiol.* **1969**, *73*, 49–60. [CrossRef]
3. Baykal-Caglar, E.; Hassan-Zadeh, E.; Saremi, B.; Huang, J. Preparation of Giant Unilamellar Vesicles from Damp Lipid Film for Better Lipid Compositional Uniformity. *Biochim. Biophys. Acta—Biomembr.* **2012**, *1818*, 2598–2604. [CrossRef] [PubMed]
4. Lind, T.K.; Cárdenas, M. Understanding the Formation of Supported Lipid Bilayers via Vesicle Fusion—A Case That Exemplifies the Need for the Complementary Method Approach (Review). *Biointerphases* **2016**, *11*, 020801. [CrossRef]
5. Rodriguez, N.; Pincet, F.; Cribier, S. Giant Vesicles Formed by Gentle Hydration and Electroformation: A Comparison by Fluorescence Microscopy. *Colloids Surf. B Biointerfaces* **2005**, *42*, 125–130. [CrossRef] [PubMed]
6. Angelova, M.I.; Dimitrov, D.S. Liposome Electro Formation. *Faraday Discuss. Chem. Soc.* **1986**, *81*, 303–311. [CrossRef]
7. Dimitrov, D.S.; Angelova, M.I. Lipid Swelling and Liposome Formation on Solid Surfaces in External Electric Fields. In *New Trends in Colloid Science*; Steinkopff: Darmstadt, Germany, 1987; Volume 56, pp. 48–56.
8. Boban, Z.; Mardešić, I.; Subczynski, W.K.; Raguz, M. Giant Unilamellar Vesicle Electroformation: What to Use, What to Avoid, and How to Quantify the Results. *Membranes* **2021**, *11*, 860. [CrossRef] [PubMed]
9. Veatch, S.L. Electro-Formation and Fluorescence Microscopy of Giant Vesicles with Coexisting Liquid Phases. In *Lipid Rafts*; Springer: Berlin/Heidelberg, Germany, 2007; Volume 398, pp. 59–72.
10. Morales-Penningston, N.F.; Wu, J.; Farkas, E.R.; Goh, S.L.; Konyakhina, T.M.; Zheng, J.Y.; Webb, W.W.; Feigenson, G.W. GUV Preparation and Imaging: Minimizing Artifacts. *Biochim. Biophys. Acta—Biomembr.* **2010**, *1798*, 1324–1332. [CrossRef] [PubMed]
11. Pott, T.; Bouvrais, H.; Méléard, P. Giant Unilamellar Vesicle Formation under Physiologically Relevant Conditions. *Chem. Phys. Lipids* **2008**, *154*, 115–119. [CrossRef]
12. Girard, P.; Pécréaux, J.; Lenoir, G.; Falson, P.; Rigaud, J.L.; Bassereau, P. A New Method for the Reconstitution of Membrane Proteins into Giant Unilamellar Vesicles. *Biophys. J.* **2004**, *87*, 419–429. [CrossRef]
13. Witkowska, A.; Jablonski, L.; Jahn, R. A Convenient Protocol for Generating Giant Unilamellar Vesicles Containing SNARE Proteins Using Electroformation. *Sci. Rep.* **2018**, *8*, 9422. [CrossRef]
14. Oropeza-Guzman, E.; Riós-Ramírez, M.; Ruiz-Suárez, J.C. Leveraging the Coffee Ring Effect for a Defect-Free Electroformation of Giant Unilamellar Vesicles. *Langmuir* **2019**, *35*, 16528–16535. [CrossRef] [PubMed]
15. Estes, D.J.; Mayer, M. Electroformation of Giant Liposomes from Spin-Coated Films of Lipids. *Colloids Surf. B Biointerfaces* **2005**, *42*, 115–123. [CrossRef]
16. Le Berre, M.; Chen, Y.; Baigl, D. From Convective Assembly to Landau−Levich Deposition of Multilayered Phospholipid Films of Controlled Thickness. *Langmuir* **2009**, *25*, 2554–2557. [CrossRef]
17. Boban, Z.; Puljas, A.; Kovač, D.; Subczynski, W.K.; Raguz, M. Effect of Electrical Parameters and Cholesterol Concentration on Giant Unilamellar Vesicles Electroformation. *Cell Biochem. Biophys.* **2020**, *78*, 157–164. [CrossRef] [PubMed]
18. Boban, Z.; Mardešić, I.; Subczynski, W.K.; Jozić, D.; Raguz, M. Optimization of Giant Unilamellar Vesicle Electroformation for Phosphatidylcholine/Sphingomyelin/Cholesterol Ternary Mixtures. *Membranes* **2022**, *12*, 525. [CrossRef] [PubMed]
19. Politano, T.J.; Froude, V.E.; Jing, B.; Zhu, Y. AC-Electric Field Dependent Electroformation of Giant Lipid Vesicles. *Colloids Surf. B Biointerfaces* **2010**, *79*, 75–82. [CrossRef]
20. Billerit, C.; Jeffries, G.D.M.; Orwar, O.; Jesorka, A. Formation of Giant Unilamellar Vesicles from Spin-Coated Lipid Films by Localized IR Heating. *Soft Matter* **2012**, *8*, 10823–10826. [CrossRef]
21. Raguz, M.; Kumar, S.N.; Zareba, M.; Ilic, N.; Mainali, L.; Subczynski, W.K. Confocal Microscopy Confirmed That in Phosphatidyl-choline Giant Unilamellar Vesicles with Very High Cholesterol Content Pure Cholesterol Bilayer Domains Form. *Cell Biochem. Biophys.* **2019**, *77*, 309–317. [CrossRef]
22. Buboltz, J.T.; Feigenson, G.W. A Novel Strategy for the Preparation of Liposomes: Rapid Solvent Exchange. *Biochim. Biophys. Acta—Biomembr.* **1999**, *1417*, 232–245. [CrossRef]
23. Buboltz, J.T. A More Efficient Device for Preparing Model-Membrane Liposomes by the Rapid Solvent Exchange Method. *Rev. Sci. Instrum.* **2009**, *80*, 124301. [CrossRef] [PubMed]
24. Li, Q.; Wang, X.; Ma, S.; Zhang, Y.; Han, X. Electroformation of Giant Unilamellar Vesicles in Saline Solution. *Colloids Surf. B Biointerfaces* **2016**, *147*, 368–375. [CrossRef] [PubMed]
25. Boban, Z.; Mardešić, I.; Jozić, S.P.; Šumanovac, J.; Subczynski, W.K.; Raguz, M. Electroformation of Giant Unilamellar Vesicles from Damp Lipid Films Formed by Vesicle Fusion. *Membranes* **2023**, *13*, 352. [CrossRef]
26. Kalb, E.; Frey, S.; Tamm, L.K. Formation of Supported Planar Bilayers by Fusion of Vesicles to Supported Phospholipid Monolayers. *BBA—Biomembr.* **1992**, *1103*, 307–316. [CrossRef] [PubMed]
27. Tabaei, S.R.; Jackman, J.A.; Kim, M.; Yorulmaz, S.; Vafaei, S.; Cho, N.J. Biomembrane Fabrication by the Solvent-Assisted Lipid Bilayer (SALB) Method. *J. Vis. Exp.* **2015**, *2015*, e53073. [CrossRef]
28. de Almeida, R.F.M.; Fedorov, A.; Prieto, M. Sphingomyelin/Phosphatidylcholine/Cholesterol Phase Diagram: Boundaries and Composition of Lipid Rafts. *Biophys. J.* **2003**, *85*, 2406–2416. [CrossRef] [PubMed]
29. Veatch, S.L.; Keller, S.L. Miscibility Phase Diagrams of Giant Vesicles Containing Sphingomyelin. *Phys. Rev. Lett.* **2005**, *94*, 148101. [CrossRef] [PubMed]

30. Kusumi, A.; Fujiwara, T.K.; Tsunoyama, T.A.; Kasai, R.S.; Liu, A.; Hirosawa, K.M.; Kinoshita, M.; Matsumori, N.; Komura, N.; Ando, H.; et al. Defining Raft Domains in the Plasma Membrane. *Traffic* **2020**, *21*, 106–137. [CrossRef] [PubMed]
31. Herrmann, A.; Huster, D.; Sto, M.; Bunge, A.; Mu, P. Characterization of the Ternary Mixture of Sphingomyelin, POPC, and Cholesterol: Support for An Inhomogeneous Lipid Distribution at High Temperatures. *Biophys. J.* **2008**, *94*, 2680–2690. [CrossRef]
32. Balleza, D.; Mescola, A.; Marín–Medina, N.; Ragazzini, G.; Pieruccini, M.; Facci, P.; Alessandrini, A. Complex Phase Behavior of GUVs Containing Different Sphingomyelins. *Biophys. J.* **2019**, *116*, 503–517. [CrossRef]
33. Róg, T.; Pasenkiewicz-Gierula, M.; Vattulainen, I.; Karttunen, M. Ordering Effects of Cholesterol and Its Analogues. *Biochim. Biophys. Acta—Biomembr.* **2009**, *1788*, 97–121. [CrossRef]
34. Gumí-Audenis, B.; Costa, L.; Carlá, F.; Comin, F.; Sanz, F.; Giannotti, M. Structure and Nanomechanics of Model Membranes by Atomic Force Microscopy and Spectroscopy: Insights into the Role of Cholesterol and Sphingolipids. *Membranes* **2016**, *6*, 58. [CrossRef]
35. Khadka, N.K.; Timsina, R.; Rowe, E.; O'Dell, M.; Mainali, L. Mechanical Properties of the High Cholesterol-Containing Membrane: An AFM Study. *Biochim. Biophys. Acta—Biomembr.* **2021**, *1863*, 183625. [CrossRef]
36. Harder, T. Formation of Functional Cell Membrane Domains: The Interplay of Lipid–and Protein–Mediated Interactions. *Philos. Trans. R. Soc. Lond. Ser. B Biol. Sci.* **2003**, *358*, 863–868. [CrossRef] [PubMed]
37. Gupta, A.; Phang, I.Y.; Wohland, T. To Hop or Not to Hop: Exceptions in the FCS Diffusion Law. *Biophys. J.* **2020**, *118*, 2434–2447. [CrossRef] [PubMed]
38. Incardona, J.P.; Eaton, S. Cholesterol in Signal Transduction. *Curr. Opin. Cell Biol.* **2000**, *12*, 193–203. [CrossRef]
39. Karal, M.A.S.; Mokta, N.A.; Levadny, V.; Belaya, M.; Ahmed, M.; Ahamed, M.K.; Ahammed, S. Effects of Cholesterol on the Size Distribution and Bending Modulus of Lipid Vesicles. *PLoS ONE* **2022**, *17*, e0263119. [CrossRef]
40. Redondo-Morata, L.; Giannotti, M.I.; Sanz, F. Influence of Cholesterol on the Phase Transition of Lipid Bilayers: A Temperature-Controlled Force Spectroscopy Study. *Langmuir* **2012**, *28*, 12851–12860. [CrossRef]
41. Mainali, L.; Raguz, M.; Subczynski, W.K. Formation of Cholesterol Bilayer Domains Precedes Formation of Cholesterol Crystals in Cholesterol/Dimyristoylphosphatidylcholine Membranes: EPR and DSC Studies. *J. Phys. Chem. B* **2013**, *117*, 8994–9003. [CrossRef]
42. Raguz, M.; Mainali, L.; Widomska, J.; Subczynski, W.K. The Immiscible Cholesterol Bilayer Domain Exists as an Integral Part of Phospholipid Bilayer Membranes. *Biochim. Biophys. Acta—Biomembr.* **2011**, *1808*, 1072–1080. [CrossRef]
43. Raguz, M.; Mainali, L.; O'Brien, W.J.; Subczynski, W.K. Lipid Domains in Intact Fiber-Cell Plasma Membranes Isolated from Cortical and Nuclear Regions of Human Eye Lenses of Donors from Different Age Groups. *Exp. Eye Res.* **2015**, *132*, 78–90. [CrossRef] [PubMed]
44. Tulenko, T.N.; Chen, M.; Mason, P.E.; Mason, R.P. Physical Effects of Cholesterol on Arterial Smooth Muscle Membranes: Evidence of Immiscible Cholesterol Domains and Alterations in Bilayer Width during Atherogenesis. *J. Lipid Res.* **1998**, *39*, 947–956. [CrossRef] [PubMed]
45. Herold, C.; Chwastek, G.; Schwille, P.; Petrov, E.P. Efficient Electroformation of Supergiant Unilamellar Vesicles Containing Cationic Lipids on ITO-Coated Electrodes. *Langmuir* **2012**, *28*, 5518–5521. [CrossRef]
46. Schindelin, J.; Arganda-Carreras, I.; Frise, E.; Kaynig, V.; Longair, M.; Pietzsch, T.; Preibisch, S.; Rueden, C.; Saalfeld, S.; Schmid, B.; et al. Fiji: An Open-Source Platform for Biological-Image Analysis. *Nat. Methods* **2012**, *9*, 676–682. [CrossRef] [PubMed]
47. R Development Core Team. *R: A Language and Environment for Statistical Computing*; R Development Core Team: Vienna, Austria, 2008.
48. Richter, R.P.; Bérat, R.; Brisson, A.R. Formation of Solid-Supported Lipid Bilayers: An Integrated View. *Langmuir* **2006**, *22*, 3497–3505. [CrossRef] [PubMed]
49. Lind, T.K.; Cárdenas, M.; Wacklin, H.P. Formation of Supported Lipid Bilayers by Vesicle Fusion: Effect of Deposition Temperature. *Langmuir* **2014**, *30*, 7259–7263. [CrossRef]
50. Jing, Y.; Trefna, H.; Persson, M.; Kasemo, B.; Svedhem, S. Formation of Supported Lipid Bilayers on Silica: Relation to Lipid Phase Transition Temperature and Liposome Size. *Soft Matter* **2014**, *10*, 187–195. [CrossRef]

7. Electroformation of Giant Unilamellar Vesicles from Damp Films in Conditions Involving High Cholesterol Contents, Charged Lipids, and Saline Solutions

MDPI

Article

Electroformation of Giant Unilamellar Vesicles from Damp Films in Conditions Involving High Cholesterol Contents, Charged Lipids, and Saline Solutions

Ivan Mardešić [1,2] , Zvonimir Boban [1] and Marija Raguz [1,*]

1 Department of Medical Physics and Biophysics, University of Split School of Medicine, 21000 Split, Croatia; ivan.mardesic@mefst.hr (I.M.); zvonimir.boban@mefst.hr (Z.B.)
2 Doctoral Study of Biophysics, Faculty of Science, University of Split, 21000 Split, Croatia
* Correspondence: marija.raguz@mefst.hr; Tel.: +385-9876-8819

Abstract: Giant unilamellar vesicles (GUVs) are frequently used as membrane models in studies of membrane properties. They are most often produced using the electroformation method. However, there are a number of parameters that can influence the success of the procedure. Some of the most common conditions that have been shown to have a negative effect on GUV electroformation are the presence of high cholesterol (Chol) concentrations, the use of mixtures containing charged lipids, and the solutions with an elevated ionic strength. High Chol concentrations are problematic for the traditional electroformation protocol as it involves the formation of a dry lipid film by complete evaporation of the organic solvent from the lipid mixture. During drying, anhydrous Chol crystals form. They are not involved in the formation of the lipid bilayer, resulting in a lower Chol concentration in the vesicle bilayer compared to the original lipid mixture. Motivated primarily by the issue of artifactual Chol demixing, we have modified the electroformation protocol by incorporating the techniques of rapid solvent exchange (RSE), ultrasonication, plasma cleaning, and spin-coating for reproducible production of GUVs from damp lipid films. Aside from decreasing Chol demixing, we have shown that the method can also be used to produce GUVs from lipid mixtures with charged lipids and in ionic solutions used as internal solutions. A high yield of GUVs was obtained for Chol/1-palmitoyl-2-oleoyl-sn-glycero-3-phosphocholine (POPC) samples with mixing ratios ranging from 0 to 2.5. We also succeeded in preparing GUVs from mixtures containing up to 60 mol% of the charged lipid 1-palmitoyl-2-oleoyl-sn-glycero-3-phospho-L-serine (POPS) and in NaCl solutions with low ionic strength (<25 mM).

Keywords: GUV; electroformation; damp lipid film; cholesterol demixing artifact; cholesterol; charged lipids; saline solution; lipid film deposition

1. Introduction

Vesicles serve as vital tools for researchers exploring the membrane properties under controlled conditions. Based on their lamellarity, they are divided into unilamellar, multilamellar (MLVs), and oligolamellar vesicles. Unilamellar vesicles consist of a single lipid bilayer, multilamellar vesicles have several concentric lipid bilayers, and oligolamellar vesicles contain smaller vesicles within the outer membrane. Unilamellar vesicles are further subdivided according to their size into small (SUVs, diameter less than 100 nm), large (LUVs, diameter from 100 nm to 1 μm), and giant unilamellar vesicles (GUVs, diameter over 1 μm). While SUVs and LUVs are frequently used for drug delivery investigations, GUVs attract more attention for studies on membrane properties and organization, mainly due to their size, which is comparable to that of eukaryotic cells [1]. Furthermore, due to their size, GUVs can be observed using light microscopy techniques, which is an additional advantage for researchers [2].

In modern research, electroformation has become one of the most widely used methods for the production of GUVs [3]. In this technique, an electric field is applied to an electrode containing lipids to generate vesicles [4]. Typically, lipids dissolved in an organic solvent are deposited onto an electrode. The solvent is then evaporated and vacuum treatment is applied to remove the residual solvent, leaving a dry lipid film. The lipid-coated and lipid-free electrodes were used to assemble the electroformation chamber, which was then filled with a chosen internal solution and connected to an alternating current generator. The hydration of the lipid film, assisted by the electric field, promotes the detachment of the lipids, which leads to the formation of vesicles.

Electroformation offers significant advantages over the natural swelling method, including a higher yield of unilamellar vesicles and less heterogeneity in composition. However, the method is not without its challenges. The traditional electroformation protocol, which involves depositing lipids using the drop-deposition method, often results in lipid films with non-uniform thickness, leading to GUVs with broad size distribution and varying compositions, ultimately reducing experimental reproducibility.

Researchers have made various attempts to improve this process [5–7]. For instance, the spin-coating technique, in which a lipid solution is deposited onto a flat glass surface coated with indium tin oxide (ITO) and spun rapidly, has been employed to create uniform lipid films [8]. This method has been validated using techniques such as ellipsometry and atomic force microscopy and has gained acceptance among researchers employing a wide range of lipid compositions for GUV production [8–14].

Another significant issue with the traditional protocol is cholesterol (Chol) demixing during the drying of the lipid film, particularly when working with lipid mixtures containing high Chol concentrations. In such cases, Chol can separate and form anhydrous Chol crystals, which do not participate in the formation of the lipid bilayer during rehydration, leading to a lower Chol concentration in the resulting bilayer (Figure 1) [9,15–17]. To address this issue, some researchers have utilized the rapid solvent exchange (RSE) technique, in which the drying phase is avoided by combining lipids dissolved in organic solvent with an aqueous solution, followed by the rapid evaporation of the organic solvent [18–20]. This method is effective in preventing Chol demixing; it primarily produces MLVs.

0.66   1.5   2   2.75

Chol/POPC mixing ratio
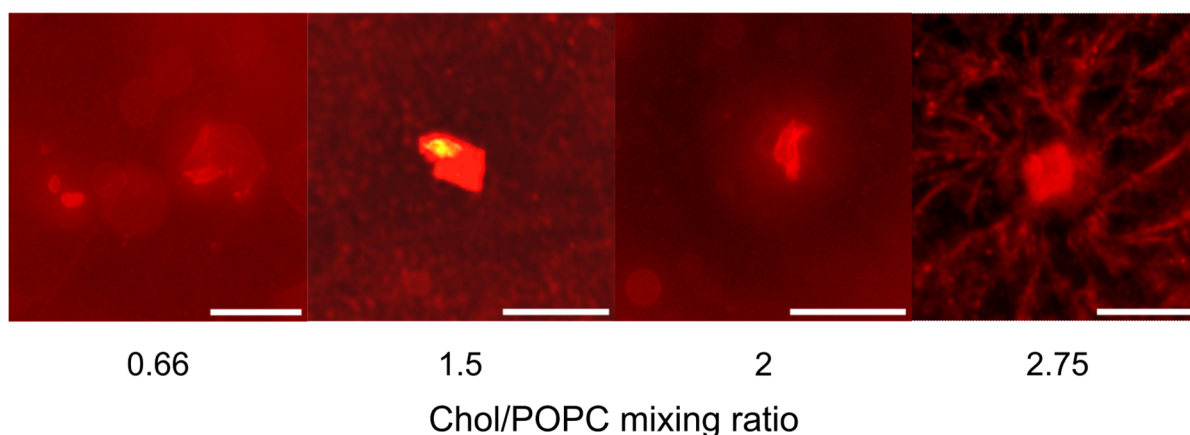
Figure 1. Examples of Chol crystals formed during the dry film phase when using the traditional electroformation protocol. The observed crystal structures are in good agreement with those observed in the study of Park et al. [21] on the phases of Chol crystallization. The scale bar represents 50 μm.

Recent advances in electroformation protocols have also focused on the cleaning of electrodes prior to lipid film deposition. Traditionally, electrodes are cleaned using organic solvents, but plasma cleaning has proven to be a more effective alternative. Plasma treatment not only cleans the electrodes but also enhances the efficiency of GUV formation, particularly when using buffers with physiological levels of charged particles, likely due to improved hydration of the lipid film [22,23].

In this study, we combine the above modifications with the traditional method of producing GUVs using an electroformation protocol from damp lipid films. This method has the potential to prevent Chol demixing during electrofromation while keeping the preparation time short and enhancing the reproducibility of the protocol. Such GUVs are of particular interest to researchers studying the role of Chol in various biological membranes, including those of the eye lens fiber cells, and in the development of atherosclerosis [20,24,25]. We show that the method is not only suitable to be applied to lipid mixtures with high Chol concentrations but can also be used to produce GUVs from mixtures with charged lipids or in ion-containing solutions.

2. Materials and Methods

2.1. Materials

1-palmitoyl-2-oleoyl-sn-glycero-3-phosphocholine (POPC), 1-palmitoyl-2-oleoyl-sn-glycero-3-phospho-L-serine (POPS), and Chol were purchased from Avanti Polar Lipids Inc. (Alabaster, AL, USA). The fluorescent dye 1,1-dioctadecyl-3,3,3,3-tetramethylindocarbocyanine Perchlorate (DiIC$_{18}$(3)) was purchased from Invitrogen, Thermo Fisher Scientific (Waltham, MA, USA). Lipids were stored at $-20\,^\circ$C when not in use. ITO-coated glass (ICG-90 INS 115, resistance 70–100 Ω and dimensions of $25 \times 75 \times 1.1$ mm) was purchased from Delta Technologies (Loveland, LO, USA). A fresh ITO-coated glass was used for each preparation to ensure efficient GUV formation [26]. Mili-Q deionized water (Merck, Rahway, NJ, USA), preheated to 60 $^\circ$C, was used as the internal chamber solution. For the saline solutions, NaCl 99.5% (Gram-mol, Zagreb, Croatia) was dissolved in Mili-Q deionized water.

2.2. Preparation of Multilamellar Vesicles Using the Rapid Solvent Exchange Method

MLVs were produced using a custom-built rapid RSE device to resolve the issue of Chol demixing. A lipid mixture dissolved in chloroform was prepared by mixing 25 mg/mL of POPC, 25 mg/mL of Chol, 10 mg/mL of POPS, and 1 mg/mL of DiIC$_{18}$(3) in the appropriate proportions. The Chol/POPC mixing ratios ranged from 0 to 2.5 (equivalent to a cholesterol mixing concentration of 0 to 71.4 mol%), while the DiIC$_{18}$(3)/POPC mixing ratio was kept constant at 1/500. When working with POPS/POPC/Chol ternary mixtures, the Chol mixing concentration was kept at 10 mol%, and the POPS mixing concentration ranged from 5 to 60 mol%. The total lipid mass per sample was 2.1 mg. Either Mili-Q water or a NaCl solution with low ionic strength (10 and 25 mM) were used as internal solutions. In total, 400 μL of the internal solution of choice was added to the lipids dissolved in the organic solvent, and the resulting mixture was vortexed (Vortex IR, Star Lab, Blakelands, UK) at a speed of 2200 rpm. While vortexing, the pressure was kept at approximately 0.05 bar using a vacuum pump (HiScroll 6, Pfeiffer Vacuum, Asslar, Germany). The sample was maintained at this pressure for 90 s to ensure the full removal of any remaining organic solvent.

2.3. Preparation of Unilamellar Vesicles by Sonication

The MLV solution prepared by the RSE method was sonicated using an ultrasonic homogenizer (SONOPLUS Ultrasonic Homogenizer HD 4050, Bandelin, Berlin, Germany) and an ultrasonic tip (Probe TS 102, Bandelin, Berlin, Germany) connected at an ultrasonic converter (UW 50, Bandelin, Berlin, Germany). If not stated differently, the sonication lasted 30 min at an amplitude of 60% (81 μm). Pulsed sonication was used (0.5 s on, 0.5 s off) to allow cooling and reduce the risk of overheating. To keep the lipids above their mixing temperature, the glass vial with the vesicle solution was heated at 60 $^\circ$C using a hotplate (Cimarec + stirring hotplate, Thermo Fisher Scientific, Waltham, MA, USA).

2.4. Preparation of the Damp Lipid Film

The ITO-coated glass stored in Mili-Q deionized water overnight was taken out and then wiped five times with lint-free cloths saturated with 70% ethanol. Afterward, the electrode underwent a 1-min oxygen plasma treatment using a plasma cleaner (PDC-

002-HPCE with PLASMAFLO PDC-FMG-2 attachment, Harrick Plasma, Ithaca, NY, USA) connected to a vacuum pump (HiScroll 6, Pfeiffer Vacuum, Asslar, Germany). Subsequently, 550 μL of a LUV suspension was applied to the hydrophilic plasma-treated ITO-coated glass electrode and spun using a spin-coater (SM-150, Sawatec, Sax, Switzerland) to obtain the lipid film. The electrode was spun at 600 rpm, reaching full speed within 1 s. The spin-coating was performed for 30 s to ensure the formation of a uniform damp lipid film. To prevent unintended evaporation, the coated ITO-coated glass was immediately placed into a Petri dish and used to assemble an electroformation chamber.

2.5. Electroformation Protocol

The electroformation chamber was assembled by sandwiching two ITO-coated glass slides (25 × 37.5 mm) with a 1.6 mm thick polytetrafluoroethylene (Teflon) spacer in between. The electrodes were made by cutting a 25 × 75 mm ITO-coated glass slide in half with a diamond pen cutter. To assemble the chamber, the lipid-coated glass was sealed to the Teflon spacer using vacuum grease, while the lipid-free electrode was sealed to the Teflon spacer on the opposite side. After the addition of 280 μL of Mili-Q water or saline solution, the stopper was sealed with vacuum grease. The care was taken that the grease did not come into contact with the water in order to prevent contamination that could affect GUV formation. The chamber was secured with clamps at three points along the electrodes—two near the stopper and one on the opposite side. The chamber was connected to a pulse generator (PSG 9080, Joy-IT, Neukirchen-Vluyn, Germany) and placed in an incubator set at 60 °C. Copper tape was applied to the outer edges of the electrodes to improve the wire–electrode contact. As in previous experiments with aqueous solutions, a voltage of 2 V and a frequency of 10 Hz were used [7,9,10,12]. In experiments using saline solution as the internal solution, a voltage of 4 V and a frequency of 500 Hz were applied. After 2 h, the pulse generator was turned off and the chamber was kept in the incubator for an hour.

2.6. Dynamic Light Scattering

Dynamic light scattering (DLS) was utilized to determine the hydrodynamic diameter and polydispersity index of the MLV and LUV suspensions (Litesizer 500, Anton Paar, Graz, Austria).

### 2.7. Fluorescence Imaging and Data Analysis

In order to comprehensively analyze the entire chamber volume, images were captured at 16 different regions of the sample. A total of 300 vesicles were randomly tracked from fluorescent images. If an image contained less than 300 vesicles, all visible vesicles were selected. To avoid bias, a subset of 100 vesicles was randomly chosen from these 300 vesicles for further analysis. Imaging was performed with a fluorescence microscope (Olympus BX51, Olympus, Tokyo, Japan), and vesicle diameters were measured using the line tool in Fiji software (ImageJ 1.53c) [27]. The numerical results are presented as the mean ± standard errors. Both data analysis and visualization were conducted using the R programming language [28].

3. Results and Discussion

3.1. The Protocol

The modifications of the protocol were inspired by the vesicle fusion method often used for the production of supported lipid bilayers [29–33]. In this method, an aqueous suspension of LUVs or SUVs is deposited on a hydrophilized surface. The hydrophilic surface causes vesicle rupturing, resulting in planar bilayers. Since our main motivation was to prevent Chol demixing induced during the drying of the lipid film, in order to utilize this new protocol, we first had to find a way to reliably create LUVs containing high Chol concentrations.

The easiest way to create vesicles is to use the hydration method. Unfortunately, this method also requires the evaporation of the organic solvent before the hydration of the film [34–36]. This is why our protocol begins with the preparation of MLVs using the RSE method (Figure 2a), which was confirmed to be effective in preventing Chol demixing [18,19]. The lipids dissolved in an organic solvent are first mixed with an aqueous solution of choice and stirred using a vortex mixer. The mixture is then subjected to a sudden vacuum, causing the organic solvent to rapidly evaporate from the mixture.
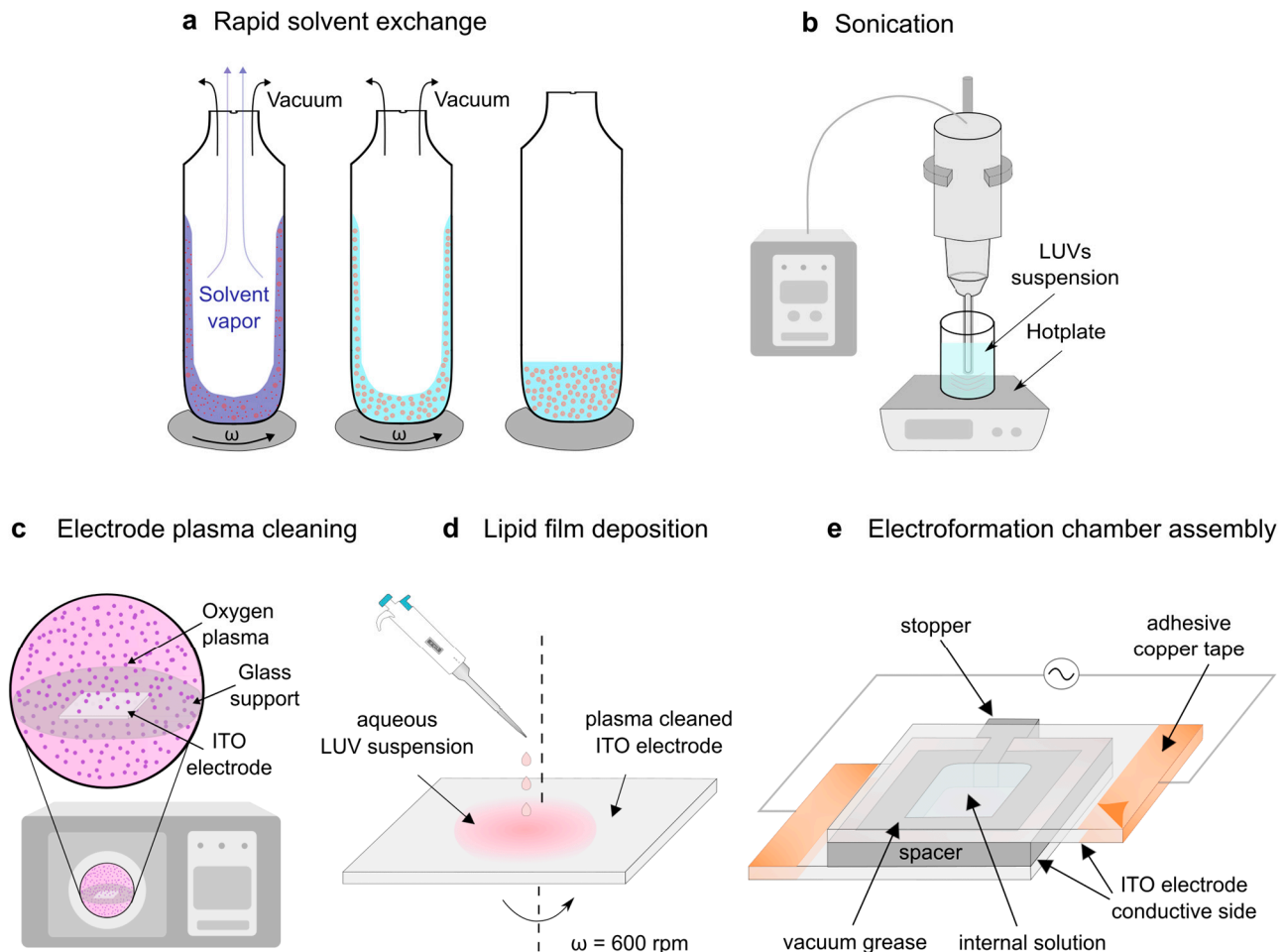
Figure 2. The modified protocol is for electroformation of GUVs from a damp lipid film. (**a**) The RSE method is used to produce an MLV solution. The RSE method is used to produce an MLV solution. An organic solvent (blue) containing lipids (red) is mixed with an aqueous solution (tube 1). The organic solvent is removed by vortexing the solution under vacuum in order to form MLVs (tube 3). (**b**) The suspension of MLVs is sonicated to produce LUVs. (**c**) A plasma cleaner is used to hydrophilize the ITO electrode. (**d**) The LUV suspension is deposited onto a plasma-cleaned ITO-coated glass and spin-coated to obtain a damp lipid film. (**e**) The coated electrode is used to assemble the electroformation chamber and connected to a voltage source to enable the growth of GUVs.

Although effective, the RSE method does not provide a homogeneous suspension of LUVs, but instead contains MLVs instead. The preparation of LUVs from a suspension of MLVs is most commonly conducted using mechanical extrusion or sonication. We tested the extrusion approach in our previous work [10,12] but found a couple of drawbacks to the method. Firstly, the method is time-consuming and always results in a loss of a small portion of the suspension volume [37]. Secondly, the extrusion of MLVs with a high Chol content results in a very large opposing force, making the extrusion process difficult, especially when using smaller pore sizes [10,12].

For this reason, we have opted for the sonication technique in this study (Figure 2b). It is much simpler and faster than extrusion [37], with only one manual action required: submerging a sonicator tip into the suspension of MLVs. It is also cheaper in the long term, as there is no need to buy disposable filters, as is the case with extrusion.

After the LUV suspension was obtained, it should be deposited onto a hydrophilized electrode surface. The hydrophilization was achieved using a plasma cleaner (Figure 2c). The traditional way of lipid deposition is the drop deposition technique, but it leads to the creation of inhomogenous lipid films, reducing the reproducibility of the experiment [7]. Therefore, we opted to deposit the suspension of LUVs using the spin-coating method (Figure 2d), which was proven effective in creating homogeneous lipid films [8,10]. Additionally, by controlling the spin-coating duration, we can reproducibly control how wet the film is and prevent it from drying out completely [12].

Now that the electrode was coated with the damp lipid film, all that remained was to create an electroformation chamber and attach it to an alternating voltage source to facilitate the growth of the GUVs (Figure 2e).

3.2. Determination of the Sonication Parameters

The size distribution of vesicles can be influenced by factors such as lipid composition, sonication duration, and sonication amplitude [37–39]. Therefore, we first tested the effect of three different sonication amplitudes at a fixed Chol/POPC ratio of 1.5 (Figure 3a). The tested amplitudes were 20, 40, and 60%, with the amplitude of 100% corresponding to an oscillation of 135 μm. The amplitude was not increased above 60% in order to avoid possible excessive damage to the vesicles. In addition, pulsed sonication (0.5 s on, 0.5 s off) was utilized to allow cooling and reduce the risk of overheating. By continuously measuring the temperature throughout the duration of sonication, we did not detect any significant increase in temperature with this approach. After inspecting the rate of decrease in average vesicle size, we decided to use an amplitude of 60%.
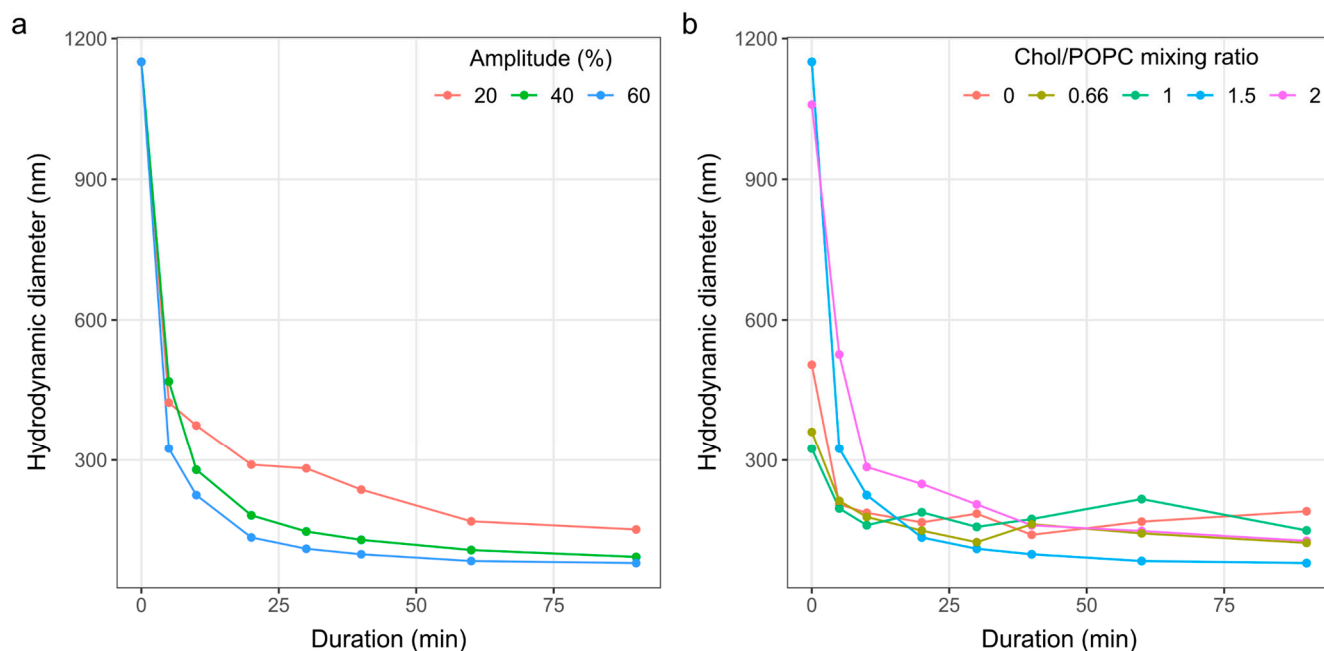

Figure 3. The effect of sonication parameters on the size of produced LUVs. (**a**) The effect of sonication duration using different sonication amplitudes for MLVs produced from a mixture with a Chol/POPC ratio of 1.5. (**b**) The effect of sonication duration for different Chol/POPC mixing ratios at a sonication amplitude of 60%.

Next, fixing the sonication amplitude at 60%, the effect of different lipid compositions on the change in particle size over time was tested (Figure 3b). Five different composi-

tions were tested, with a Chol/POPC ratio ranging from 0 to 2. Similar to another study investigating the influence of increasing Chol concentration in the sonicated vesicles [38], we observed that vesicles with a lower Chol content broke more easily. However, after approximately 30 min, there seemed to be no appreciable additional decrease in average diameter with time. This saturation behavior is consistent with other studies on liposome sonication [39,40]. Furthermore, prolonged sonication induces the formation of free radicals [40], altering the properties of membrane lipids. Therefore, we settled on a pulsed sonication duration of 30 min.

3.3. The Effect of Chol Content

After finding the optimal sonication parameters, we tested the effect of increasing the Chol concentration on GUV electroformation using our modified protocol (Figure 4). The results indicate a decrease in the average diameter of GUVs with increasing Chol/POPC ratio, with a size range similar to that observed in previous studies [12].
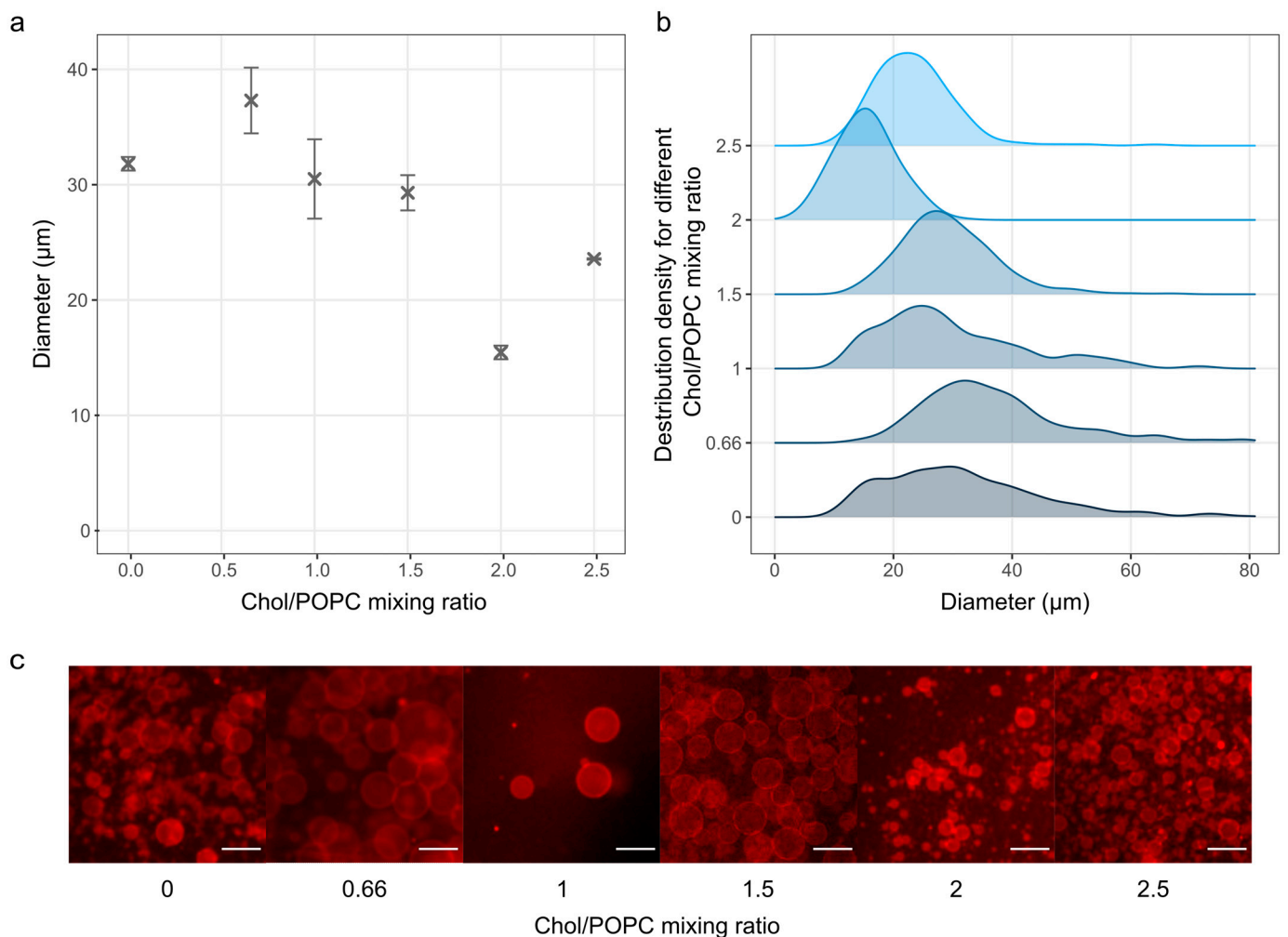

Figure 4. The effect of increasing the Chol content on the electroformation of GUVs. (**a**) Size of GUVs as a function of the different Chol mixing ratios. The points and bars represent mean values and standard errors. The mean values were calculated by averaging the mean diameters from three independent samples for each concentration. (**b**) Size distribution densities for different Chol contents. Each distribution density represents 300 vesicles (100 vesicles from each of the three samples). (**c**) Fluorescence microscopy images for each sample. The scale bar represents 50 μm.

This trend could be a result of reduced membrane elasticity and increased rigidity when more Chol is incorporated, which hinders vesicle formation. The effect is especially

pronounced when the Chol/POPC mixing ratio exceeds 1.5 (more than 60 mol% Chol in the mixture), where GUV membranes are expected to contain pure cholesterol bilayer domains (CBDs) [17]. An increase at a ratio of 2.5 (71.5 mol% Chol in the mixture) could be explained by Chol demixing due to the Chol/POPC ratio being higher than the Chol solubility limit of 66 mol% [41]. The demixing was also evident from a high number of Chol crystals observed during microscopy after the Chol/POPC ratio exceeded two. No Chol crystals were detected at the Chol/POPC mixing ratio lower than 2. At a ratio of 2, a negligible number of crystals were found, which was much lower than the number observed at the same ratio when using the traditional protocol. As expected, many crystals appeared on the surface after exceeding the Chol solubility limit at a Chol/POPC ratio of 2.5.

3.4. The Effect of Charged Lipids

The effect of different concentrations of a negatively charged POPS lipid was also tested (Figure 5).
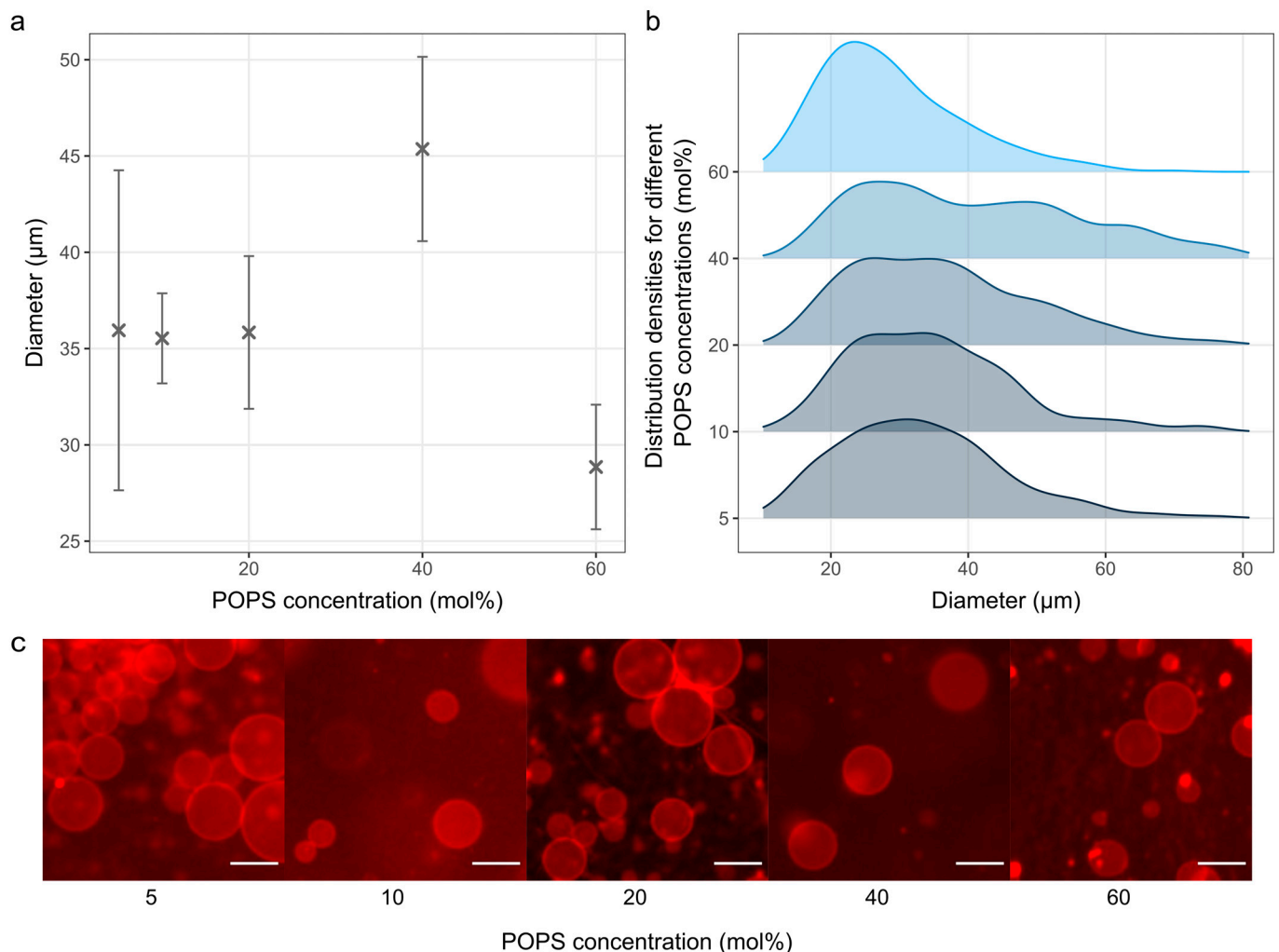
Figure 5. Electroformation from damp lipid films using different concentrations of POPS. (**a**) GUV size as a function of POPS concentrations. The points and bars represent mean values and standard errors. Mean values were calculated by averaging the mean diameters of three independent samples for each concentration. (**b**) Size distribution densities of GUVs for different POPS concentrations. Each distribution density represents 300 vesicles (100 vesicles from each of the three samples). (**c**) Fluorescence microscopy images for each sample. The scale bar represents 50 μm.

We succeeded in producing GUVs from a ternary POPS/POPC/Chol mixture with a POPS concentration ranging from 5 to 60 mol%, and a fixed Chol concentration of 10 mol%. The number of vesicles produced at POPS concentrations higher than 60 mol% was negligible.

Regarding the amount of POPS incorporated into the membrane, it has been shown that the incorporation of negatively charged lipids reduces membrane stability due to the reduction in membrane edge tension, which can lead to the complete collapse of the vesicle [42]. The results using POPC/POPG mixtures indicate high instability after 50 mol% of POPG [42], which is in line with the results presented here.

In comparable studies (using DOPS instead of POPS), an even lower amount of charged lipids was used for testing, namely about 30 mol% [23,43]. The average diameters of the obtained vesicles with such a composition were about 10 μm [43] and 20 μm [23], which is much smaller compared to our results with similar concentrations of charged lipids.

It should also be noted that one of these studies performed a comprehensive optimization of the electrical parameters for each lipid composition [23], whereas we contented ourselves with the commonly used values. Additionally, in the aforementioned studies, the drop deposition method was used (with or without subsequent smearing) to deposit the lipid film. Although this approach is inherently less reproducible, it has the advantage of resulting in a lipid film with regions of varying thicknesses, ensuring that there is always a portion of the lipid film that has the optimal thickness for that lipid composition. Our protocol uses the spin-coating technique instead, which can lead to greater homogeneity of film thickness, but requires more optimization because film thickness varies greatly with different lipid compositions and lipid concentrations [8,11]. Consequently, even though the present results with POPS are already quite good, we expect even better outcomes once the fine-tuning of the electrical parameters and film thickness is performed.

3.5. The Effect of Using Saline Solutions

GUVs prepared from a Chol/POPC mixture with a fixed Chol concentration of 10 mol% can also be successfully produced even when saline solutions were used during electroformation (Figure 6). We selected a voltage of 4 V and a frequency of 500 Hz according to the literature [22]. The average GUV diameters and standard errors were 11.2 ± 2.6 μm and 7 ± 0.3 μm for NaCl concentrations of 10 and 25 mM, respectively.
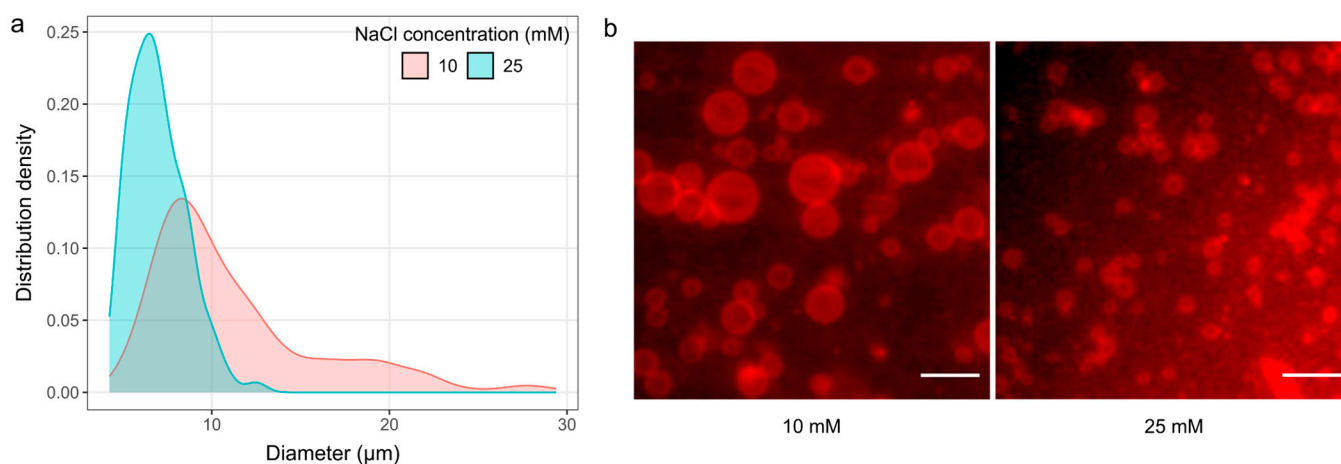
Figure 6. Electroformation from damp lipid films using saline solutions for the Chol/POPC mixture with a fixed Chol concentration of 10 mol%. (**a**) Size distribution of GUVs for different salt concentrations. Each distribution density represents 300 vesicles (100 vesicles from each of the three samples). (**b**) Fluorescence microscopy images for each sample. The scale bar represents 50 μm.

Previous studies have shown that cleaning the electrodes with plasma [22] or applying preformed liposome suspensions during film deposition [43,44] can promote GUV

electroformation under ionic conditions. Our modified protocol applies both of these modifications, and the results obtained are in agreement with those presented in their studies under similar conditions [22].

It is important to note that visibly wet lipid films were used for these experiments, as the duration of spin-coating was only 30 s. Since the amount of Chol in the mixture here was low, we could have dried the film even more, which would probably have given us even better results [10].

4. Conclusions

GUVs are extensively used in studies on membrane properties and are most commonly produced using the electroformation method. In this study, a modified protocol is described that addresses some of the shortcomings of the traditional method, offering a more efficient and reproducible approach for the preparation of GUVs, particularly for experiments requiring high Chol concentrations. In order to eliminate the dry lipid film phase and reduce Chol demixing, we used techniques that have been shown to be beneficial for GUV production under other conditions, such as when using charged lipids or ionic solutions.

Initially, the RSE method was used to avoid drying the lipid film and Chol demixing artifact. Sonication is a new method included in this protocol. We concluded that a sonication time of 30 min is sufficient to form LUVs. Replacing the extrusion step with sonication has further improved our protocol. Sonication is less time-consuming and results in a smaller amount of lipids used in the protocol. The extrusion of MLVs with a high Chol content, which results in a very large opposing force and makes the extrusion process difficult, was a problematic step in our previous protocol. Applying the sonication method instead of extrusion in our protocol makes the process shorter and easier to perform. We have also included plasma cleaning of the electrode, which has been shown to promote vesicle formation when using charged lipids or saline solution. To ensure methodological reproducibility, the solution of LUVs was applied to the electrode by spin-coating instead of drop deposition.

We tested our modified protocol using lipid mixtures with very high Chol concentrations, charged lipids (POPS), and saline solutions. Compared to other studies testing GUV electroformation under similar conditions, the results obtained were similar or better than the data found in the literature [22]. Furthermore, by bypassing the dry phase, our protocol should be more suitable for protein insertion into GUVs and further reduce the risk of protein denaturation [45,46].

In the future, we plan to test the performance of the new protocol using a larger number of lipid species and ionic solutions to further customize the protocol for the best possible outcomes.

Author Contributions: Conceptualization, I.M., Z.B. and M.R.; methodology, I.M. and Z.B.; software, I.M. and Z.B.; validation, I.M. and Z.B.; formal analysis, I.M. and Z.B.; investigation, I.M. and Z.B.; resources, M.R.; data curation, I.M. and Z.B.; writing—original draft preparation, I.M. and Z.B.; writing—review and editing, I.M., Z.B. and M.R.; visualization, I.M. and Z.B.; supervision, M.R.; project administration, M.R.; funding acquisition, M.R. All authors have read and agreed to the published version of the manuscript.

References

1. Rideau, E.; Dimova, R.; Schwille, P.; Wurm, F.R.; Landfester, K. Liposomes and Polymersomes: A Comparative Review towards Cell Mimicking. *Chem. Soc. Rev.* **2018**, *47*, 8572–8610. [CrossRef] [PubMed]
2. Gudheti, M.V.; Mlodzianoski, M.; Hess, S.T. Imaging and Shape Analysis of GUVs as Model Plasma Membranes: Effect of Trans DOPC on Membrane Properties. *Biophys. J.* **2007**, *93*, 2011–2023. [CrossRef] [PubMed]
3. Angelova, M.I.; Dimitrov, D.S. Liposome Electroformation. *Faraday Discuss. Chem. Soc.* **1986**, *81*, 303. [CrossRef]
4. Angelova, M.; Dimitrov, D.S. Angelova, M.; Dimitrov, D.S. A Mechanism of Liposome Electroformation. In *Trends in Colloid and Interface Science II*; Steinkopff: Darmstadt, Germany, 1988; Volume 67, pp. 59–67.
5. Veatch, S.L. Electro-Formation and Fluorescence Microscopy of Giant Vesicles with Coexisting Liquid Phases. *Methods Mol Biol.* **2007**, *398*, 59–72. [PubMed]
6. Morales-Penningston, N.F.; Wu, J.; Farkas, E.R.; Goh, S.L.; Konyakhina, T.M.; Zheng, J.Y.; Webb, W.W.; Feigenson, G.W. GUV Preparation and Imaging: Minimizing Artifacts. *Biochim. Biophys. Acta—Biomembr.* **2010**, *1798*, 1324–1332. [CrossRef]
7. Boban, Z.; Mardešić, I.; Subczynski, W.K.; Raguz, M. Giant Unilamellar Vesicle Electroformation: What to Use, What to Avoid, and How to Quantify the Results. *Membranes* **2021**, *11*, 860. [CrossRef]
8. Estes, D.J.; Mayer, M. Electroformation of Giant Liposomes from Spin-Coated Films of Lipids. *Colloids Surf. B Biointerfaces* **2005**, *42*, 115–123. [CrossRef]
9. Boban, Z.; Puljas, A.; Kovač, D.; Subczynski, W.K.; Raguz, M. Effect of Electrical Parameters and Cholesterol Concentration on Giant Unilamellar Vesicles Electroformation. *Cell Biochem. Biophys.* **2020**, *78*, 157–164. [CrossRef]
10. Boban, Z.; Mardešić, I.; Jozić, S.P.; Šumanovac, J.; Subczynski, W.K.; Raguz, M. Electroformation of Giant Unilamellar Vesicles from Damp Lipid Films Formed by Vesicle Fusion. *Membranes* **2023**, *13*, 352. [CrossRef]
11. Boban, Z.; Mardešić, I.; Subczynski, W.K.; Jozić, D.; Raguz, M. Optimization of Giant Unilamellar Vesicle Electroformation for Phosphatidylcholine/Sphingomyelin/Cholesterol Ternary Mixtures. *Membranes* **2022**, *12*, 525. [CrossRef]
12. Mardešić, I.; Boban, Z.; Raguz, M. Electroformation of Giant Unilamellar Vesicles from Damp Lipid Films with a Focus on Vesicles with High Cholesterol Content. *Membranes* **2024**, *14*, 79. [CrossRef] [PubMed]
13. Politano, T.J.; Froude, V.E.; Jing, B.; Zhu, Y. AC-Electric Field Dependent Electroformation of Giant Lipid Vesicles. *Colloids Surf. B Biointerfaces* **2010**, *79*, 75–82. [CrossRef] [PubMed]
14. Billerit, C.; Jeffries, G.D.M.; Orwar, O.; Jesorka, A. Formation of Giant Unilamellar Vesicles from Spin-Coated Lipid Films by Localized IR Heating. *Soft Matter* **2012**, *8*, 10823–10826. [CrossRef]
15. Baykal-Caglar, E.; Hassan-Zadeh, E.; Saremi, B.; Huang, J. Preparation of Giant Unilamellar Vesicles from Damp Lipid Film for Better Lipid Compositional Uniformity. *Biochim. Biophys. Acta—Biomembr.* **2012**, *1818*, 2598–2604. [CrossRef]
16. Raguz, M.; Kumar, S.N.; Zareba, M.; Ilic, N.; Mainali, L.; Subczynski, W.K. Confocal Microscopy Confirmed That in Phosphatidyl-choline Giant Unilamellar Vesicles with Very High Cholesterol Content Pure Cholesterol Bilayer Domains Form. *Cell Biochem. Biophys.* **2019**, *77*, 309–317. [CrossRef]
17. Mainali, L.; Raguz, M.; Subczynski, W.K. Formation of Cholesterol Bilayer Domains Precedes Formation of Cholesterol Crystals in Cholesterol/Dimyristoylphosphatidylcholine Membranes: EPR and DSC Studies. *J. Phys. Chem. B* **2013**, *117*, 8994–9003. [CrossRef]
18. Buboltz, J.T.; Feigenson, G.W. A Novel Strategy for the Preparation of Liposomes: Rapid Solvent Exchange. *Biochim. Biophys. Acta—Biomembr.* **1999**, *1417*, 232–245. [CrossRef]
19. Buboltz, J.T. A More Efficient Device for Preparing Model-Membrane Liposomes by the Rapid Solvent Exchange Method. *Rev. Sci. Instrum.* **2009**, *80*, 124301. [CrossRef]
20. Mainali, L.; Raguz, M.; O'Brien, W.J.; Subczynski, W.K. Properties of Membranes Derived from the Total Lipids Extracted from the Human Lens Cortex and Nucleus. *Biochim. Biophys. Acta—Biomembr.* **2013**, *1828*, 1432–1440. [CrossRef]
21. Park, S.; Sut, T.N.; Ma, G.J.; Parikh, A.N.; Cho, N.J. Crystallization of Cholesterol in Phospholipid Membranes Follows Ostwald's Rule of Stages. *J. Am. Chem. Soc.* **2020**, *142*, 21872–21882. [CrossRef]
22. Li, Q.; Wang, X.; Ma, S.; Zhang, Y.; Han, X. Electroformation of Giant Unilamellar Vesicles in Saline Solution. *Colloids Surf. B Biointerfaces* **2016**, *147*, 368–375. [CrossRef] [PubMed]
23. Ghellab, S.E.; Mu, W.; Li, Q.; Han, X. Prediction of the Size of Electroformed Giant Unilamellar Vesicle Using Response Surface Methodology. *Biophys. Chem.* **2019**, *253*, 106217. [CrossRef] [PubMed]
24. Preston Mason, R.; Tulenko, T.N.; Jacob, R.F. Direct Evidence for Cholesterol Crystalline Domains in Biological Membranes: Role in Human Pathobiology. *Biochim. Biophys. Acta—Biomembr.* **2003**, *1610*, 198–207. [CrossRef] [PubMed]
25. Mainali, L.; O'Brien, W.J.; Subczynski, W.K. Detection of Cholesterol Bilayer Domains in Intact Biological Membranes: Method-ology Development and Its Application to Studies of Eye Lens Fiber Cell Plasma Membranes. *Exp. Eye Res.* **2019**, *178*, 72–81. [CrossRef]
26. Herold, C.; Chwastek, G.; Schwille, P.; Petrov, E.P. Efficient Electroformation of Supergiant Unilamellar Vesicles Containing Cationic Lipids on ITO-Coated Electrodes. *Langmuir* **2012**, *28*, 5518–5521. [CrossRef]
27. Schindelin, J.; Arganda-Carreras, I.; Frise, E.; Kaynig, V.; Longair, M.; Pietzsch, T.; Preibisch, S.; Rueden, C.; Saalfeld, S.; Schmid, B.; et al. Fiji: An Open-Source Platform for Biological-Image Analysis. *Nat. Methods* **2012**, *9*, 676–682. [CrossRef]
28. R Development Core Team. *R: A Language and Environment for Statistical Computing*; R Development Core Team: Vienna, Austria, 2008.

29. Richter, R.P.; Bérat, R.; Brisson, A.R. Formation of Solid-Supported Lipid Bilayers: An Integrated View. *Langmuir* **2006**, *22*, 3497–3505. [CrossRef]

30. Brian, A.A.; McConnell, H.M. Allogeneic Stimulation of Cytotoxic T Cells by Supported Planar Membranes. *Proc. Natl. Acad. Sci. USA* **1984**, *81*, 6159–6163. [CrossRef]

31. Lind, T.K.; Cárdenas, M.; Wacklin, H.P. Formation of Supported Lipid Bilayers by Vesicle Fusion: Effect of Deposition Temperature. *Langmuir* **2014**, *30*, 7259–7263. [CrossRef]

32. Jackman, J.A.; Cho, N.-J. Supported Lipid Bilayer Formation: Beyond Vesicle Fusion. *Langmuir* **2020**, *36*, 1387–1400. [CrossRef]

33. Tero, R. Substrate Effects on the Formation Process, Structure and Physicochemical Properties of Supported Lipid Bilayers. *Materials* **2012**, *5*, 2658–2680. [CrossRef]

34. Reeves, J.P.; Dowben, R.M. Formation and Properties of Thin-Walled Phospholipid Vesicles. *J. Cell. Physiol.* **1969**, *73*, 49–60. [CrossRef] [PubMed]

35. Darszon, A.; Vandenberg, C.A.; Schönfeld, M.; Ellisman, M.H.; Spitzer, N.C.; Montal, M. Reassembly of Protein-Lipid Complexes into Large Bilayer Vesicles: Perspectives for Membrane Reconstitution. *Proc. Natl. Acad. Sci. USA* **1980**, *77*, 239–243. [CrossRef] [PubMed]

36. Rodriguez, N.; Pincet, F.; Cribier, S. Giant Vesicles Formed by Gentle Hydration and Electroformation: A Comparison by Fluorescence Microscopy. *Colloids Surf. B Biointerfaces* **2005**, *42*, 125–130. [CrossRef] [PubMed]

37. Cho, N.J.; Hwang, L.Y.; Solandt, J.J.R.; Frank, C.W. Comparison of Extruded and Sonicated Vesicles for Planar Bilayer Self-Assembly. *Materials* **2013**, *6*, 3294–3308. [CrossRef]

38. Lapinski, M.M.; Castro-Forero, A.; Greiner, A.J.; Ofoli, R.Y.; Blanchard, G.J. Comparison of Liposomes Formed by Sonication and Extrusion: Rotational and Translational Diffusion of an Embedded Chromophore. *Langmuir* **2007**, *23*, 11677–11683. [CrossRef]

39. Woodbury, D.J.; Richardson, E.S.; Grigg, A.W.; Welling, R.D.; Knudson, B.H. Reducing Liposome Size with Ultrasound: Bimodal Size Distributions. *J. Liposome Res.* **2006**, *16*, 57–80. [CrossRef]

40. Maulucci, G.; De Spirito, M.; Arcovito, G.; Boffi, F.; Castellano, A.C.; Briganti, G. Particle Size Distribution in DMPC Vesicles Solutions Undergoing Different Sonication Times. *Biophys. J.* **2005**, *88*, 3545–3550. [CrossRef]

41. Huang, J.; Feigenson, G.W. A Microscopic Interaction Model of Maximum Solubility of Cholesterol in Lipid Bilayers. *Biophys. J.* **1999**, *76*, 2142–2157. [CrossRef]

42. Lira, R.B.; Leomil, F.S.C.; Melo, R.J.; Riske, K.A.; Dimova, R. To Close or to Collapse: The Role of Charges on Membrane Stability upon Pore Formation. *Adv. Sci.* **2021**, *8*, e2004068. [CrossRef]

43. Uzun, H.D.; Tiris, Z.; Czarnetzki, M.; López-Marqués, R.L.; Günther Pomorski, T. Electroformation of Giant Unilamellar Vesicles from Large Liposomes. *Eur. Phys. J. Spec. Top.* **2024**, *123*. [CrossRef]

44. Pott, T.; Bouvrais, H.; Méléard, P. Giant Unilamellar Vesicle Formation under Physiologically Relevant Conditions. *Chem. Phys. Lipids* **2008**, *154*, 115–119. [CrossRef] [PubMed]

45. Girard, P.; Pécréaux, J.; Lenoir, G.; Falson, P.; Rigaud, J.L.; Bassereau, P. A New Method for the Reconstitution of Membrane Proteins into Giant Unilamellar Vesicles. *Biophys. J.* **2004**, *87*, 419–429. [CrossRef] [PubMed]

46. Witkowska, A.; Jablonski, L.; Jahn, R. A Convenient Protocol for Generating Giant Unilamellar Vesicles Containing SNARE Proteins Using Electroformation. *Sci. Rep.* **2018**, *8*, 9422. [CrossRef]

8. CONCLUSIONS AND FUTURE PERSPECTIVE

The long term aim for this thesis was to investigate CBDs properties. We believe this domain is not investigated enough regarding their important biological functions. In the first article, we reviewed all the membrane models and experimental techniques that were used to investigate CBDs properties. Producing membrane models with very high Chol content is challenging, so we reviewed all the protocols that are suitable for research of domains' properties. We also summarised all the known properties of CBDs and their function in biological membrane. We were specially motivated by the beneficial function in the fiber cell plasma membrane of the eye lens. In these plasma membranes, CBDs ensures that the surrounding PL bilayer is always saturated with Chol. These domains form buffering capacity for Chol in the surrounding phospholipid bilayer. The saturation of bilayers with Chol ensures that the membrane physical properties of these bilayers become consistent and independent of the compositions. These properties ensure the proper functioning of the eye lens fiber cell membranes through changes in the lipid composition that occurs with age. Another function is that CBDs is maximising hydrophobic barrier. CBDs also increase the barrier to oxygen that protects lens from oxidative stress and developing cataract. Furthermore, the saturation of Chol should smooth the membrane surface, reducing light scattering and helping to maintain lens transparency.

After all the detail research about CBDs, we decided to use GUVs as membrane models for investigating CBDs properties. Electroformation is the method most often used for their production. In second and third article, we conducted experiments to optimize and improve the electroformation protocol for generating GUVs with high Chol content, charged lipids and in ionic solutions. The motivation was to modify traditional electroformation protocol in order to improve method to produce GUVs with lipid composition that resemble the composition of the lipid portion of the eye lens fiber cell membranes. The traditional electroformation protocol often yields low GUV production, particularly for lipid mixtures containing charged lipids or high Chol levels. A major issue with the conventional method is that drying the lipid film induces Chol demixing.

To address this issue, in the previous experimental article done by our group, we developed a novel protocol that integrates RSE, extrusion, plasma cleaning, and spin-coating to generate GUVs from a damp lipid film. Method was developed but not optimised. In the second article of thesis, using this improved method, we first optimized various parameters such as: spin-coating duration, liposome deposition and lipid composition. As a result, we successfully produced GUVs with high Chol content without encountering Chol demixing artifact. For Chol/POPC mixing ratios greater

than 1.5, where the GUVs may contain CBDs, a significant decrease in the average GUV diameter was measured. It was about 40% lower compared to that of the pure POPC bilayer.

Despite successful production of GUVs with high Chol contents, there were still some limitations in the protocol. The most significant challenge was the extrusion of vesicles with high Chol content due to the increased flow resistance. To overcome this issue, we wrote third article that is included in this thesis, where we replaced the extrusion step with sonication to obtain LUVs. The main advantage of sonication is its simplicity compared to extrusion. The sonication duration and amplitude were optimized for different lipid compositions. Applying the new protocol, we not only achieved the successful formation of GUVs with high Chol content but also obtained a high yield when charged lipids (up to 60 mol% POPS) or ionic solutions (up to 25 mM NaCl solution) were used.

We believe that this improved and optimized electroformation protocol will enable the study of the physical properties and lateral organization of the plasma membranes with very high Chol content, such as those found in fiber cell plasma membranes of the eye lens. Furthermore, the protocol can be adapted for protein incorporation into GUVs, minimizing the risk of protein denaturation by avoiding the use of organic solvents and lipid film drying.

9. CURRICULUM VITAE

IVAN MARDEŠIĆ

Date of birth: 9th August 1995

e-mail: imardesi@mefst.hr

EDUCATION

• 09/2020.-today Postgraduate university study in Biophysics, Faculty of Science, University of Split

• 09/2017.-09/2019. Graduate university study in Biophysics, Faculty of Science, University of Split

• 09/2014.-09/2017. Undergraduate university study in Physics, Faculty of Science, University of Split

EMPLOYMENT

• 03/2019.-today Research Assistant at University of Split School of Medicine

PROJECTS

• 2020.-today: Croatian Science Foundation (Croatia) under Grant IP-2019-04-1958

AWARDS

• Dean award, Faculty of Science, University of Split, 2019

TEACHING

• University of Split School of Medicine

ARTICLES

1. Boban, Z.; Mardešić, I.; Subczynski, W.K.; Raguz, M. Giant Unilamellar Vesicle Electroformation: What to Use, What to Avoid, and How to Quantify the Results. Membranes (Basel). 2021, 11, 860, doi:10.3390/membranes11110860.

2. Boban, Z.; Mardešić, I.; Subczynski, W.K.; Jozić, D.; Raguz, M. Optimization of Giant Unilamellar Vesicle Electroformation for Phosphatidylcholine/Sphingomyelin/Cholesterol Ternary Mixtures. Membranes (Basel). 2022, 12, 525, doi:10.3390/membranes12050525.

3. Boban, Z.; Mardešić, I.; Jozić, S.P.; Šumanovac, J.; Subczynski, W.K.; Raguz, M. Electroformation of Giant Unilamellar Vesicles from Damp Lipid Films Formed by Vesicle Fusion. Membranes (Basel). 2023, 13, 352, doi:10.3390/membranes13030352.

4. Mardešić, I.; Boban, Z.; Subczynski, W.K.; Raguz, M. Membrane Models and Experiments Suitable for Studies of the Cholesterol Bilayer Domains. Membranes (Basel). 2023, 13, doi:10.3390/membranes13030320.

5. Mardešić, I.; Boban, Z.; Raguz, M. Electroformation of Giant Unilamellar Vesicles from Damp Lipid Films with a Focus on Vesicles with High Cholesterol Content. Membranes (Basel). 2024, 14, 79, doi:10.3390/membranes14040079.

6. Mardešić, I.; Boban, Z.; Raguz, M. Electroformation of Giant Unilamellar Vesicles from Damp Films in Conditions Involving High Cholesterol Contents, Charged Lipids, and Saline Solutions. Membranes 2024, 14, 215. https://doi.org/10.3390/membranes14100215